

*ESF-IMPACT Workshop*

**OCEANIC IMPACTS: MECHANISMS AND  
ENVIRONMENTAL PERTURBATIONS**

APRIL 15 - APRIL 17, 1999

Alfred Wegener Institute for Polar and Marine Research  
Bremerhaven, Germany

*Abstracts*

---

**Edited by Rainer Gersonde and Alexander Deutsch**

Ber. Polarforsch. 343 (1999)  
ISSN 0176 - 5027



## CONTENTS

<b>Preface</b>	..... 3
<b>Acknowledgements</b>	..... 6
<b>Program</b>	..... 7
<b>Abstracts</b>	
P. Agrinier, A. Deutsch, U. Schärer and I. Martinez: On the kinetics of reaction of CO <sub>2</sub> with hot CaO during impact events: An experimental study.	.....11
L. Ainsaar and M. Semidor: Long-term effect of the Kärđla impact crater (Hiiumaa, Estonia) on the middle Ordovician carbonate sedimentation.	.....13
N. Artemieva and V.Shuvalov: Shock zones on the ocean floor - Numerical simulations.	.....16
H. Bahlburg and P. Claeys: Tsunami deposit or not: The problem of interpreting the siliciclastic K/T sections in northeastern Mexico.	.....19
R. Coccioni, D. Basso, H. Brinkhuis, S. Galeotti, S. Gardin, S. Monechi, E. Morettini, M. Renard, S. Spezzaferrri, and M. van der Hoeven: Environmental perturbation following a late Eocene impact event: Evidence from the Massignano Section, Italy.	.....21
I. von Dalwigk and J. Ormö: Formation of resurge gullies at impacts at sea: the Lockne crater, Sweden.	.....24
J. Ebbing, P. Janle, J. Koulouris and B. Milkereit: Palaeotopography of the Chicxulub impact crater and implications for oceanic craters.	.....25
V. Feldman and S.Kotelnikov: The methods of shock pressure estimation in impacted rocks.	.....28
J.-A. Flores, F. J. Sierro and R. Gersonde: Calcareous plankton stratigraphies from the "Eltanin" asteroid impact area: Strategies for geological and paleoceanographic reconstruction.	.....29
M.V.Gerasimov, Y. P. Dikov, O . I. Yakovlev and F.Wlotzka: Experimental investigation of the role of water in the impact vaporization chemistry.	.....31
R. Gersonde, F. T. Kyte, A. Abelmann, U. Bleil, B. Diekmann, J.A. Flores, K. Gohl, G. Kuhn and F. J. Sierro: A late Pliocene asteroid impact into the deep ocean (Bellingshausen Sea) - Its documentation and paleoenvironmental implications.	.....33
A. Glikson: Post-LHB bombardment rates and oceanic impact records.	.....35
C. B. Harbitz, U. M. Kolderup and A. Makurat. Tsunami prediction, monitoring and warning in Norway.	.....36
B. Ivanov: Comet impacts to the ocean: Numerical analysis of Eltanin-scale events.	.....38
A. P. Jones, G. D. Price and P. Claeys: A petrological model for oceanic impact melting and the origin of komatiites.	.....41
B. Kettrup and A. Deutsch: Geochemical investigations of K/T boundary rocks: The search for precursor lithologies.	.....44

B. A. Klumov: Large meteoroid impact into oceanic site: Impact on ozone layer.	.....47
J. Koulouris, P. Janle, B. Milkereit, and S. Werner: Significance of large ocean impact craters.	.....48
F. T. Kyte and R. Gersonde: Meteoritic ejecta deposits from the late Pliocene impact of the Eltanin Asteroid.	.....50
M. Lindström: The present status of the Lockne marine impact structure (Ordovician, Sweden).	.....54
F. Martinez-Ruiz, M. Ortega Huertas and I. Palomo: The Cretaceous-Tertiary event: Impact spherules and geochemical signatures from areas of SE Spain and Site 1049 (ODP Leg 171B).	.....57
V. L. Masaitis: The Kaluga impact event and its proven and possible geological consequences.	.....60
J. F. Monteiro, A. Ribeiro and J. Munha: The Tore "Sea-Mount": A possible megaimpact crater in deep ocean.	.....64
J. R. Morrow, C. A. Sandberg, and W. Ziegler: Recognition of mid-Frasnian (early late Devonian) oceanic impacts: Alamo, Nevada, Usa, and Amönau, Hessen, Germany.	.....66
J. Ormö and M. Lindström: Geological characteristics of marine-target craters.	.....70
J. B. Plescia: Mulkarra impact, South Australia: A complex impact structure.	.....74
C. W. Poag, J. B. Plescia and P. C. Molzer: Chesapeake Bay impact structure: Geology and geophysics.	.....79
A. Preisinger, S. Aslanian, H. Summesberger and H. Stradner: 5 Million years of Milankovitch cycles in marine sediments across the K/T boundary at the black sea coast near Bjala, Bulgaria.	.....84
J. Smit: Ejecta deposits of the Chicxulub impact.	.....87
K. Suuroja, V. Puura and S. Suuroja: Kärđla Crater (Hiiumaa Island, Estonia) - The result of an impact in a shallow epicontinental sea.	.....89
A. V. Teterov and L. V. Rudak: Atmospheric perturbations and tsunamis caused by an impact of a cosmic body into an ocean.	.....92
A. V. Teterov: Underwater cratering at impacts into oceans.	.....93
R. Törnberg: Component analysis of the resurge deposits in the marine Lockne and Tvären impact structures.	.....95
F. Tsikalas, J. I. Faleide, O. Eldholm, and S. T. Gudlaugsson: Porosity variation, seismic-amplitude anomalies and hydrocarbon potential of the Mjøltnir impact crater.	.....97
S. A. Vishnevsky and V. F. Korobkov: Marine impact site Shiyli: Origin of central uplift due to elastic response of target rocks.	....100
D. Völker and V. Spieß: The seismic fingerprint of the Eltanin impact.	....102
Å. Wallin: Middle Ordovician acritarchs from impact structures in Sweden.	....103
K. Wünnemann and M. A. Lange: Numerical modeling of oceanic impact events.	....106
<b>List of Participants</b>	....107

## **Preface**

From April 15 to April 17, 1999, 63 scientists from 14 European countries, Russia and the US met at the Alfred Wegener Institute for Polar and Marine Research in Bremerhaven, Germany, to present and discuss the results of recent research on oceanic impacts. The workshop „Oceanic Impacts: Mechanisms and Environmental Perturbations” was organized by Alex Deutsch (University of Münster) and Rainer Gersonde (Alfred Wegener Institute, Bremerhaven), assisted by the co-conveners Bernd Milkereit (University of Kiel) and Jan Smit (Vrije Univ. Amsterdam). Main scopes of the oral and poster presentations and plenary discussions were the development of methods for the identification of oceanic impacts, the documentation and modelling of related mechanisms and environmental perturbations in ocean and atmosphere, as well as the potential of impact structures as hydrocarbon reservoirs.

Of the ~165 known terrestrial impact structures only ~13% have been identified to originate in marine environments. Most of the marine impacts have been reported from shallow water marginal or epicontinental seas where characteristic craterform structures are developed, except the Eltanin impact discovered from a deep sea basin (Fig. 1, Tab. 1). In contrast to continental impacts, oceanic impacts will generate megatsunamis that could potentially devastate coastlines. The ejection of large quantities of water and salt into the atmosphere might lead to depletion of the ozone shield and acidification of surface regions. This could affect the Earth's albedo and the power of greenhouse forcing. It is now generally accepted that the shallow water Chicxulub impact at the Cretaceous/Tertiary (K/T) boundary resulted in a global catastrophe leading to the K/T mass extinction. This severe disruption of the biosphere has been linked with processes such as the deposition of heat on the planet's surface, and breaking of the food chains by a sudden change in the Earth's climate. The latter was most probably caused by the enormous quantities of H<sub>2</sub>O, impact-released gases such as CO<sub>2</sub>, SO<sub>2</sub>, and dust, which were injected into the atmosphere. Despite the great potential of oceanic impacts for causing sudden disturbance of Earth's climate and biological evolution our knowledge on these processes is still quite limited.

Possible reasons for the mismatch between the numbers of detected continental and deep sea impacts include the relatively young average age of oceanic basins resulting from tectonic plate movements, the burial of marine impact structures under a post-impact sedimentary cover, the deceleration and disintegration of small projectiles in the water column excluding the formation of crater structures or sediment disturbances at the deep sea floor, the inaccessibility of the deep ocean, and the lack of systematic programs for the detection of oceanic impacts.

To date, the key site for deep ocean impact studies is the late Pliocene Eltanin impact in the 5000 m deep Bellingshausen Sea (Fig. 1). The Eltanin impact was documented based on combined bathymetric, seismic and sediment coring surveys of the impact area. This study resulted in the description of a typical sequence of sediment beds formed as a consequence of the impact-

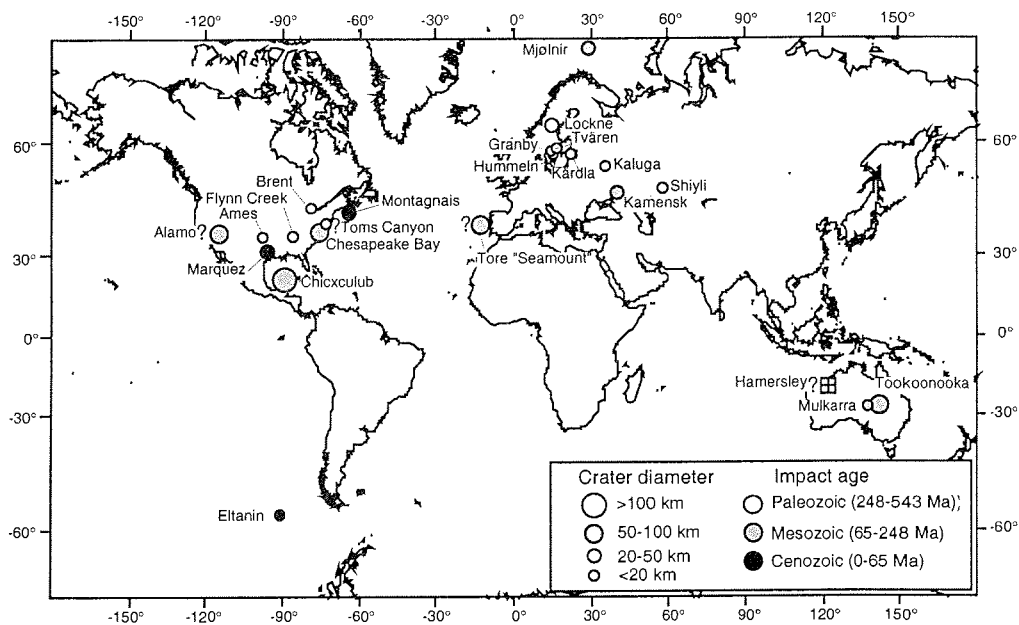


Figure 1 Location of marine impact structures (see also Tab. 1)

Name	Target Water Depth [km]	Locality	Diameter of the Structure [km]	Age* [Ma]
<b>Deep Ocean Impacts</b>				
Eltanin	ca. 5000	?north of San Martin Seamounts ca. 57°S,91°W	no cratering observed	2.15
<b>Shallow Water Impacts</b>				
Chesapeake Bay	200-500	37°16'N,76°0.7'W	85	35.5
Shiyli	ca.300	49°10'N,57°51'E	3.2	45
Montagnais	<600	42°53'N, 64°13'W	45	50.5
Marquez	shallow	31°17'N,96°18'W	22	58
Kamensk	100-200	48°20'N, 40°15'E	38	65
Chicxculub	100-200	21°20'N,89°30'W	180	65
Mulkarra	very shallow	27°51'S, 138°55'E	17	105
Tookoonooka	paralic	27°07'S, 142°50'E	55-65	128
Mjolnir	300-500	73°45'N,29°45'E	40	140
Flynn Creek	ca. 10	36°17'N,85°40'W	3.8	360
Kaluga	?100-400	54°30'N, 36°15'E	15	380
Ames	10-50	36°15'N, 98°10'W	15	450-460
Brent	0-25	45°05'N,78°20'W	4	453
Kårdla	25-75	57°00'N,22°42'E	14	455
Lockne	>200	63°00'N,14°48'E	24	455
Tvären	100-150	58°46'N, 17°25'E	2	457
Granby	50-100	58°25'N,14° 56'E	3	465
Hummeln	25-75	57°22'N,16°15'E	1.2	465
<b>Potential Marine Impact Structures</b>				
Toms Canyon	200-500	39°08'N,72°51'W	20-22	?35.5
Tore "Seamount"	deep sea	39°30'N, 13°W	122 (long), 86 (wide)	91
Alamo	deep sea	?37°35'N, 116°W	no crater observed	370
Hamersley	?deep sea	NW Australia	no crater observed	2540

\* for some of age data, precision is less than 10% rel.

Table 1 Marine impact structure data (for geographical presentation see Fig. 1)

related oceanic excavation and shock waves, and subsequent turbulence in the water column. This sediment sequence could be related with a zone of acoustically transparent sediments representing a seismic fingerprint of the Eltanin impact. The geological and seismical structures reported from the Eltanin impact area can be used as a baseline for the identification of other deep ocean impacts. The sediment cores recovered during the first survey of the Eltanin impact area with RV „Polarstern“ (expedition ANT-XII/4) are stored on the AWI-core repository and have been presented during the workshop.

Combined with seismic and sediment core data numeric modeling represents the most important tool to understand complex impact-related processes, such as short-term effects (pressure, velocities, shock waves) in the water column, large scale oceanic phenomena (e.g. tsunami generation and propagation), the effects of shock waves and oceanic processes on the sediment cover and basement, as well as perturbations in atmosphere and environment. Such studies will also help to develop scenarios for the identification and documentation of deep sea impacts. Impact-related tsunamis should cause significant devastations in shore-line areas. This should also account for smaller impactors that would not cause significant disturbances at the deep ocean sea floor. However the identification of tsunami-related deposits is rather problematic because of the lack of accepted definitions of facies models diagnostic for tsunami-related deposits. Also the realistic modelling of impact generated tsunamis and their propagation across the ocean is still under debate.

Impacts into shallow water, epicontinental or passive margin targets have been studied on Paleozoic, Mesozoic and Cenozoic craters located in Baltoscandia, Russia, North America and Australia. This comprises some of the largest terrestrial craters yet known, such as the Chicxulub structure in northern Yucatan (Fig. 1, Tab. 1). Most of these craters are buried beneath a thick post-impact sedimentary cover. Consequently the morphology and geological peculiarities of these structures can only be unveiled by densely spaced geophysical survey arrays and borehole studies. At water depths up to a few tens of meters, the final crater largely resembles impact structures on land targets. If, however, the water depth at the impact site was on the order of a few hundred meters, the crater displays characteristic features such as resurge deposits (e.g., Lockne) and radially arranged resurge gullies. Erosion by resurging can effectively modify and flatten the original crater structure. Resurge deposits can reach a thickness of up to several hundred meters in the crater center. They generally consist of breccias and turbidite-like beds composed of ejecta and material eroded from sedimentary beds in the surroundings of the crater. The formation of gullies depends upon the water depth at the impact site. Therefore, the partial or total destruction of the crater rim represents an independent criterion for the estimation of the paleowater depth at the impact site. Large impacts into shallow-water targets cause vaporization of target rocks in the presence of water. This other specific aspect of marine impacts may lead to significant generation of gases such as  $\text{NH}_3$  and  $\text{H}_2\text{SO}_4$  that could have an impact on the atmosphere chemistry and thus on Earth's climate and life.

Seismic data indicate an enhanced impact-related rock porosity and density of faulting in the marginal zone e.g. of the shallow water Mjølner structure on the Barents Shelf. These features have high potential for hydrocarbon reservoirs highlighting the economic importance of impact structures. Given the interest of the hydrocarbon exploiting industry and the large amounts of proprietary 2D and 3D seismic data, it can be speculated that in the near future a number of still „hidden“ impact structures will be identified at passive margins.

International programs to augment our knowledge on marine impact include a drilling project at Chixculub (Chixculub Scientific Drilling Project, CSDP) within the framework of the International Continental Drilling Program (ICDP), which is currently implemented (<http://icdp.gfz-potsdam.de/html/chixculub/news/news4.html>). Drilling of a 2-3 km deep hole in the crater has been scheduled to begin early next year. A second expedition to the Eltanin impact site with RV „Polarstern“ including seismic and sediment coring surveys is planned for 2001 (contact [rgersonde@awi-bremerhaven.de](mailto:rgersonde@awi-bremerhaven.de)). The results of the cruise should also help to define a proposal for drilling the impact region in the frame of the post-2003 Ocean Drilling Program (ODP). During summer 2000 an expedition with N/O „Atalante“ will examine the origin of the so-called Tore „Seamount“ located 300 km off Portugal, that was proposed to represent a deep ocean impact structure (contact [jfmontei@fc.ul.pt](mailto:jfmontei@fc.ul.pt)).

A special Deep Sea Research issue will be collated in spring 2000 for publication of papers related to oceanic impact features and numerical modelling of associated processes. Hopefully this should help to improve our understanding and exploration of oceanic impacts.

## **Acknowledgements**

The workshop „Oceanic Impacts: Mechanisms and Environmental Perturbations“ has been generously supported by the European Science Foundation (ESF) through the ESF scientific program „Responses of the Earth System to Impact Processes (IMPACT)“. The workshop represented the second in a series of workshops supported by the European Science Foundation (ESF) within the broadly interdisciplinary ESF IMPACT program that was started in 1998. ESF IMPACT is focused on the understanding of the effects of asteroid and comet impacts on the development and evolution of Earth. Further information on IMPACT is available under <http://www.esf.org/lp/IMPACTa.html> and <http://psri.open.ac.uk/esf/>. An IMPACT newsletter can be obtained from the European science Foundation, 1 quai Lezay-Marnésia, F-67080 Strasbourg CEXED, France (contact Mrs. Catherine Lobstein, ESF Administrative Assistant, e-mail: [clobstein@esf.org](mailto:clobstein@esf.org), Tel. +33 (0)3 88 76 71 30, Fax: +33 (0)3 88 37 05 32).

Further support came from the Alfred Wegener Institute for Polar and Marine Research, Bremerhaven, hosting the workshop and the Institute for Planetology at the University Münster.

## Program schedule

Thursday, April 15, 1999

- 12:00-13:30 Registration, Installation of posters  
13:30-14:00 Welcome by AWI representative Prof. Dr. H. Miller and IMPACT-coordinator Prof. Dr. Christian Koeberl, Vienna  
Introduction to workshop themes, program schedule, organization of working groups and general logistics (Dr. Rainer Gersonde, AWI)
- 14:00-14:25 J. Ormö and M. Lindström: Geological characteristics of marine-target craters.

### Session Cretaceous and Paleogene Impacts and related Studies I

(Chair: A. Deutsch)

- 14:25-14:50 J. Smit: Ejecta deposits of the Chicxulub Impact.  
14:50-15:15 B. Kettrup and A. Deutsch: Geochemical investigations of K/T boundary rocks: The Search for precursor lithologies.  
15:15-15:40 F. Martinez-Ruiz, M. Ortega Huertas, and I. Palomo: The Cretaceous-Tertiary event: Impact spherules and geochemical signatures from areas of SE Spain and Site 1049 (ODP Leg 171b)  
15:40-16:05 A. Preisinger, S. Aslanian, H. Summesberger, and H. Stradner: 5 Million Years of Milankovitch Cycles in marine sediments across the K/T Boundary at the Black Sea coast near Bjala, Bulgaria.  
16:05-16:40 Coffee/tea break, Registration, Poster installation

### Session Cretaceous and Paleogene Impacts and related Studies II

(Chair: C. Koeberl)

- 16:40-17:05 C. Wylie Poag, J. B. Plescia and P. C. Molzer: Chesapeake Bay impact structure: Geology and geophysics.  
17:05-17:30 R. Coccioni, D. Basso, H. Brinkhuis, S. Galeotti, S. Gardin, S., Monechi, E. Morettini, M. Renard, S. Spezzaferri, and M. van der Hoeven: Environmental perturbation following a late Eocene impact event: Evidence from the Massignano Section, Italy.  
17:30-17:55 B. Ivanov and B. Milkereit: The present status of Chicxulub impact crater drilling  
17:55-18:10 Registration  
19:00 - Icebreaker Buffet Party

Friday, April 16, 1999

**Session Oral Poster Presentation (audience hall)** (Chair: R. Gersonde)

- 8:30-9:00 3-min. presentations with 1-2 overheads
- P1: J. Koulouris, P. Janle, B. Milkereit, and S. Werner: Significance of large ocean impact craters.
- P2: A.V.Teterev: Underwater cratering at impacts into oceans.
- P3: A.V.Teterev and L.V.Rudak: Atmospheric perturbations and tsunamis caused by an impact of a cosmic body into an ocean.
- P4: K. Wünnemann and M. A. Lange: Numerical modeling of oceanic impact events.
- P5: K. Suuroja, V. Puura, and S. Suuroja: Kärđla Crater (Hiiumaa Island, Estonia) - The result of an impact in a shallow epicontinental sea.
- P6: S.A.Vishnevsky and V. F. Korobkov: Marine impact site Shiyli: Origin of central uplift due to elastic response of target rocks.
- P7: J. Ebbing, P. Janle, J. Koulouris, and B. Milkereit: Palaeotopography of the Chicxulub impact crater and implications for oceanic craters.
- P8: H. Bahlburg and P. Claeys: Tsunami deposit or not: The problem of interpreting the siliciclastic K/T sections in northeastern Mexico.

**Session Deep Ocean Impacts I** (Chair: J. Smit)

- 9:00-9:25 R. Gersonde, F. T. Kyte, A. Abelmann, U. Bleil, B. Diekmann, J.A. Flores, K. Gohl, G. Kuhn, and F. J. Sierro: A late Pliocene asteroid impact into the deep ocean (Bellingshausen Sea) - Its documentation and paleoenvironmental implications.
- 9:25-9:50 F. T. Kyte and R. Gersonde: Meteoritic ejecta deposits from the Late Pliocene impact of the Eltanin Asteroid.
- 9:50-10:15 J.-A. Flores, F.J. Sierro and R. Gersonde: Calcareous plankton stratigraphies from the "Eltanin" Asteroid impact area: Strategies for geological and paleoceanographic reconstruction.
- 10:15-10:45 Coffee/tea break, Poster discussion

**Session Deep Ocean Impacts and Modelling** (Chair: B. Milkereit)

- 10:45-11:10 D. Völker and V. Spieß: The seismic fingerprint of the Eltanin impact.
- 11:10-11:35 B. Ivanov: Comet impacts to the ocean: Numerical analysis of Eltanin scale events.
- 11:35-12:00 B. A. Klumov: Large meteoroid impact into oceanic site: Impact on ozone layer.
- 12:00-12:25 N. Artemieva and V. Shuvalov: Shock zones on the ocean floor - Numerical simulations.

12:30-14:00 Lunch break, Poster discussion (13:15-14:00: Guided tour to Eltanin Impact sediment cores by R. Gersonde and F. Kyte)

**Session Impact modelling and experiments** (Chair: B. Ivanov)

- 14:00-14:25 M. V. Gerasimov, Y. P. Dikov, O. I. Yakovlev and F. Wlotzka: Experimental investigation of the role of water in the impact vaporization chemistry.
- 14:25-14:50 A. P. Jones, G. D. Price, and P. Claeys: A petrological model for oceanic impact melting and the origin of Komatiites.
- 14:50-15:15 P. Agrinier, A. Deutsch, U. Schärer, and I. Martinez: On the kinetics of reaction of CO<sub>2</sub> with hot CaO during impact events: An experimental study.
- 15:15-15:40 J. F. Monteiro, A. Ribeiro and J. Munha: The Tore "Sea-Mount": A possible megaimpact crater in deep ocean.
- 15:40-16:10 Coffee/tea break, Poster discussion
- 16:10-17:30 Plenary discussion on „Eltanin Impact Research“ (Chairs: R. Gersonde, F. Kyte)  
Discussion of further research strategies, modelling of deep ocean impacts and related environmental perturbations (including tour to Eltanin Impact sediment cores)
- 17:30-19:00 Plenary discussion on „Strategies for the discovery of oceanic impacts“ (Chairs: B. Milkereit, V. Spiess, B. Ivanov)
- 19:00 - Buffet Party

**Saturday, April 17, 1999**

**Session Marine Impacts in Northern Europe** (Chair: P. Claeys)

- 8:45-9:10 F. Tsikalas, J. I. Faleide, O. Eldholm, and S. T. Gudlaugsson: Porosity variation, seismic-amplitude anomalies and hydrocarbon potential of the Mjølner impact crater.
- 9:10-9:35 M. Lindström: The present status of the Lockne marine impact structure.
- 9:35-10:00 I. von Dalwigk and J. Ormö: Formation of resurge gullies at impacts at sea: The Lockne Crater, Sweden.
- 10:00-10:25 R. Törnberg: Component analysis of the resurge deposits in the marine Lockne and Tvären impact structures.
- 10:25-10:50 Coffee/tea break, Poster discussion

**Session Marine Impacts** (Chair: M. Lindström)

- 10:50-11:15 L. Ainsaar and M. Semidor: Long-term effect of the Kärda impact crater (Hiiumaa, Estonia) on the middle Ordovician carbonate sedimentation.
- 11:15-11:40 V. L. Masaitis: The Kaluga impact event and its proven and possible geological consequences.
- 11:40-12:05 J.B. Plescia: Mulkarra Impact, South Australia: A complex impact structure.
- 12:05-13:00 Plenary Discussion
- 13.00-14:00 Lunch
- 14:00 End of workshop



## On the Kinetics of Reaction of CO<sub>2</sub> with hot CaO during Impact Events: An Experimental Study

P. Agrinier<sup>1</sup>, A. Deutsch<sup>2</sup>, U. Schärer<sup>3</sup>, and I. Martinez<sup>1</sup>.

1) Laboratoire de Géochimie des Isotopes Stables, IPGP 75252 Paris cedex 05 France (piag@ccr.jussieu.fr); 2) Institut f. Planetologie, Univ. Münster, D-48149 Münster, Germany (deutschca@uni-muenster.de); 3) Laboratoire de Géochronologie, IPGP 75252 Paris cedex 05 France (scharer@ipgp.jussieu.fr).

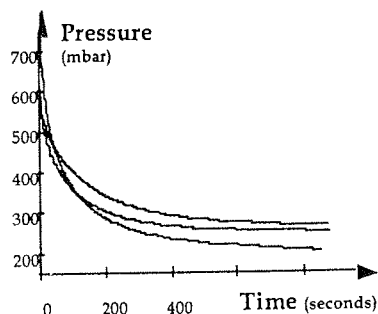
CO<sub>2</sub> losses induced by large impact events on carbonatic sediments are an important process that fundamentally influence the chemical composition of the atmosphere. Such catastrophic volatile release was proposed to be large enough to modify the climate of the Earth, noticeably during the K/T boundary event. In this context, rising concentrations of CO<sub>2</sub> are a widely discussed (O'Keefe and Ahrens, 1989; Pierazzo et al., 1998; Pope et al., 1997; Pierazzo and Melosh, *subm.*). Because the amplitude of the greenhouse effect is directly linked to the amount of CO<sub>2</sub> released, estimating the total amount of impact produced volatiles is of particular importance.

Although carbonates are stable under dynamic compression during passage of the shock-wave, they decompose into CaO + CO<sub>2</sub> during the high temperature regime that persists after pressure drop (Martinez et al., 1995). From ATEM of carbonates in the Haughton impact structure it could be shown that shocked carbonates are composed of relatively undisturbed limestone clasts embedded in a fine grained carbonate-rich matrix. These carbonates partly result from back reaction of CO<sub>2</sub> with CaO (Redeker and Stöffler, 1988; Metzler, 1988; Martinez et al., 1994), suggesting that CO<sub>2</sub> back-reaction at high temperatures plays an important role for the budget of impact released volatiles. This feature is in agreement with thermodynamical data which indicate that CaO very efficiently traps CO<sub>2</sub> at high temperature (< 1100K); therefore, the CaO + CO<sub>2</sub> ⇌ CaCO<sub>3</sub> equilibrium should control CO<sub>2</sub> pressures during post impact processes. A critical parameter for such back reaction is whether or not reaction kinetics are sufficiently fast relative to the over-all duration of the impact process (in maximum a few minutes).

We have investigated the CaO + CO<sub>2</sub> ⇒ CaCO<sub>3</sub> reaction to determine the parameters that rule its kinetics. From a theoretical point of view, evaluations of the reaction rate can be derived from a phenomenological description: as temperatures of the hot CaO + CO<sub>2</sub> mixture decrease, CaO forms small solid grains that react with CO<sub>2</sub> to form CaCO<sub>3</sub> shields on the surface of the CaO grains. In consequence, to form more CaCO<sub>3</sub>, CO<sub>2</sub> must penetrate these CaCO<sub>3</sub> shields to reach reactive CaO and the resistance to CaCO<sub>3</sub> formation consist of the transport of CO<sub>2</sub> through the CaCO<sub>3</sub> shield. Numerical simulations are used to determine the rate of CO<sub>2</sub> back reaction. For CaO grains (r = 1 μm in radius), transport of CO<sub>2</sub> in the CaCO<sub>3</sub> shield (D = 10<sup>-10</sup> cm<sup>2</sup> s<sup>-1</sup>) and an initial CO<sub>2</sub> concentration (C<sub>0</sub> = 3.10<sup>-3</sup> mole cm<sup>-3</sup> ⇌ ≈ 300 bars at 1100K), it would take less than about 10 seconds to trap 50% of the original CO<sub>2</sub> and less than 100 seconds to trap 90% of the initial CO<sub>2</sub>. Such high

theoretical reaction rates suggest that most of the CO<sub>2</sub> could be back-reacted; however, as usual for diffusion controlled processes, the time needed to react a given amount of CO<sub>2</sub> is proportional to DC<sub>0</sub>r<sup>-2</sup>. Doubling r quadruples the reaction time, and doubling D or C<sub>0</sub> reduces it by half. This shows that the size of CaO grains is a particularly critical parameter.

To further investigate these findings, we have performed experiments to explore the kinetic of the CaO + CO<sub>2</sub> => CaCO<sub>3</sub> back-reaction at various temperatures. Calcium carbonate crystals (1 μm) were thermally decomposed to produce CaO and CO<sub>2</sub> under continuous control of the reaction by precise measurement and trapping of the released CO<sub>2</sub>. The obtained CaO was exposed to CO<sub>2</sub> to allow the back-reaction at 970K. The change of the CO<sub>2</sub> pressure versus time was monitored, and results are illustrated below.



The pressure-time plot shows that the CO<sub>2</sub> pressure is reduced to less than half of its initial value in less than 400 seconds indicating that more than 50% of the initial CO<sub>2</sub> has back-reacted. Although the experiments have been conducted at an initial CO<sub>2</sub> pressure (= 1 bar) much lower than typical for large impacts, they confirm that the kinetics of the CaO + CO<sub>2</sub> => CaCO<sub>3</sub> reaction are fast enough to control CO<sub>2</sub> pressures in the impact produced vapor plume.

Ignoring the potential of these back-reactions may lead to large overestimates of impact related CO<sub>2</sub> release into the atmosphere and, hence, the importance of environmental changes by large impacts. Similar kinetic studies are required for the case of impact produced SO<sub>2</sub> liberation from gypsum and anhydrite. The release of large quantities of this gaseous species from the platform sediments at the Chixculub target site have been advocated to explain the K/T boundary crisis (Gullett et al., 1988). In this context it must be emphasized that kinetic studies for coal-based power plants (Chen et al., 1994) show that SO<sub>2</sub> rapidly reacts with hot CaO most likely reducing the total volume release to about the same degree as for CO<sub>2</sub>.

#### References

- Chen, G., Tyburczy, J.A. and Ahrens T. J. (1994) Shock-induced devolatilization of calcium sulfate and implications for K-T extinctions. *EPSL* **128**: 615.
- Gullett B.K. et al. (1988) *Reactivity of solids* **6**: 263.

- Martinez, I. et al. (1994) CO<sub>2</sub> production by impact into carbonates? A SEM-ATEM and stable isotope ( $\delta^{13}\text{C}$ ,  $\delta^{18}\text{O}$ ) study of carbonates from the Haughton impact crater. *EPSL* **121**: 559.
- Martinez, I. et al. (1995) Shock recovery experiments on dolomite and thermodynamical modeling of impact induced decarbonation. *J. Geophys. Res.* **100**:15,465-15,476.
- Metzler, A. (1988) *Meteoritics* **23**: 197.
- O'Keefe J.D. and Ahrens T.J. (1989) Impact production of CO<sub>2</sub> by the Cretaceous/Tertiary extinction bolide and the resultant heating of the Earth. *Nature* **338**: 247.
- Pierazzo, E. and Melosh, H.J. (1999 subm.) Hydrocode modeling of Chicxulub as an oblique impact event. *EPSL*.
- Pierazzo, E., Kring, D.A. and Melosh, H.J. (1998) Hydrocode simulation of the Chicxulub impact event and the production of climatically active gases. *J. Geophys. Res.* **108**: 28,607-28,625
- Pope, K., Baines, K.H. and Ocampo, A.C. (1997) Energy, volatile production, and climatic effects of the Chicxulub Cretaceous/Tertiary impact *J. Geophys. Res.* **102**: 21,645-21,664.
- Redeker H.-J. and Stöffler D. (1988) *Meteoritics* **23**: 185.

### **Long-Term Effect of the Kärdla Impact Crater (Hiiumaa, Estonia) on the Middle Ordovician Carbonate Sedimentation**

L. Ainsaar and M. Semidor

Institute of Geology, University of Tartu, Vanemuise 46, Tartu 51014, Estonia  
(lainsaar@math.ut.ee).

#### Introduction

Kärdla impact crater was formed in Baltoscandian shelf sea in the early Caradoc, at the beginning of the Idavere (=early Haljala) age. The area was characterized by temperate climate open shelf with relatively low-rate carbonate sedimentation. The sea depth is supposed to have been about 20 m (Puura and Suuroja, 1992) or 50-100 m (Lindström, 1995) at the impact moment.

Kärdla crater is covered by Ordovician carbonate sediments with a thickness ranging from 15 to 275 m. The crater rim is composed by three separated basement highs. Top of the buried rim is up to 100 m higher from the base of post-impact sediments outside the crater and 290 m of that in the crater depression at present situation (Puura and Suuroja, 1992). These highs formed islands or shoals in the Middle Ordovician shelf sea and influenced the sedimentation in surrounding, otherwise sedimentary starved area. The existence of these highs in the flat-bottom Ordovician sea and changes in their influence give us an unique opportunity to study the shallow facies distribution as well as sea level history, whereas normal the nearshore area of this sea is purely preserved in the geological record. For this purpose the composition of the post-impact Middle Ordovician (Caradoc) carbonate rocks was studied in

four boring cores drilled between 0.2 km and 7 km east from the crater rim (Fig. 1). The carbonate component of the samples was dissolved in diluted (3.5%) hydrochloric acid and the insoluble residue (i.r.) was fractionated by gravity sedimentation and sieving.

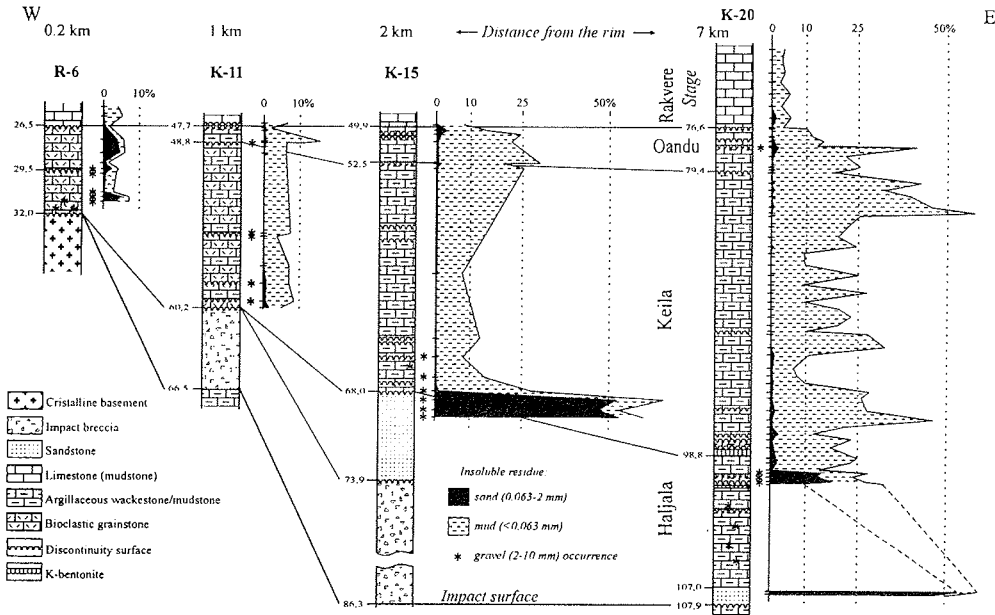


Figure 1 Composition of post-impact carbonate rocks on the eastern slope of the Kärda crater rim.

Composition of post-impact sediments

The post-impact carbonate sedimentary rocks lay in the crater surrounding area directly on the fractured and eroded basement and sedimentary rocks (target surface), on the fall-out breccia layer, or on the redeposited sandy ejecta layer. The sedimentary gap between the impact-related rocks and sedimentary cover is the biggest on the rim, gradually decreasing outside from the rim (Fig. 1; Puura and Suuroja, 1992).

The impact-related sandstone bed is rich of carbonate and terrigenous component of it consists mainly of sand fraction with some gravel fragments (Fig. 1; Kleesment et al., 1987). The upper part of the Haljala Stage, the Keila and Oandu Stage are characterized by argillaceous wackestones/mudstones with numerous discontinuity surfaces in the studied sections. The insoluble residue of these beds consists mainly of clay and silt. High sand content together with gravel occurrences is documented from upper Haljala Stage near the discontinuity surfaces. Slightly elevated sand content (up to 10% from i.r.) is also measured in the limestones from lower part of the Keila Stage and

in the Oandu Stage around the discontinuity surfaces (Fig. 1). The limestone (mudstone) of the Rakvere Stage contains less than 5% of i.r. (clay and fine silt material). The basal part of post-impact beds on the rim is characterized by grainstone containing abundant echinoderm fragments (Puura and Suuroja, 1992) and has possibly Oanduan age. The i.r. of this limestone (3-7% of the rock) is rich in terrigenous sand and gravel fraction in the lower part, and in authigenic sulfides in the upper part in R-6 core section (Fig. 1). Basement fragments of gravel size are found in the Oandu Stage up to 7 km from the rim.

#### Discussion

Non-carbonate material in the post-impact sediments near the crater is derived from four sources: (1) land area on Fennoscandian Shield, (2) fractured Precambrian crystalline rocks on the elevated rim, (3) Cambrian and Lower Ordovician terrigenous rocks near the elevated rim, and (4) diagenetic formation of silicates and sulfides. The Caradocian limestones of North Estonia normally contain only mud-size terrigenous material with minor diagenetic fine-grained minerals (e.g. Põlma, 1982). Presence of sand- and gravel-sized terrigenous material in the studied sections is evidently the result of crater rim influence to sedimentation. The occurrence of this material in particular stratigraphic intervals reflects the intensity of wave action and sea level changes in the area.

According to mineral and grain-size composition the impact-related sandstone in studied sections is similar to Cambrian-Lower Ordovician quartzose sediments and is redeposited from these sandstones (Kleesment et al., 1987). The post-impact carbonate deposition together with limited input of rim material began in the Haljala age in distal areas in and shifted towards the crater rim during the Keila age as a reflection of crater area subsidence. During most of the Caradocian, transport distance of sand material did not exceed 1-3 km from non-deposition area surrounding the rim. Gravel occurrences are related mainly to the discontinuity surfaces of probably subaqual origin in the basal part of post-impact sediments.

The formation of shallow water bioclastic accumulations in Oanduan (or latest Keilan) time on the Kärda rim is contemporaneous with similar processes in the Vasalemma region in North Estonia (e.g. Männil, 1966) and is related to climatic and sea level changes in the basin. The occurrence of terrigenous gravel in the Oandu stage in the distal section supports the opinion about sea-level fall in this period (Ainsaar et al., 1996). A major transgression in the Rakvere age, about 15 million years after the impact, finally covered the crater rims with carbonate mud.

#### References

- Ainsaar, L., Kirsimäe, K. and Meidla, T. (1996) Regression in Caradoc: evidences from southwestern Estonia (Ristik la core). In: *WOGOGOB-94 Symposium. Working Group of Ordovician Geology of Baltoscandia, Bornholm-94*. Stouge, S. (ed.), *Geological Survey of Denmark and Greenland, Report 98*: 5-12.

- Lindström, M. (1995) 6 Ordovician impacts in Fennoscandia. In: *The 22nd Nordic Geological Winter Meeting*, 8-11 January 1996, Turku, Finland, Kohonen, T. and Lindberg, B. (eds). Abstracts:121.
- Kleesment, A.-L., Pirrus, E., Suuroja, K. and Tiirmaa, R. (1987) Geology of the north-eastern outer slope of the mound of the Kärđla buried crater. *Proceedings of the Academy of Sciences of the Estonian SSR. Geology* **36**: 131-139 (in Russian).
- Männil, R. (1966) Evolution of the Baltic Basin during the Ordovician. Valgus, Tallinn: 200 pp. (in Russian).
- Pölma, L. (1982) Comparative lithology of the Ordovician carbonate rocks in the northern and middle East Baltic. Valgus, Tallinn: 164 pp. (in Russian).
- Puura, V. and Suuroja, K. (1992) Ordovician impact crater at Kärđla, Hiiumaa Island, Estonia. *Tectonophysics* **216**: 143-156.

## **Shock Zones on the Ocean Floor - Numerical Simulations**

N. Artemieva and V. Shuvalov

Institute for Dynamics of Geospheres, Moscow, Russia (art@idg.chph.ras.ru).

### Introduction

Shock metamorphism (SM) is a set of physical, chemical and mineralogical changes in the rocks under the shock loading. The indicators of the SM in quartz are well known (Stoffler, 1972), namely, planar features and cracks (under the pressures 5-35 GPa), quartz modification to stishovite (15-40 GPa) or coesite (30-50 GPa) and melting (50-65 GPa). Shock modifications of quartz have been for the first time found in Meteor Crater (Arizona) and it is precisely these elements that proved the impact origin. Thus, detection of shock zones all over the world is an important tool in the detection of ancient impacts (even though the ancient crater itself can not be distinguished after a certain period of time). The most part of the Earth's surface is (and probably was) covered by oceans, therefore a considerable part of cosmic bodies impacted the ground surface passing through water layers of different depth. These layers may attenuate shocks strongly. Because of this, the question arises - what are the impact parameters (impactor size, velocity, material and ocean depth) which cause the shock zone formation on the floor?

Numerical simulations of the meteoroid impacts into the ocean (Ahrens and O'Keefe, 1983; Roddy et al., 1987; Nemtchinov et al., 1994) have been conducted for huge impactors with diameter of 2-10 km and energy  $10^5$ -  $10^8$  Mt. Such events are of great interest from the viewpoint of extinction of terrestrial life and planets' evolution. Undeniably, these impactors reach the ocean floor, form an underwater crater (with SM) and giant waves, but they are rather rare events (just several cases in the course of the Earth's geological history). The impacts of smaller bodies (hundreds meters in diameter) take place in a shorter time interval (around every 10,000 years). But it is not clear yet whether it is possible to find shock zones for the case of the small bodies impacts into the ocean.

Laboratory experiments (Gault and Sonett, 1982) have demonstrated that for the impactor velocity of 5-6 km/s the floor crater doesn't arise if the ratio of the water depth to the transient crater diameter in deep water exceeds 4 and the floor changes are very small if this ratio is more than 0.4. Assuming that the crater diameter is 10-20 times greater than the impactor diameter (Melosh, 1989), one can conclude that only asteroids and comets with diameter exceeding 100-500 m may result in SM on the ocean floor (1-4 km beneath the surface). Nevertheless, the extrapolation of the experimental results to the velocities typical for asteroids ( $V=15-30$  km/s) leads to the mistakes, because the depth of the impactor penetration into the water  $l$  (and, hence, shock wave in the water) strongly depends on the velocity ( $l \sim V^{0.58}$ ).

In this study numerical simulations of the vertical impacts of comets and asteroids with different velocities into the water are conducted to find the range of parameters giving rise to shock metamorphism in the floor material.

#### Self-similarity of the impacts

Hydrodynamic equations descriptive of the impact process are self-similar, i.e. they do not change if we multiply all linear dimensions and time by constant value  $k$ , except of the gravity, which is not essential at the initial stage of the impact and hydrostatic pressure on the floor, which is small (0.04 GPa) in comparison with the shock pressure necessary for SM (minimum 5 GPa). Thus, it is possible to perform the calculations for fixed value of impactor diameter and than to recalculate the critical in SM-sense pressures for all the other diameters (i.e. if the pressure after the impact with impactor diameter  $d$  equals  $P_{sm}$  at the depth  $H$ , then the same value of pressure will be at the depth  $kH$  for impact diameter  $kd$ ).

#### Hydrocode and EOS in use

The SOVA code (Shuvalov et al., 1998), which is similar to the commonly accepted in the US CTH code, is used in this study. The code allows to model multidimensional, multimaterial, large deformation gasdynamics flows with strong discontinuities ( $10^5-10^{10}$  in pressure and density) with a high level of accuracy. Different equations of state (tabular or analytical) are possible. In this study we used the tabular equation of state for atmospheric gas, ANEOS or RUGEOS (Zamyshlyayev and Evterev, 1990) equation of state for granite and ANEOS for water, supplemented by data in the two-phase region from (Rivkin and Aleksandrov, 1975).

#### Results of the modeling

At the first stage the impact into the deep water (without floor) was studied to define pressure in the shock as a function of the depth. Thus, the critical pressures (5-50 GPa) are defined, taking into account that the shock wave is amplified by the reflection from the floor. Estimations with the real Hugoniot curves have shown, that the pressure in the reflected water shock wave (RSW) and granite one, respectively, is twice as large as in the induced shock (ISW) - see table. In reality, the floor of the ocean is covered by sediment material (not pure granite) which is of smaller density. At least, it may be suggested, that the SW in the floor material is of the same pressure amplitude as in the water.

Density, g/cm <sup>3</sup>		Pressure, GPa	
ISW	RSW	ISW	RSW
1.41	1.53	2.3	5.1
1.61	1.79	7.7	14.8
1.88	2.15	22.0	40.0

Numerical simulations of the asteroid impact (density of the impactor 2.65 g/cm<sup>3</sup>) have shown that critical pressures of 5, 15 and 40 GPa were achieved at the depth to the impactor diameter ratios 5, 3.6 and 2.4 for the value of preimpact velocity of 15 km/s and 9.4, 6.6 and 5.2 - for 50 km/s.

At the next stage modeling of the impact into the water of finite depth was performed to take into account the complex flows near the floor and to determine the size of SM affected region. Numerical simulations were performed for comets and asteroids with the velocities of 15-50 km/s and the size to depth ratio ranging from 0.1 to 1.

#### References

- Ahrens, T.J. and O'Keefe, J.D. (1983) Impact of an asteroid or comet in the ocean and extinction of terrestrial life. *JGR* **88A**: 799-806.
- Gault, D.E. and Sonett, Ch.P. (1982) Laboratory simulation of pelagic asteroidal impact: atmospheric injection, benthic topography, and the surface wave radiation field. *Geol. Soc. Amer. Spec.* **190**: 69-92.
- Melosh, H.J. (1989) Impact cratering. A geological process. New York.
- Nemtchinov, I.V., Popov S.P. and Teterev, A.V. (1994) The estimates of characteristics of waves and tsunamis caused by impacts of asteroids and comets in oceans and seas. *Solar System Research.* **28**: 81-99.
- Rivkin, S.L. and Aleksandrov, A.A. (1975) Thermodynamical properties of water and water vapor. *M. Energy.*
- Roddy, D.J., Schuster, S.H. et al. (1987) Computer simulations of large asteroid impacts into oceanic and continental sites. *Int. J. Impact Engng.* **65**: 525-541.
- Shuvalov, V.V., Artemieva, N.A. and Kosarev I.B. (1998) 3D hydrodynamic code SOVA for interfacial flows, application to Shoemaker-Levy 9 Comet impact problem. *Int. J. Imp. Engng* (accepted).
- Stöffler, D. (1972) Deformation and transformation of rock-forming minerals by natural and experimental shock processes. *Fortschritte der Mineralogie* **49**: 50-113.
- Zamyshlyayev, B.V. and Evterev L.S. (1990) Nauka.

## **Tsunami Deposit or not: The Problem of Interpreting the Siliciclastic K/T Sections in Northeastern Mexico**

H. Bahlburg<sup>1</sup> and P. Claeys<sup>2</sup>

1) Geologisch-Paläontologisches Institut, Universität Münster, Correnstraße 24, 48149 Münster (bahlbur@uni-muenster.de); 2) Institut für Mineralogie, Museum für Naturkunde, Invalidenstr. 43, 10115 Berlin (philippe.claeys@rz.hu-berlin.de).

In the Gulf of Mexico region, a one to four m thick, high-energy coarse clastic deposit occurs at the K/T boundary. It has been suggested that the anomalous thickness of the K/T sections from Alabama (USA) to Vera Cruz (Mexico) is due to the proximity of the Chicxulub impact crater (Smit et al., 1996). This sedimentary sequence can be subdivided into three units. The basal unit 1 (or spherule bed) is a coarse, poorly cemented cross-bedded calcarenite. It contains rounded or elongated clay spherules a few mm in size, planktic foraminifera and rip up clasts of the underlying marls. Some rare spherules (<5%) still contain relict impact glass in their center and a few quartz grains present evidence of shock metamorphism. Unit 2 is a coarse parallel- and cross-bedded sandstone texturally and petrographically distinct from unit 1. It contains abundant detrital quartz grains, planktic foraminifera, mixed debris of shallow water benthic organisms, and abundant plant fragments. Paleocurrent measurements at different levels in unit 2 indicate that currents were bi-directional, differing by 180°. Unit 3 consist of a fining-upward sequence of three to five current-ripple layers of fine sand to silt separated by subcentimetric layers of clay enriched in Ir (Smit et al., 1992) and cosmic spinels (Rocchia et al., 1996).

Three sets of mutually exclusive interpretations of these K/T deposits were put forward by different study groups, all of them necessarily ambiguous. (i) The tsunami and seiche model (Bourgeois et al., 1988; Smit et al., 1996) essentially proposes that tsunami waves transport sediment. Usually they do not, as long as the wave does not take up the whole water column, as e.g. in the breaker zone of modern coasts, and maybe in the case of a Chicxulub tsunami at landfall. Bourgeois et al. (1988) conclude that the tsunami had a height of 50-100 m at landfall. This would amount to a run-up height of the tsunami on the shore exceeding the height at landfall at least 1.5 to 2 times. Seiches, in turn, do not transport sediment. (ii) The turbidite model (Bohor, 1996) interprets the rocks under discussion as deposits of a single turbidite depositional event. This is problematic as the inferred Bouma B division, i.e. the upper plane bed depositional phase of a turbidity current, comprising Unit 2 shows alternations of parallel laminations and ripple cross laminations (Bouma C), and erosional surfaces. This implies, unrealistically, that the assumed depositing turbidity current alternated between supercritical and subcritical flow in very short time intervals on an essentially unchanging depositional slope. (iii) The incised valley fill model (Stinnesbeck et al., 1993; Stinnesbeck and Keller, 1997) in turn faces several problems, one of which is the fact that in terms of known exposures across northeastern Mexico only incised valley fills were found but no interchannel areas.

In view of these discrepancies it appears timely to approach the problem along new lines. Published interpretations are based on meticulous but largely descriptive field observations. This is quite understandably so because there is, for example, no accepted facies model allowing the prediction of a sequence of diagnostic depositional features produced by a tsunami. Based on the assumption that the K/T deposits in northeastern Mexico are connected, in a yet unspecified way, to a tsunami caused by the Chicxulub impact, we propose a study in which the propagation of a tsunami across a shelf basin and its eventual landfall are numerically simulated. We anticipate that first order results will be obtained which describe velocity distributions and particle pathways in the propagating Chicxulub tsunami and, in particular, during its buildup at landfall. Once these fundamental problems are elucidated results will be compared to known and inferred tsunami deposits including the K/T rocks in northeastern Mexico.

#### References

- Bohor, B.F. (1996) A sediment gravity flow hypothesis for siliciclastic units at the K/T boundary, northeastern Mexico. *Geol. Soc. Amer. Spec. Pap.* **307**: 183-196
- Bourgeois, J., Hansen, T.A., Wiberg, P.L., and Kauffman, E.G. (1988) A tsunami deposit at the Cretaceous-Tertiary boundary in Texas. *Science* **241**: 567-570.
- Rocchia, R., Robin, E., Froget, L., and Gayraud, J. (1996) Stratigraphic distribution of extraterrestrial markers at the Cretaceous-Tertiary boundary in the Gulf of Mexico area: implications for the temporal complexity of the event. *Geol. Soc. Amer. Spec. Pap.* **307**: 279-286.
- Smit, J., Montanari, A., Swinburne, N.H.M., Alvarez, W., Hildebrand, A.R., Margolis, S.V., Claeys, P., Lowrie, W., and Asaro, F. (1992) Tektite-bearing, deep-water clastic unit at the Cretaceous-Tertiary boundary in northeastern Mexico. *Geology* **20**: 99-103.
- Smit, J., Roep, T.B., Alvarez, W., Montanari, A., Claeys, P., Grajales Nishimura, J.M., and Bermudez, J. (1996) Coarse-grained, clastic sandstone complex at the K/T boundary around the Gulf of Mexico: deposition by tsunami waves induced by the Chicxulub impact? *Geol. Soc. Amer. Spec. Pap.* **307**: 151-182.
- Stinnesbeck, W., Barbarin, J.M., Keller, G., Lopez-Oliva, J.G., Pivnik, D.A., Lyons, J.B., Officer, C.B., Adatte, T., Graup, G., Rocchia, R., and Robin, E. (1993) Deposition of channel deposits near the Cretaceous-tertiary boundary in northeastern Mexico: catastrophic or „normal“ sedimentary deposits? *Geology* **21**: 797-800.
- Stinnesbeck, W., and Keller, G. (1996) K/T boundary coarse-grained siliciclastic deposits in northeastern Mexico and northeastern Brazil: evidence for mega-tsunami or sea-level changes? *Geol. Soc. Amer. Spec. Pap.* **307**: 197-210.

## **Environmental Perturbation Following a Late Eocene Impact Event: Evidence from the Massignano Section, Italy**

R. Coccioni<sup>1</sup>, D. Basso<sup>2</sup>, H. Brinkhuis<sup>3</sup>, S. Galeotti<sup>1</sup>, S. Gardin<sup>4</sup>, S. Monechi<sup>5</sup>, E. Moretini<sup>6</sup>, M. Renard<sup>4</sup>, S. Spezzaferri<sup>7</sup>, and M. van der Hoeven<sup>3</sup>

1) Istituto di Geologia e Centro di Palinologia dell'Università, Campus Scientifico, Località Crocicchia, 61209 Urbino, Italy; 2) University of Milano, Department of Earth Sciences, Via Mangiagalli 34, 20133-Milano, Italy; 3) Laboratory of Palaeobotany and Palynology, Institute of Palaeoclimate and Palaeoenvironment Utrecht, Utrecht University, Budapestlaan 4, 3584 CD Utrecht, The Netherlands; 4) ESA-CNRS 7073 1761 Département de Géologie Sédimentaire, Université Pierre et Marie Curie, 4 Place Jussieu, 75252 Paris, France; 5) Dipartimento di Scienze della Terra, Via La Pira 4, 50121 Firenze, Italy; 6) Dipartimento di Scienze della Terra, Piazza Università, 06100 Perugia, Italy; 7) Geology Institute, ETH-Zentrum, Sonneggstrasse 5, 8092 Zurich, Switzerland

The late Eocene is characterised by an intriguing concentration of extraterrestrial body impact evidence with the two largest known impact craters of the Cenozoic Era occurring almost synchronously at about 35.6 Ma (Koeberl et al., 1996; Bottomley et al., 1997). These two major events were accompanied by other minors impacts during this time-interval (Montanari et al., 1998). <sup>3</sup>He-based evidence indicate that these multiple impacts are part of a comet shower which, in many cases, produced impact debris (see Farley et al., 1998).

Cosmic signatures together with evidence of several volcanic events, are recorded in the 23 m-thick Massignano Section (Central Italy), the Global Stratotype Section and Point for the Eocene-Oligocene boundary (Fig. 1). Two Ir-rich layers occur at 5.65 m and 10.25 m and they are associated with major spikes of extraterrestrial <sup>3</sup>He. The Ir-rich horizon at 5.65 m also contains shocked quartz and Ni-rich spinels. It is interpreted as an impact layer dated as old as 35.7±0.4 Ma, probably related to the Popigai event (Montanari et al., 1993; Clymer et al., 1996). Therefore, the Massignano outcrop provides a unique opportunity to explore whether the late Eocene impact(s) had any effect on the biosphere. With this goal, a high resolution, multidisciplinary analysis based on dinoflagellate cysts (dinocysts), calcareous nannofossils, foraminifera, and geochemistry (stable isotopes and trace elements) has been carried out between 4 m and 8 m above the base of the Massignano section.

Microfossil-based SST curves provide evidence for a gradual cooling throughout the studied interval. By contrast  $\delta^{18}\text{O}$  curve indicates a slight warming. The high degree of covariance between  $\delta^{18}\text{O}$  and  $\delta^{13}\text{C}$ , however, suggests that the oxygen isotope record at Massignano is diagenetically corrupted as already pointed out by Vonhof et al. (1998). The overall cooling is accompanied by a trend towards a slight decline of pelagic productivity as indicated by planktic foraminiferal and  $\delta^{13}\text{C}$  records. On the other hand, calcareous nannofossil fertility proxies show rather stable average values whereas the bloom of *T. pelagica* which occurs in the first 50 cm above the impact layer might indicate increased eutrophication. We speculate that temperature and surface water conditions played a major role in controlling

the distribution of nannofossil. However, the trophic structure influenced, although partially, the distributions of some nannofossil (e.g. *Discoaster* spp.) and dinoflagellate groups.

In this framework of gradual cooling and surface water structure re-organization, a significant break in both  $\delta^{13}\text{C}$  and planktic foraminiferal records occurs at 6.1 m and allows the distinction of two discrete intervals characterized by peculiar average values of several parameters. The 6.1-8 m interval is characterized by a) lower temperature and pelagic productivity, and higher dissolved oxygen content of surface waters; b) increased abundance of deep and/or cooler and intermediate water planktic foraminifera, and thus, possibly, a shallower thermocline; c) lower dissolved oxygen content on the sea floor; d) higher average concentration of Fe and Mn. In addition, larger fluctuations of several parameters testify a less stable environment. Prior to the break recognized at 6.1 m, the sea floor experienced a gradual decrease of oxygenation as indicated by benthic foraminifera in correspondence to the transition from reddish to greenish-gray sediments. At this level reduced oxygenation led to better preservation of dinoflagellates giving good palynological record for the first time at the impact layer. The bloom of *T. pelagica* which would suggest increased eutrophication just above the impact layer might also result from better preservation.

More significant changes in both geochemical and biotic records seem to coincide with volcanoclastic layers. However, not all proxies show this consistent pattern. The calcareous nannofossil record possibly indicate increased oligotrophy during deposition of these layers. In correspondence to the volcanoclastic layers the relative abundance of agglutinating foraminifera always increases probably in consequence of lowered pH of bottom waters due to the onset of volcano-derived material on the sea floor. Changes across volcanoclastic layers may be explained in terms of local effects, possibly related to reduced light penetration, and/or chemical changes in the water mass invoking large but short-duration environmental response. According to the estimated sedimentation rate of 0.65 cm/ka, the cyclical distribution of volcanoclastic layers seems to have a periodicity of about 100 ka. It is, therefore, surprisingly compatible with the short eccentricity cycles of Earth orbit. It is obviously hard to distinguish between coincidence and causal link(s) merely based on our data and we feel that any conclusion as regards this aspect would be speculative.

Perhaps surprisingly, no drastic changes of both biological and geochemical records occur in correspondence to the impact layer. The manifold and, to some extent, controversial signal recorded by biotic and geochemical proxies can be better regarded as the response to an extremely complex and dynamic scenario influenced by global cooling and volcanic activity. However, the possibility that impact related processes might have emphasized the Late Eocene global cooling through a series of positive feedback mechanisms unravelling ~70 ka after the impact, cannot be ruled out. In fact, the Massignano Ir-rich layer seems to be coeval with the impactoclastic layer of ODP Site 689B which is followed by a rapid cooling of surface waters (Vonhof et al., 1998).

A multivariate statistical treatment of quantitative data of planktonic foraminifera and calcareous nannofossils also indicates that an environmental break took place after the impact leading to accelerated pulses of climatic deterioration.

The lack of a sudden environmental response to an extraterrestrial body(ies) impact might depend on several factors such as the small size of the impactor(s), the latitude of the impact site and its nature including marine vs. continental and type of target rock. A major role, moreover, might have been played by pre-impact environmental conditions which, in the late Eocene, were certainly further than, for instance, pre-Cretaceous-Tertiary boundary ones to threshold limits.

#### References

- Bottomley, R., Grieve, R., York, D., and Masaitis, V. (1997) The age of the Popigai impact event and its relation to events at the Eocene/Oligocene boundary. *Nature* **388**: 365-368.
- Clymer, A.K., Bice, D.M., and Montanari, A. (1996) Shocked quartz from the late Eocene: Impact evidence from Massignano, Italy. *Geology* **24**: 483-486.
- Farley, K.A., Montanari, A., Shoemaker, E.M., and Shoemaker, C.S. (1998) Geochemical Evidence for a Comet Shower in the Late Eocene. *Science* **280**:1250-1253.
- Koeberl, C., Poag, C.W., Reimold, W.H., and Brandt, D. (1996) Impact Origin of the Chesapeake Bay Structure and the Source of the North American Tektites. *Science* **271**:1263-1266.
- Montanari, A., Asaro, F., Michel, H.V., and Kennett, J.P. (1993) Iridium anomalies of late Eocene age at Massignano (Italy), and ODP Site 689B (Maud Rise, Antarctic). *Palaios* **8**: 420-437.
- Montanari, A., Campo Bagatin, A., Montanari, A., and Farinella, P. (1998) Earth cratering record and impact energy flux in the last 150 Ma. *Planetary and Space Science* **46**: 271-281.
- Vonhof, H.B., Smit, J., Brinkhuis, H., and Montanari, A. (1998) Late Eocene Impacts accelerated global cooling? In: *The Strontium Stratigraphic Record of Selected Geologic Events*, H.B. Vonhof (PhD Thesis), Academisch Proefschrift, University of Utrecht, p.77-90.

## **Formation of Resurge Gullies at Impacts at Sea: The Lockne Crater, Sweden**

I. von Dalwigk and J. Ormö.

Department of Geology and Geochemistry, Stockholm University, S-10691 Stockholm, Sweden  
(ilka@geo.su.se).

The surface of the Earth is constantly the target of extraterrestrial bombardment. Meteorite impacts on Earth take place on continents, as well as in shallow and deep seas. Water covers 70% of the Earth's surface; nevertheless, impact crater studies had for a long time to concentrate on craters formed on continents. However, recent studies show that marine-target craters differ in several aspects from craters formed on land. One of the important lithological differences is the abundant resurge deposits in craters where the water depth of the impact site was sufficient to overcome any rim wall formed. At some of the impact structures where resurge sediments occur within the crater, it has been suggested that the resurge has eroded deep, radial gullies through the rim e.g. at the Lockne (Lindström et al., 1996), Kärddla (Puura and Suuroja, 1992), and Kamensk craters (Movshovich and Milyavsky, 1990).

Four such gullies, each of them transecting radially through the rim of the inner crater, are identified at the Lockne crater.

The Lockne crater (63°00'20"N, 14°49'30"E) is a marine-target crater, formed in a shelf sea, approximately 460.4 Ma years ago (Grahn, 1997). The crater structure consists of a 12 km wide inner crater surrounded by an outer, inclined surface that extends to almost 12 km from the centre of the crater (Sturkell, 1998).

The aim of this study is to investigate the mechanisms behind the formation of the radial gullies. The many well-exposed outcrops in these gullies allow us to reconstruct the process of their formation.

The part of the crater cavity that formed in the seawater almost instantly collapsed and the seawater forcefully flooded the crater. The dense, ejecta loaded flow dragged along the largest ejecta clasts and parts of the underlying shattered sedimentary strata. The fragments may be up to tens of meters in diameter. The entrained material disintegrated during transport and constitutes today the dominantly monomictic lower part of the resurge sequence. The very high sediment load of the resurging water increased the density and the viscosity of the flow, thereby also increasing its erosive power. The flow eroded the outer crater, cut down at zones of weakness and became in this way concentrated to certain points, which further increased the erosional force. The erosion in the gullies proceeded as headward erosion down to the transition zone between the brecciated and the less disintegrated crystalline basement. The size of the resurge gullies at Lockne ranges from 100 to 1000 metres across, 20 to 100 metres in depth and 0.5 to 3 km in length. Their floor

is covered with resurge deposits that are partially overlain by sedimentary rocks deposited when the normal sedimentation continued.

However, gully formation appears to be dependent upon the water depth at the site of the impact. On these criteria Ormö and Lindström (pers. comm.) identify Lockne as a crater formed in a deep shelf environment. At shallow water depths the water can not break through the rim wall of the crater. For impacts at a greater water depth the formation of resurge gullies is more accentuated and the destruction of the crater rim more complete than for impacts in relative shallow water, e.g. Kärda.

#### References

- Grahn, Y. (1997) Chitinozoan biostratigraphy of the early Caradocian Lockne impact structure, Jämtland, Sweden. *Meteoritics and Planetary Science* **32**: No.6: 745-751.
- Lindström, M., Sturkell, E.F.F., Törnberg, R. and Ormö, J. (1996) The marine impact crater at Lockne, central Sweden. *GFF* **118**: 193-206.
- Movshovich, E.V. and Milyavsky, A.E. (1990) Morphology and inner structure of Kamensk and Gusev astroblemes. In: *Impact craters of the Mesozoic-Cenozoic boundary*, Masaitis, V.L. (ed.) pp. 110-146 (Nauka, Leningrad).
- Puura, V. and Suuroja, K. (1992) Ordovician impact crater at Kärda, Hiiumaa Island, Estonia. *Tectonophysics* **216**: 143-156.
- Quaide, W.L. and Oberbeck, V.R. (1968) Thickness determinations of the lunar surface layer from lunar impact craters. *J. Geophys. Res.* **73**: 5247-5270.
- Sturkell, E.F.F. (1998) Resurge morphology of the marine Lockne impact crater, Jämtland, central Sweden. *Geological Magazine* **135**: 121-127.

## **Palaeotopography of the Chicxulub Impact Crater and Implications for Oceanic Craters**

J. Ebbing, P. Janle, J. Koulouris, and B. Milkereit.

Institut für Geowissenschaften der Christian-Albrechts-Universität, Kiel, Otto-Hahn-Platz 1, 24118 Kiel, Germany.

The Chicxulub impact structure in Mexico is buried beneath a 300-1000m thick sedimentary cover of tertiary age. It is the only crater of three of this size with a suspected intact topography. The impact took place in a shallow marine environment. The other two craters, Vredefort in South Africa and Sudbury in Canada, exhibit erosion levels of a few km at the surface. The palaeotopography of Chicxulub will be reconstructed from seismic profile data, and implications for oceanic craters will be discussed in this investigation. As large impact craters with intact topographies at the surface are only available at extraterrestrial planetary surfaces, the complex crater Keeler on the Moon with a diameter of 169 km will be used here for comparison. Keeler shows a

complex terracing, interpreted as slumped blocks in the last phase of the impact and early post impact history, and a central uplift.

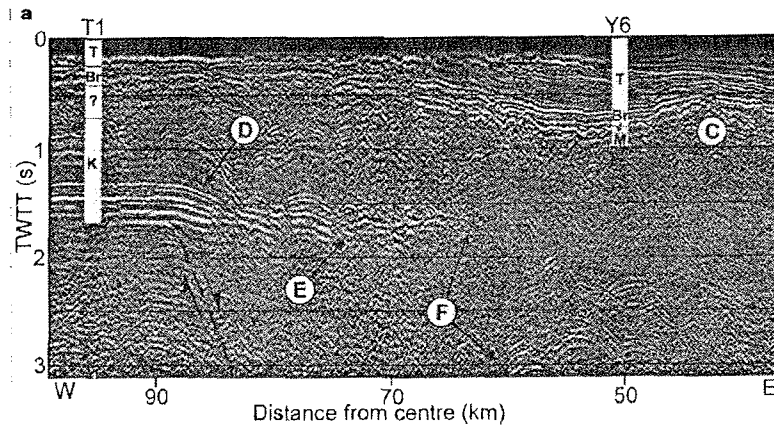


Figure 1: Seismic reflection data along part of Chicx-A profile. The stratigraphy in wells Ticul (T1) and Yucatan (Y6) has been projected on to the section. The undulation of the K/T-boundary is clearly seen. Further the tertiary infill thickens towards the crater center (Morgan et al., 1997).

The investigation of the palaeotopography of the Chicxulub crater is based on the seismic data collected across the offshore portion of the structure (Morgan et al., 1997). Figure 1 shows one example of the seismic profiles. The thickening of the tertiary infill respectively the crater depression is clearly seen. Further, the K/T-boundary shows undulations in the crater area. Around 60 km distance from the crater center deeper reflections reveal a disturbance, which is interpreted as a slumped block. Morgan et al. (1997) postulated that in the central crater area the tertiary layer is flat with no disturbances. Two of the profiles are radial to the centre of the crater; the other two profiles cross the northern offshore part parallel to the coast. The tertiary thicknesses are given in TWT which are converted to km with an average velocity of 2000 m/s for the infill. In the next step the thicknesses have been extrapolated between the profiles assuming a circular structure centered at Chicxulub Puerto. Undulations of the K/T-boundary in the profiles are particularly weighted for the extrapolation. The reconstructed palaeotopography has been controlled with borehole data of Lopez Ramos (1975). The correlation was in general quite good; only for the outer crater areas on the landsite the tertiary layer was thinner than in our model extrapolation.

The reconstructed palaeotopography (Fig. 2) shows in the outer part from West to East a depression followed by a topographic high adjacent to a second depression. Only the eastern part shows another broad interior ring next to another depression. This sequence can be interpreted as terracing respectively slumped blocks. The central area shows diffuse highs and lows of the palaeotopography. Based on the available data it cannot be decided whether this is representative for a central uplift or a peak ring.

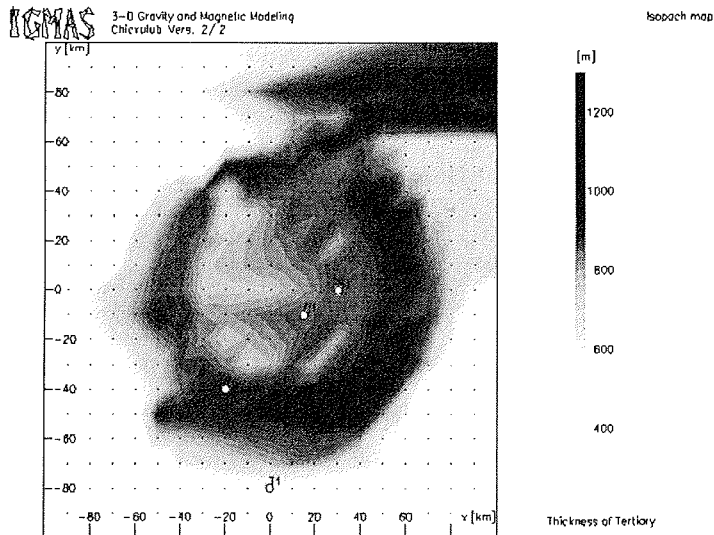


Figure 2: The reconstructed palaeotopography of the Chicxulub impact structure shows the thickness of the tertiary infill. Compared to the lunar crater Keeler the palaeotopography of Chicxulub has a rather destroyed and smoothed appearance. C1, S1, T1 and Y6 are drilling sites.

Compared to the lunar Keeler crater the palaeotopography of Chicxulub has a rather smooth appearance. This can be explained by strong erosional processes due to high-energy water wave action (backwash effects) in the late impact phase or just after the impact (Morgan et al., 1997).

The 3D gravity contribution of the tertiary infill has been calculated assuming a density difference of  $\approx 0.3 \text{ g/cm}^3$  between the infill and the Cretaceous. In general, there is no correlation between this contribution and the Bouguer anomalies. This confirms the interpretation of the smoothed K/T-topography above. Thus the sources of the Bouguer anomalies should be located in deeper levels. This is in agreement with the circular shaped Bouguer anomalies of Vredefort, reflecting density contrasts of the deeper structure of the crater.

The implications for oceanic impact craters are discussed now. Due to backwash effects the concise terracing and central uplift as seen at Keeler crater will be smoothed in the case of marine impact craters. Thus side scan sonar images should deliver only smooth circular structures in the case of young impact craters. In general the palaeotopography is not expected to be a suitable signature of larger marine impacts.

#### References

Lopez Ramos, E. (1975) Geologic Summary of the Yucatan peninsula. In: Nairn, A.E.M., Stehli, F.G. (eds.) The ocean basins and margins, Volume

3, The Gulf of Mexico and the Caribbean. *Plenum Press*, New York: 257-282.

Morgan, J., Warner, M. and the Chicxulub Working Group, Brittan, J., Buffler, R., Camargo, A., Christeson, G., Denton, P., Hildebrand, A., Hobbs, R., Macintyre, H., Mackenzie, G., Maguire, P., Marin, L., Nakamura, Y., Pilkington, M., Sharpton, V., Snyder, D., Suarez, G. and Trejo, A. (1997) Size and morphology of the Chicxulub impact crater. *Nature* **390**: 472-476.

## **The Methods of Shock Pressure Estimation in Impacted Rocks.**

V. Feldman and S. Kotelnikov.

Moscow State University, Geological Faculty, Petrology Chair, Vorob'evy Gory, Moscow, Russia (feldman@geol.msu.ru).

The estimation of shock pressure, which acted upon investigated rocks, is the very important stage of study of impact craters and meteorites. This pressure is calculated frequently with help of investigation of general alterations of main minerals, such as the appearance of planar deformations, kink-bands, isotropisation, shock decomposition etc. Such methods allow to get only a probable pressure range. More precise estimations can be made using pressure dependence of any mineral characteristics. Perspective minerals for shock geobarometry are quartz and feldspars, some of their characteristics (the density, the index of refraction, the lattice parameters and others) are regularly changed by shock. The appearance of different orientations of planar elements as a result of pressure increase is used successfully for shock estimations. However, this method can be employed only up to 30 GPa (quartz is turned into diaplectic glass at higher pressures). As for feldspars, the properties alterations by shock depend on the composition in considerable extent.

Therefore very important problem is the investigation of mafic minerals, which are stable to impact influence, besides they compose of main part in shocked meteorites and oceanic rocks. The study of olivine and pyroxene shows that the lattice parameters, chemical composition, the index of refraction are not changed by shock significantly. Our investigation of experimentally and naturally deformed clinopyroxene detected the increase of the number of planar deformations with rare indexes and the decrease of angle of optical under shock. However, these effects can be caused by some reasons and cannot be estimated precisely enough. Our recent investigations show that most convenient effect for geobarometry constructions is clinopyroxene X-ray maxima broadening. The reasons of this broadening are the decrease of coherent dispersion blocks and planar deformation. However, in our case the division of these effects is impossible and we can only calculate the value of

the peak broadening. It is likely that this effect does not depend from clinopyroxene composition (it is the same for experimentally deformed diopside and augite). The identical character of the broadening alteration was observed for minerals shocked in nature and in experiments. Besides it is very important that all powder diffractogram data give the total information about properties of very many crystals in investigated sample (in contrast to planar deformations study, for instance).

Then the clinopyroxene X-ray maxima broadening is very perspective effect for shock geobarometer construction. We suppose that the same results can be obtained for the other minerals, which are stable to shock compression, such as enstatite and olivine.

#### References

- Dodd, R.T. and Jarosewich, E. (1979) Incipient melting in and shock classification of L-group chondrites. *Earth Planet. Sci. Lett* **44**: 335-340.
- Feldman, V.I. (1994) The conditions of shock metamorphism. In: *Large meteorite impacts and Planetary Evolution*, Boulder, Colorado, : Dressler B.O., Grieve R.A.F., Sharpton V.L. (eds), *Geological Society of America Special. Paper* **293**.
- Kotelnikov, S.I., Feldman, V.I. and Juk, A.Z. (1996) The comparison of shock effects in naturally and experimentally deformed clinopyroxene. **27th Lun. and Plan. Sci. Conf.** 693-694.
- Rusakov, A.A. (1977) X-ray study of metals. Moscow, in Russian.
- Stöffler, D. (1972) Deformation and transformation of rock-forming minerals by natural and experimental shock process. 1. Behaviour of minerals under shock compression. *Fortschr. Mineral.* **49**, **1**: 50-113.
- Stöffler, D. (1974) Deformation and transformation of rock-forming minerals by natural and experimental shock process. 2. Physical properties of shocked minerals. *Fortschr. Mineral.*, **51**, **2**: 256-289.
- Stöffler, D. (1971) Progressive metamorphism and classification of shocked and brecciated crystalline rocks at impact craters. *J. Geophys. Res.* **76**, **23**: 5541-5551.

### **Calcareous Plankton Stratigraphies from the "Eltanin" Asteroid Impact Area: Strategies for Geological and Paleoceanographic Reconstruction**

J.-A. Flores<sup>1</sup>, F.J. Sierro<sup>1</sup>, and R. Gersonde<sup>2</sup>.

1) Department of Geology, University of Salamanca, S-37008 Salamanca, Spain (flores@gugu.usal.es), 2) Alfred-Wegener-Institute for Polar and Marine Research, Postbox 120161, D-27515 Bremerhaven, Germany

In this study calcareous nannofossils and planktic foraminifera are analyzed in late Pliocene-Pleistocene cores along the impact area of the Eltanin Asteroid in the Bellinghausen Sea (Gersonde et al., 1997). Conventional qualitative and

quantitative analyses were carried out in RV“Polarstern“ cores PS2708-1, PS2709-1, PS2704-1 and USNS“Eltanin“ Core E13-4. The calcareous plankton analyses focused in three different aspects:

1) Biostratigraphy (and biochronology) from the autochthonous sediments above and below the impact event. Plio-Pleistocene events identified in stratigraphy unit (SU) I allow us to correlate the palomagnetic signal with the magnetostratigraphic scale, supporting stratigraphies carried out by other micropaleontological groups. The identification of Chron C2n, as well as several hiatuses was crucial. In the same sense, calcareous nannofossils and planktic foraminifera were used to unambiguously date the middle Eocene autochthonous SU V.

2) Evaluation of reworking and sediment mixture inside the sedimentary units. The relationship between autochthonous (Plio-Pleistocene) vs. reworked (Paleogene) microfossils between SU I (autochthonous ) and SU II and SU III (resuspended bottom and ejecta sediments) is used as additional data to interpret the sediment origin and degree of mixture. Standard stratigraphies were also used to date blocks and sediment fragments in the chaotic SU in order to understand the sediment disturbance induced by the impact. The record and identification of carbonated units characterized by well preserved calcareous nannofossils and planktic foraminifera below the is useful to reconstruct sedimentary processes.

3) (Paleo)Ecological behaviour and evolution of coccolithophores and planktic foraminifera. Calcareous plankton give information about different oceanic parameters (e.g. water temperature, productivity) and its evolution after impact. Regarding this aspect, no significant change in assemblages was observed at ca. 2.15 Ma for comparison with other areas.

#### References

Gersonde, R., Kyte, F.T., Bleil, U., Diekmann, B., Flores, J.A., Gohl, K., Grahl, G., Hagen, R., Kuhn, K., Sierro, F.J., Völker, D., Abelmann, A. and Bostwick, J.A. (1997) Geological record and reconstruction of the late Pliocene impact of the Eltanin asteroid in the Southern Ocean. *Nature* **390**:357-363.

## Experimental Investigation of the Role of Water in the Impact Vaporization Chemistry.

M.V.Gerasimov<sup>1</sup>, Yu.P.Dikov<sup>2</sup>, O.I.Yakovlev<sup>3</sup>, and F.Wlotzka<sup>4</sup>.

1) Space Research Inst., Profsoyuznaya st., 84/32, Moscow, 117810, (mgerasim@mx.iki.rssi.ru); 2) Inst. of Ore Deposits, Petrography, Mineralogy and Analytical Chem., Staromonetny per., 35, Moscow, 109017; 3) Vernadsky Inst. of Geochem. and Analytical Chem., Kosygina st., 19, Moscow, 117975; 4) Max-Planck-Inst. für Chemie, Mainz, F.R.Germany, (wlotzka@mpch-mainz.mpg.de).

The investigation of oceanic impacts is important for the understanding of the Earth's evolution since the probability of such impacts is higher than of impacts into continents. The possibility of the early origin of the ocean due to impact-induced degassing also imply that at the late stage of accretion large masses of water could be involved in impacts and could play a certain role in the processing of the silicate material. The role of water vapor in the chemistry of impacting material is not yet clear.

Our experimental approach included small scale impacts using light-gas-gun (LGG) facility and simulation of impact vaporization by use of laser pulse (LP) technique (Gerasimov et al., 1999). In our experiments we used a wide range of targets including different silicate types from ultramafic to acidic and different salts modeling some specific sediments (e.g. gypsum, anhydrite and calcite for Chixculub case). Water was included in the system whether by its presence in the structure of target samples (e.g. serpentine) or by performance of experiments in a wet atmosphere. The role of water was discriminated by comparison of wet and dry experimental runs.

LGG and LP experiments on high-temperature vaporization of mafic and ultramafic rocks and minerals have shown that condensing silicates provide intense formation of hydroxides with mainly all rock forming elements (except Ca) by counteraction with water vapor at the hot stage of expansion of a vapor cloud (Gerasimov et al., 1994a; Yakovlev et al., 1995). The amount of water in forming hydrated silicates could be about 10 wt.%. Investigation of condensed material by X-ray photoelectron spectroscopy (XPS) technique shows that formation of hydroxides was accompanied by a noticeable change of the redox potential of the silicates. Forming silicates at dry conditions had some portion of elements in reduced state but no reduced state of elements was observed during experiments at wet conditions.

The chemistry of other volatile elements was also changed at wet conditions compared to dry conditions. Experiments in CO<sub>2</sub> wet and dry atmospheres indicated that the presence of water in the system increases the reduction of carbon and provides higher production of elemental carbon and of rather complex organics. Experiments in N<sub>2</sub> wet and dry atmospheres indicated that the presence of water vapor provided the formation of N-H bonds which are probably could be related to the formation of NH<sub>3</sub> gas molecules or to the formation of -NH<sub>2</sub> groups in organics (Gerasimov, 1999). Experiments with

gypsum have a strong indication that counteraction of water vapor and sulfur can result in the formation of sulphuric acid ( $H_2SO_4$ ) (Gerasimov et al., 1994b).

Based on experimental results, the role of water in impact chemistry is not negligible. The involving of water changes the chemical processing of rock forming elements and of other volatiles as well and result in the change of redox behavior of the system, in the ingassing of water into the rocks, in the formation of hydrogen containing components such as hydrocarbons, amino groups and other. The formation of such gases as  $NH_3$ ,  $H_2SO_4$  could have a sufficient impact on the stability of the atmosphere.

#### References

- Gerasimov, M.V., Dikov, Y.P., Yakovlev, O.I. and Wlotzka, F. (1994a) Water-vapor trapping from the atmosphere by condensed silicate material produced during pulsed evaporation, *Geochemistry International* **31**: 135-146.
- Gerasimov, M.V., Dikov, Y.P., Yakovlev, O.I. and Wlotzka, F. (1994b) High-temperature vaporization of gypsum and anhydrite: experimental results, In: *Lunar and Planetary Science XXV*, Lunar and Planet. Inst. (Abstracts), Houston, Texas, pp. 413-414.
- Gerasimov, M.V. (1999) Physics and chemistry of impacts. In: *Laboratory Astrophysics and Space Research*, P. Ehrenfreund, K. Krafft, H. Kochan, V. Pirronello, (eds.), *Astrophysics and Space Science Library* **236**, Kluwer Academic Publishers, Dordrecht, p. 279-330.
- Gerasimov, M.V., Dikov, Y.P., Yakovlev, O.I. and Wlotzka, F. (1999) Nitrogen impact-induced outgassing and ingassing during the Earth's accretion stage. In: *Lunar and Planetary Science XXX*, Abstract 1593, Houston (CD-ROM).
- Yakovlev, O.I., Dikov, Y.P. and Gerasimov, M.V. (1995) Experimental study of shock and pulse evaporation of ultrabasite, *Geokhimiya* No **8**: 1235-1248 (in Russian).

## **A Late Pliocene Asteroid Impact into the Deep Ocean (Bellingshausen Sea) - Its Documentation and Paleoenvironmental Implications.**

R. Gersonde<sup>1</sup>, F. T. Kyte<sup>2</sup>, A. Abelmann<sup>1</sup>, U. Bleil<sup>3</sup>, B. Diekmann<sup>1</sup>, J.A. Flores<sup>4</sup>, K. Gohl<sup>1</sup>, G. Kuhn<sup>1</sup>, and F. J. Sierro<sup>4</sup>.

1) Alfred-Wegener-Institute for Polar and Marine Research, Postbox 120161, D-27515 Bremerhaven, Germany (rgersonde@awi-bremerhaven.de); 2) Institute of Geophysics and Planetary Physics, UCLA, Los Angeles, 90095, USA; 3) Fachbereich 5, Geowissenschaften, University Bremen, Postbox 330440, D-28334 Bremen; 4) Department of Geology, University of Salamanca, S-37008 Salamanca, Spain.

Of the ca. 150 impact structures known on our planet the impact of the Eltanin asteroid is yet the only known affecting a deep ocean basin. The impact was discovered in 1981 in sediment cores already recovered in the mid sixties during USNS Eltanin expeditions to the Bellingshausen Sea (eastern Pacific sector of the Southern Ocean) based on iridium measurements (Kyte et al., 1981). The Ir was contained in mm-sized, vesicular impact melt that formed by shock-melting of the asteroid during the impact (Kyte and Brownlee, 1985). Several mm-sized unmelted meteorite fragments were also identified and named the Eltanin meteorite, an anomalous mesosiderite. However, a comprehensive documentation of the imprint of the Eltanin impact event was only possible after revisiting the impact area during expedition ANT-XII/4 with RV Polarstern (spring 1995). Bathymetric and seismic survey combined with sediment coring now allows the delineation of the disturbances of the deep sea sedimentary record caused by the impact, the development of an impact scenario, and an accurate age determination of the impact (Gersonde et al., 1997).

The impact, the related vapour explosion, and the subsequently generated giant waves removed an Eocene - late Pliocene sediment sequence and disturbed the sediments over a distance of several hundred of kilometers. The created deposit consisting of stirred up sediments forms a seismically transparent layer which has an average thickness of 20-40 m, the Eltanin-Polarstern Transparent Zone (EPTZ). In the vicinity of a seamount structure (San Martin Seamounts), which is located in the impact area reaching a water depths of 2500 m, the disturbed sediments are covered by a several dcm-thick, laminated, well sorted, and upward graded interval, representing carbonate turbidites originating from the top of the seamounts. This is followed by a distinct depositional episode, recording fallout out of meteoritic and sedimentary debris ejected by the vapour explosion into the high atmosphere. The meteorite debris ranges up to 1.5 cm in size. The fallout layer is topped by upward graded, fine-grained sediment material that apparently deposited at high sedimentation rates from a sediment cloud in the 5 km water column.

Data on the concentrations of impact debris and iridium and the apparent distribution and volume of disturbed sediments indicate that the minimum size of the impactor was 1 km. At typical asteroidal velocities (20 km/s) kinetic

energy is 100 GT of TNT, approaching a size with potential for global environmental consequences. The impact-generated mega-tsunamis would reach the South American and the Antarctic continent at a height of up to tens of meters over deep water, reaching runup heights on the continental margins 10-25 times higher. This would cause major devastation in the shelf and coastal areas. Anomalous geological deposits recorded from the Antarctic continent, New Zealand and the Peruvian coast could be related. Large volumes of meteorite and sediment fragments, dust and vapour would be ejected in the high atmosphere and lead to climate deteriorations. Biostratigraphic and paleomagnetic dating place the impact in a time period immediately below the magnetostratigraphic Reunion-event (C2r.1n) in the lower Matuyama Chron, dated to 2.15 - 2.14 Ma. It thus is close to marine isotope stage 82, which represents a major cooling event after the establishment of northern hemisphere ice sheets. At that time interval distinct changes in sedimentary facies indicate a reorganisation of water mass circulation in the Southern Ocean.

The impact and the related ejection of debris into the high atmosphere represents a most likely mechanism to resolve the enigma about the occurrence of Cenozoic marine microfossils in the Transantarctic Sirius Group, interpreted to indicate significant instabilities of the East Antarctic Ice Sheet (EAIS) (Harwood, 1983). A special controversy rised about the presence of a significant mid-Pliocene reduction of the EAIS. The comparison of microfossil assemblages distributed by the impact and the species reported from the Sirius Group, as well as the age of the impact event strongly support the idea, that the marine Sirius microfossils were transported onto the Antarctic continent by ejection of deep sea sediments due to the asteroid impact, at a distance of 4000 km from the impact site.

The first comprehensive documentation of an asteroid impact into the deep ocean will be a baseline for the identification of further deep sea impacts, which according to impact probability models should occur at relatively short geological time intervals. Modelling Earth's environmental and climatic response on the Eltanin impact will help to understand the influence of short-term catastrophic events on Earth's climate history caused by the collision with asteroide bodies.

#### References

- Gersonde, R., Kyte, F.T., Bleil, U., Diekmann, B., Flores, J.A., Gohl, K., Grahl, G., Hagen, R., Kuhn, K., Sierro, F.J., Völker, D., Abelmann, A. and Bostwick, J.A. (1997) Geological record and reconstruction of the late Pliocene impact of the Eltanin asteroid in the Southern Ocean. *Nature* **390**:357-363.
- Harwood, D. M. (1983) Diatoms from the Sirius Formation, Transantarctic Mountains. *Antarctic Journal* **18**:98-100.
- Kyte, F.T. and Brownlee, D.E. (1985) Unmelted meteoritic debris in the Late Pliocene Ir anomaly: evidence for the impact of a nonchondritic asteroid. *Geochim. Cosmochim. Acta* **49**:1095-1108.
- Kyte, F.T., Zhou, L., and Wasson, J.T. (1988) New evidence on the size and possible effects of a late Pliocene oceanic impact. *Science* **241**:63-65.

Kyte, F.T., Zhou, Z., and Wasson, J.T. (1981) High noble metal concentrations in a late Pliocene sediment. *Nature* **292**:417-420.

## Post-Lhb Bombardment Rates and Oceanic Impact Records

A. Glikson.

Research School of Earth Science, Australian National University, Canberra, A.C.T. 0200  
(andrew.glikson@anu.edu.au).

The waning of the Late Heavy Bombardment (LHB) in the Earth-Moon system about 3.9-3.8 Ga - involving a decline of impact rates by about two orders of magnitude (for craters larger than 18 km-diameter from  $4-9 \times 10^{-13} \text{ km}^{-2} \text{ yr}^{-1}$  to  $4-6 \times 10^{-15} \text{ km}^{-2} \text{ yr}^{-1}$ ; Baldwin, 1986; Ryder, 1990), is widely assumed to signify a transition from a crustal regime dominated by extraterrestrial impacts to one dominated by internal mantle-crust dynamics. By contrast, post-LHB impact rates indicated by lunar and terrestrial crater counts and by astronomical observations, when combined with crater size versus cumulative crater size-frequency relationships ( $N \propto D_c^{-1.8}$  to  $N \propto D_c^{-2.0}$ ;  $D_c$  = crater diameter;  $N$  = cumulative number of craters with diameters  $>D_c$ ; Shoemaker and Shoemaker, 1996), imply formation of over 450 craters of  $\geq 100$  km- diameter, including over 50 craters of  $\geq 300$  km-diameter. A confirmation of these rates on the larger end of the scale is provided by observation of very large asteroids such as Swift Tuttle ( $D_p = 24$  km). Estimates of the distribution of continental crust in the Archaean at less than 20 percent of the Earth surface (McCulloch and Bennett, 1994) require that the bulk of the post-LHB impacts occurred on oceanic crust, including the proximity of ocean spreading loci. Modelling of the consequences of impact by projectiles  $\gg 10$  km-diameter on thin, thermally active, oceanic crust and shallow lithosphere suggest that adiabatic melting of impact-rebounded mantle should result in volcanic activity on a scale exceeding that of oceanic Large Igneous Provinces (LIP) (Coffin and Eldholm, 1994). The formation of very large ( $D_c \geq 500$  km) oceanic craters, predicted by the impact rates, may trigger episodic re-arrangement of mantle convection systems and plate tectonic patterns. Evidence for distal condensates of large oceanic impacts is beginning to emerge, including (1) a c.3.26 Ga oceanic crater indicated by impact condensate spherules, iridium anomalies, Ni-rich quench spinels and  $^{53}\text{Cr}/^{52}\text{Cr}$  isotopic evidence from the basal Fig Tree Group, Barberton Mountain Land, Transvaal (Lowe et al, 1998; Byerly and Lowe, 1994; Shukolayukov et al., 1998). Mass balance calculations based on Iridium and Chromium suggest a chondritic projectile  $D_p > 30$  km in diameter, implying a crater of  $D_c > 600$  km diameter; (2) c.2.63 Ga, c.2.56 Ga and c.2.49 Ga spherule units in the Hamersley Basin, Western Australia (Simonson and Hassler, 1997). The absence of shocked quartz grains militates for oceanic impacts. The near-contemporaneity of the c.3.26 Ga event and major magmatic and tectonic activity in the Pilbara Craton, Western Australia, draws attention to the potential global consequences of very large impacts. Independent confirmation of the rate and size distribution of large impacts on Phanerozoic oceanic crust is provided by the progressive

unravelling of new buried impact structures on continental shelves (Gorter, 1998). Recent discoveries include the 120-130 km-diameter Woodleigh multi-ring structure, south Carnarvon Basin, Western Australia (Mory et al., in prep.), of pre-lower Jurassic age - rendering it a potential candidate for a Permian-Triassic boundary impact. The progressive identification of distal impact signatures in pre-200 Ma sediments promises to provide new clues to the "mare incognita" of hitherto subducted oceanic regimes.

#### References

- Baldwin, R. B. (1986) Relative and absolute ages of individual craters and the rates of infalls on the Moon in the post-Imbrium period. *Icarus* **61**:63-91.
- Byerly, G. R., and Lowe, D. R. (1994) Spinels from Archean impact spherules. *Geochim. Cosmochim. Acta* **58**:3469-3486.
- Coffin, M. F. and Eldholm, O. (1994) Large igneous provinces: crustal structure, dimensions and external consequences. *Rev. Geophys.* **32**:1-36.
- Gorter, J.D. (1998) The petroleum potential of Australian impact structures. *Aust. Petrol. Explor. Assoc. J.* **1998**:159-186.
- Lowe, D.R., Byerly, G.R., Asaro, F. and Kyte, F.T. (1989) Geological and geochemical record of 3400 m.y.-old terrestrial meteorite impacts. *Science* **245**:959-962.
- McCulloch, M. T. and Bennett, V. C. (1994) Progressive growth of the Earth's continental crust and depleted mantle: Geochemical constraints. *Geochim. Cosmochim. Acta* **58**:4717-4738.
- Mory, A.J., Iasky, R.P. and Glikson, A.Y. (in prep.) Woodleigh, Carnarvon Basin, Western Australia: a new multi-ring structure, 120 km in diameter, of probable impact origin.
- Ryder, G. (1990) Lunar samples, lunar accretion and the early bombardment of the Moon. *Eos* **71**:313-322.
- Shoemaker, E. M. and Shoemaker, C. S. (1996) The Proterozoic impact record of Australia. *Aust. Geol. Surv. Org. J. Aust. Geol. Geophys.* **16/4**:379-398.
- Shukolayukov, A., Kyte, F.T., Lugmair, G.W. and Lowe, D.R. (1998) The oldest impact deposits on Earth - first confirmation of an extraterrestrial component (abstract), *Cambridge meeting on Impacts and the Early Earth*.
- Simonson, B.M. and Hassler, S.W. (1997) Revised correlations in the Hamersley Basin based on a horizon of resedimented impact spherules. *Aust. J. Earth Sci.* **44**:37-48.

### **Tsunami Prediction, Monitoring and Warning in Norway**

C. B. Harbitz, U. M. Kolderup and A. Makurat  
Norwegian Geotechnical Institute, P.O.Box 3930 Ullevaal Hageby, 0806 Oslo, Norway

The three most severe events of landslide generated tsunamis in the Norwegian history, taking a toll of 174 deaths in addition to huge material damage, have all occurred in this century. NGI is today in a key position concerning monitoring, warning, detection and analyses of natural hazards

due to snow avalanches, landslides, and subaqueous mass flows, as well as secondary effects such as destructive water waves. A careful registration of historic events have been undertaken by NGI for decades, and constituted the basis for the Norwegian contribution to the European GITEC tsunami catalogue. At present, seven areas in Norway are equipped with rock slide monitoring and warning systems designed by NGI due to significant probability of slide-induced, destructive tsunamis. Brief examples of monitoring and warning systems and computational predictions on tsunami wave heights, currents and impact are shown.

It is more and more accepted that submarine slides are the principal cause of large tsunamis (long waves set in motion by an impulsive perturbation of the sea, intermediate between tides and swell waves in the spectrum of gravity water waves), while e.g. earthquakes play an indirect role as the slide triggering mechanism. It should be noted that most slides are triggered by a combination of several release mechanisms.

Simulations of the Second Storegga Slide (ca. 8000 years BP) generated tsunami are described by Harbitz (1992) and Pedersen et al. (1995). The calculated run-up heights agree remarkably well with possible tsunami wave heights deduced from geological evidences along the eastern coast of Scotland and the western coast of Norway. Simulations of tsunamis generated by the 1969 Gorrige Bank earthquake SW of Portugal are presented by Gjevik et al. (1997). Examples of tsunami simulations are also presented on internet (<http://www.math.uio.no/gitec/>).

The work conducted by NGI so far on tsunamis caused by submarine slides, will be a good starting point for the planned activities on impact related tsunami generation and propagation. This work will be done in co-operation with the Institute for Geology, University of Oslo, Norway.

#### References

- Gjevik, B., Pedersen, G., Dybesland, E., Harbitz, C., Miranda, P.M.A, Babtista, M.A., Mendes-Victor, L., Heinrich, P., Roche, R. and Guesmia, M. (1997) Modelling Tsunamis from Earthquake sources near Gorrige Bank Southwest of Portugal. *Journal of Geophysical Research* **102**, No. C13, 27,931-27,949.
- Harbitz, C.B. (1992) Model simulations of tsunamis generated by the Storegga Slides. *Marine Geology* **105**:1-21.
- Pedersen, G., Gjevik, B., Harbitz, C.B., Dybesland, E., Johnsgard, H. and Langtangen, H.P. (1995) Tsunami case studies and model analysis; Final GITEC report. Preprint Series, Dept. of Mathematics, University of Oslo, No. 4.

## Comet Impacts to the Ocean: Numerical Analysis of Eltanin Scale Events

B. Ivanov.

Institute for Dynamics of Geospheres, Russian Acad. Sci., Leninsky Prospect 38-6 Moscow Russia 117321 (baivanov@glasnet.ru).

The discovery of the Eltanin impact site (Kyte et al., 1981; Gersonde et al., 1997) proved the possibility to find the footprint of an impact event even in the absence of a visible impact crater at the oceanic bottom. The recovered fragments of the Eltanin meteorite (Kyte and Brownlee, 1985) allow to identify the nature of a projectile. The absence of a visible crater allows to restrict the possible diameter of the Eltanin projectile in the range of 1 to 4 km (Gersonde et al., 1997). The aim of the presented work is to analyse possible effects of a cometary impact at a scale comparable with what is known about the Eltanin Impact Site (EIS). The specific goal of the current stage of the project is to find the range of impact conditions when shock pressure in rocks at the oceanic bottom is enough high just for beginning of the impact melting. For typical basaltic rocks the melting pressure is about 50 GPa.

Using the multimaterial Eulerian numerical code based on the SALE program (Amsden et al., 1980) the impact of comets with diameters 1 to 4 km were simulated. Both the ocean (5 km deep) and the comet nuclei were treated as water with the Tillotson EOS (O'Keefe and Ahrens, 1982). The oceanic bottom was described as a rigid surface. To find the minimum size of a projectile the vertical impact was computed as the main variant. The shock loading just below the point of impact depends on the projectile size and velocity.

For short-periodic comets the average impact velocity is close to  $30 \text{ km s}^{-1}$ . At this impact velocity the ice sphere of 1.4 km diameter create the maximum pressure at the ocean floor of the order of 20 GPa, while the 2.0 km body impact resulted in the reflected shock wave pressure of 70 GPa. The similar loading was computed for the impact of a  $\sim 1.6 \text{ km}$  water sphere with the impact velocity of  $50 \text{ km s}^{-1}$  (typical for long period comets). In both cases the floor area loaded above 50 GPa has a radius of  $\sim 1.5 \text{ km}$  - slightly larger than a projectile radius.

The typical graphic output for the general mass movement is presented on Figure 1. The light grey shading designates zone with a density above  $0.5 \text{ g cm}^{-3}$ , the dark grey shading shows dense water vapors with a density from 0.1 to  $0.5 \text{ g cm}^{-3}$ . Figure 2 demonstrates the pressure history at the oceanic bottom near to the sub-impact point.

While the cometary impacts into ocean were computed by many authors (e.g. O'Keefe and Ahrens, 1982; Hills et al., 1994), the main attention was devoted to surface waves (tsunami). However calculations demonstrate another important phenomena: a huge water velocity in respect to the ocean floor.

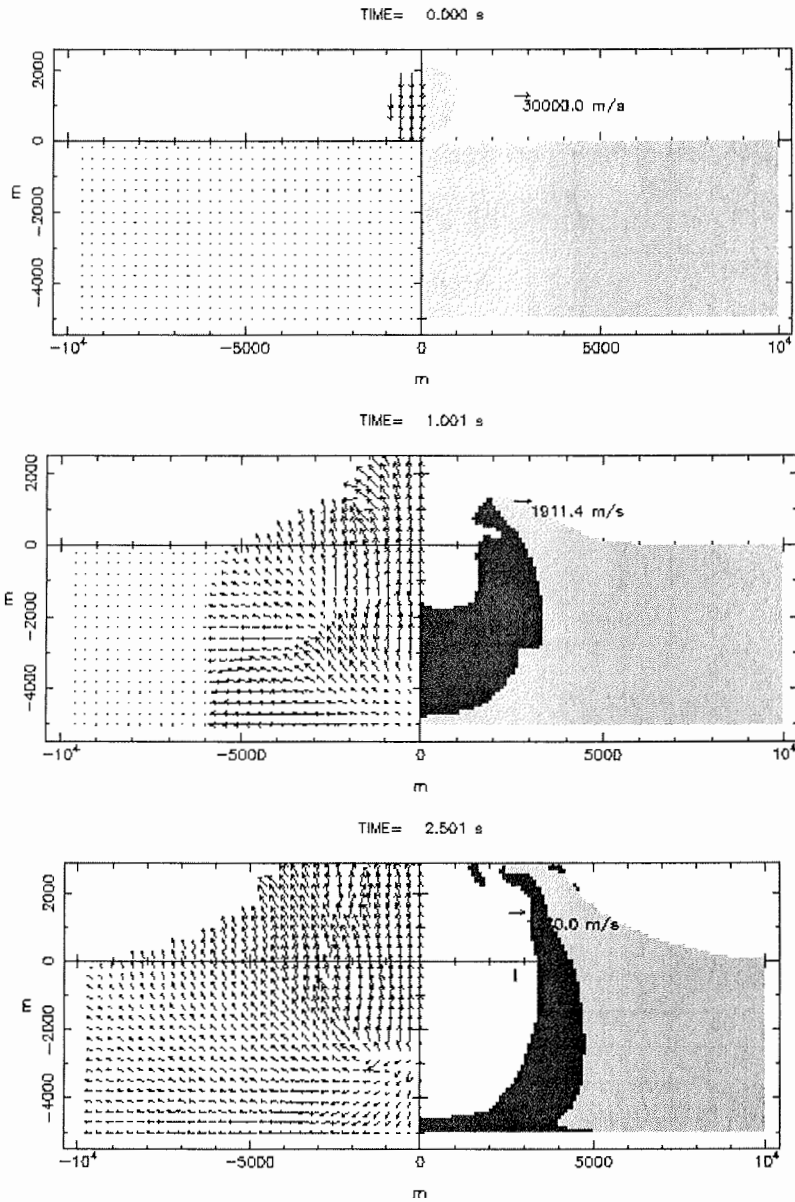


Figure 1 The general picture of the material motion after the vertical impact of a comet with a diameter of 2 km and velocity of 30 km/s. Left hand side show the velocity field, right hand side show zones of water density above 50% of a normal value (light grey) and between 10% and 50% of a normal value (dark grey).

In the vicinity of the impact point the water motion behind the shock wave (with a triple shock configuration in a certain range) occurs with velocities of  $100 \text{ m s}^{-1}$  up to distances of 20 km from the sub-impact point (Fig. 3). This strong water stream seems to be a good mechanism for the initial disturbance of sediments.

The future work includes the simulation of the oceanic bottom deformation to reveal the specifics of the impact crater formation under the deep water layer.

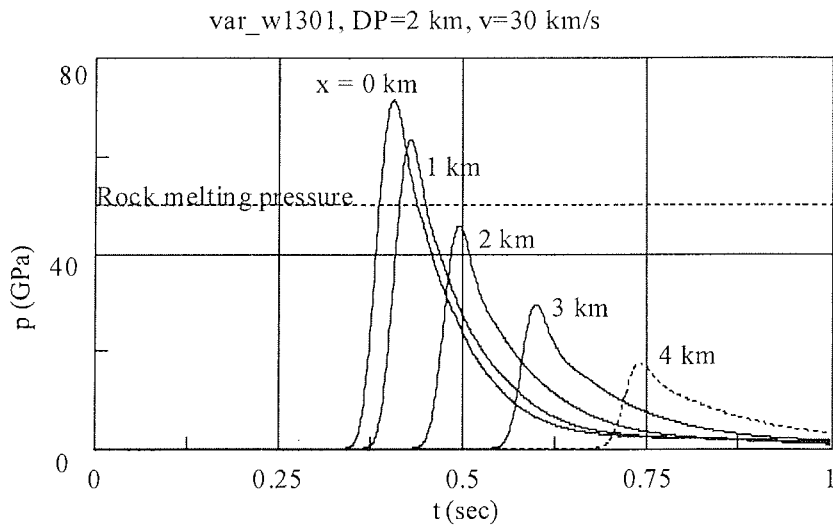


Figure 2 Pressure at the rigid oceanic floor vs time at distances from the sub-impact point,  $x$ , equal 0, 1, 2, 3, and 4 km. The typical shock melting pressure for rocks ( $\sim 50 \text{ GPa}$ ) is shown with a dashed line.

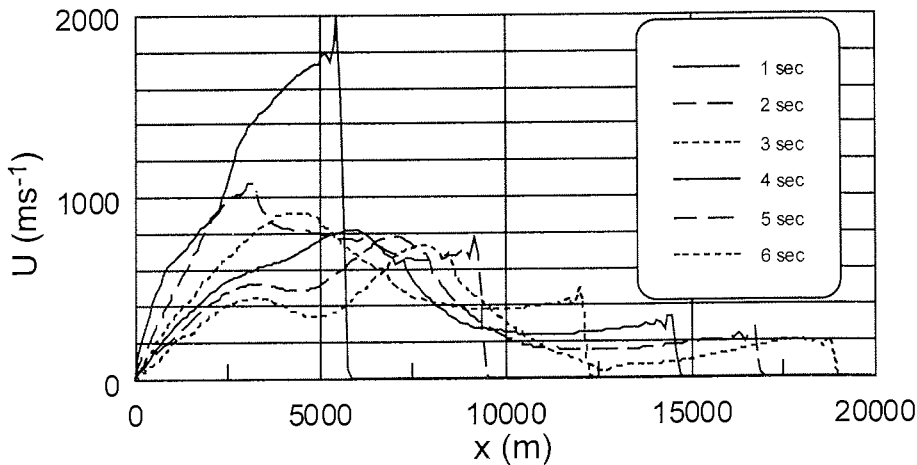


Figure 3 The radial flow velocity profiles at the oceanic floor at first seconds after the impact.

### References

- Amsden, A.A., Ruppel, H.M. and Hirt, C.W. (1980) SALE: A Simplified ALE Computer Program for Fluid Flow at All Speeds LA-8095, Los Alamos National Laboratory, Los Alamos, N. M.
- Gersonde, R., Kyte, F.T., Bleil, U., Diekmann, B., Flores, J.A., Gohl, K., Grahl, G., Hagen, R., Kuhn, K., Sierro, F.J., Völker, D., Abelmann, A. and Bostwick, J.A. (1997) Geological record and reconstruction of the late Pliocene impact of the Eltanin asteroid in the Southern Ocean. *Nature* **390**:357-363.
- Hills, J.G., Nemtchinov, I.V., Popov, S.P. and Teterov, A.V. (1994) Tsunami generated by small asteroid impacts. In: *Hazards due to comets and asteroids*, T. Gehrels (ed.), Univ. Arizona Press, pp. 779-789.
- Kyte, F.T., Zhou, Z. and Wasson, J.T. (1981) High noble metal concentration in a late Pliocene sediments. *Nature* **292**: 417-420.
- Kyte, F.T. and Brownlee, D.E. (1985) Unmelted meteoritic debris in the Late Pliocene Ir anomaly: Evidence for the impact of a nonchondritic asteroid. *Geochim. Cosmochim. Acta* **49**: 1095-1108.
- O'Keefe, J.D. and Ahrens, T.J. (1982) The interaction of the Cretaceous/Tertiary extinction bolide with the atmosphere, ocean and solid Earth. *Geol. Soc. of America Spec. Pap.* **190**: 103-120.

## **A Petrological Model for Oceanic Impact Melting and the Origin of Komatiites.**

A.P. Jones, G.D. Price, and P. Claeys.

Department of Geological Sciences, University College London, Gower Street, London WC1E 6BT England. (ucfbhaj@ucl.ac.uk).

We present a new general model for impact melting phenomena caused by large impacts into oceanic lithosphere. Melting is expected to be much more common than for impacts into continental lithosphere, due to increased geothermal gradients, and much greater thermal melt potentials with increasing depth. Melting will occur either as (a) direct transfer of kinetic energy or (b) pressure release melting following crater excavation.

Perhaps surprisingly decompression melting (b) is likely to produce the major geological signature. Melting is an inevitable consequence of adiabatic decompression following crater excavation. The solid-melt transition would be nearly instantaneous (~sound velocity) and orders of magnitude faster than gravitational crater relaxation. Melt delivery to the surface, total melt volumes and the magmatic lag post-shock depend on a number of parameters. These are best visualised in terms of end-member models, defining geochemical, petrological, mineralogical and "plate-tectonic" conditions. Degrees of partial melting and melt compositions are easily obtained from published

experimental petrological data. For oceanic lithosphere the highest degrees of partial melting are expected in oceanic lithosphere with high geothermal gradients, corresponding to current day young crust. High degrees of partial melting are easily sufficient to generate komatiite melts from shallow mantle peridotite; there is little difference between "enriched" or "depleted" mantle, or "wet" or "dry" mantle. The limiting case is for 1.2 GPa pressure release, equivalent to ~35 km transient crater depth, in near-solidus (young) oceanic lithosphere, following a ~Chicxulub sized (Cx) event. Larger impacts would also generate peridotitic or komatiitic melts from greater depths. A Cx-sized impact into colder oceanic lithosphere ("old") would generate proportionally less melting of picritic or basaltic composition, depending also on mantle composition. Post-melt extraction could produce regional mantle anomalies, secondary melting and longer-lived plume-like activity. We propose that spinifex-textured komatiites of peridotitic composition are the expected response to large impacts in peridotitic mantle. Current day distributions favour this product from oceanic lithosphere, but Archaean tectonic conditions may have been different. If komatiites are indeed impact melts, this might uniquely explain many komatiite enigmas including eg; their close association with tholeiites (pre-impact magmatism), positive N isotope ratios (air-like), superheat sufficient to thermally erode their bases (thermal limit = complete melting of peridotite), storage of high degree partial melts in the mantle (none required).

The first known komatiites of post Precambrian age are typical spinifex-textured glassy flows of Mesozoic or Tertiary age from Gorgona Island. They are interlayered with basalts in a km-scale sequence of ultramafic igneous rocks which resemble an uplifted fragment of oceanic crust and are capped by Tertiary sediments. A feature of the Gorgona komatiites is the close association with a large volume chaotic to stratified ultramafic breccia (23-27 wt% MgO) with glassy picritic blocks in a fine grained matrix of plastically deformed high-Mg glassy globules (Echeverria, 1980; Echeverria and Aitken 1986). Conventional petrological and geochemical modelling requires a separate magmatic source for the komatiites, which might be related to plume-related thickened oceanic crust (Echeverria, 1980; Echeverria and Aitken 1986; Storey et al., 1991). We postulate instead, that the Gorgona komatiites resulted from decompression melting following an oceanic impact. The Gorgona komatiites are seemingly close in both age and location to the K/T Chicxulub event, though we also consider other possible sources.

If komatiites are indeed the long sought after evidence of large oceanic impacts, then they may be unrelated to long term heat flow in the early Earth.

#### References

- Echeverria, L.M. (1980) Tertiary or Mesozoic komatiites from Gorgona Island. *Contrib. Mineral. Petrol.*, **73**: 253-266.
- Echeverria, L.M. and Aitken, B.G. (1986) Pyroclastic rocks: another manifestation of ultramafic volcanism on Gorgona Island, Columbia. *Contrib. Mineral. Petrol.*, **92**: 428-436.
- Storey, M., Mahoney, J.J., Kroenke, L.W. and Saunders, A.D. (1991) Are oceanic plateaus sites of komatiite formation? *Geology*, **19**: 376-379.

## Geochemical Investigations of K/T Boundary Rocks: The Search for Precursor Lithologies

B. Kettrup and A. Deutsch.

Inst. f. Planetologie, Wilhelm-Klemm-Strasse 10, D-48149 Münster, Germany (kettrup@uni-muenster.de).

### Introduction

It has been demonstrated convincingly that geochemical and isotopic characteristics of impact melt lithologies (melt rocks, melt particles in suevites) can be used to constrain their precursor materials, and to relate ejected impact melt glass to the respective source crater. In this context, the 195 km sized 65 Ma old Chicxulub structure (Hildebrand et al., 1991; Morgan et al., 1997) and its ejecta which is world-wide distributed at the K/T boundary, represent ideal study objects. The target at the Chicxulub impact site consisted of shallow water, and up to 2.9 km thick Cretaceous platform sediments resting on continental crust (Fig. 1). At present, both these rock components are inaccessible in outcrops close to the crater, yet they form clasts in breccias. Such breccias have been drilled by PEMEX and UNAM. In addition, the sediments (Lopes Ramos, 1975; Ward et al., 1995; Sharpton et al., 1992) reach surface about 350 km off the presumed crater rim, whereas the nature of the basement is still a matter of debate.

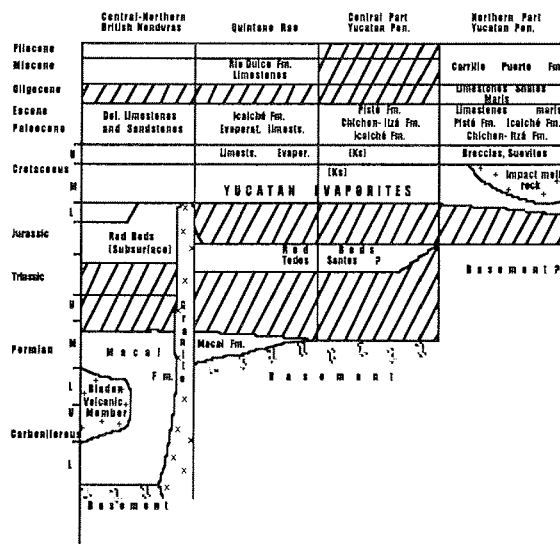


Figure 1 Generalized stratigraphic correlation chart for the Yucatan Peninsula (after Lopes Ramos, 1975).

### Samples, results

Here we present Rb-Sr and Nd-Sm isotope data for carefully cleaned Chicxulub impactites, i.e., suevites and impact melt rocks, and handpicked fragments from these breccias (PEMEX drillcores Yucatan-6 N14-19, and Chicxulub-1, Bottom) as well as for black glass from the K/T boundary at Beloc, Haiti. Major element, REE data and  $\delta^{18}\text{O}$  data of these specimen have been reported elsewhere (Dißmann et al., 1998; Kettrup and Deutsch, 1998).

The Nd model parameters of all analysed impactites are very homogeneous:  $T_{DM}^{Nd}$  is  $1.12 \text{ Ga} \pm 0.03$  (mean  $\pm 1\sigma D$ ,  $n = 8$ ), and  $T_{CHUR}$   $0.565 \pm 0.038 \text{ Ga}$ . In accordance with U-Pb data for zircons from distal ejecta deposits (Krogh et al., 1993) these data point to a Pan-African age of the crystalline basement in the Chicxulub target region.

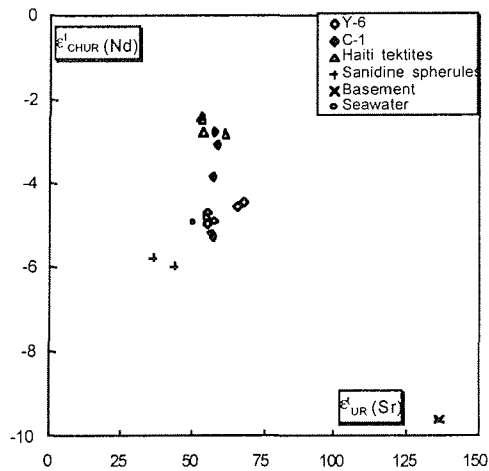


Figure 2 Data sources: Haiti tektites (Premo and Izett., 1992), impact melt lithologies from Y-6, C-1 (Dißmann et al., 1998; Kettrup and Deutsch 1998; Blum et al., 1993), seawater (Vonhof, 1998; Faure, 1986) and Sanidine spherules from the K/T boundary, Caravaca, Spain (DePaolo et al., 1983).

Moreover, the model ages are clearly distinct from the Proterozoic basement in the Sierra Madre terrane (localities Novillo and Molango) west of Yucatan ( $T_{DM}^{Nd}$  of  $1.52 \text{ Ga} \pm 0.06$  (Patchett and Ruiz, 1987) In the time-corrected ( $T = 65 \text{ Ma}$ )  $\epsilon_{Nd}$ - $\epsilon_{Sr}$ -diagram of Figure 2, the impact related lithologies plot in a field which is defined by  $\epsilon_{Nd}$  of  $-2$  up to  $-6$ , and  $\epsilon_{Sr}$  of  $55$  to  $69$ . This variation in  $\epsilon_{Nd}$  exceeds that known for impact melt rocks of other craters. Compared to the Y-6 samples, C-1 and Haiti tektites show less negative  $\epsilon_{Nd}$  values. Typical for the upper continental crust, one crystalline clast separated from Y-6 N14, display a more negative  $\epsilon_{Nd}$ -value and highly radiogenic Sr; it's  $T_{DM}^{Nd}$  of  $1.38 \text{ Ga}$  is slightly higher than that of the impactites (Y-6, C-1 in Fig. 2), and of Haitian tektites ( $\approx 1.05 \text{ Ga}$  (Premo and Izett, 1992). The data array in Figure 2 indicates that the Sm-Nd system of the impactites and Haitian tektites is not defined by a mixture of such a basement component and Cretaceous sediments (represented in the diagram as "seawater"). Additional target rocks recovered from Chicxulub drill cores are shown in the Sm/Nd vs. ppm Nd diagram of Fig.

3. In this diagram, data points for Haiti tektites plot off the field, delimited by potential target rocks.

#### Discussion and outlook

Despite the restricted data set (due to the non-availability of samples!), our Sr, Nd isotope investigation yielded one result which is fundamental for the origin of the Chicxulub impact melt lithologies: They are not the product of simple mixing of two components, i.e., Cretaceous platform sediments and a homogeneous basement. At least one precursor component is missing specified by high a Nd content, a low Sm/Nd ratio, and a relatively high  $^{143}\text{Nd}/^{144}\text{Nd}$  ratio (i.e.,  $\epsilon_{\text{Nd}}^{T=65\text{Ma}}$  of about  $-2$ ). Rocks with such a specification are more than unusual. We therefore, argue, that probably two different precursor components have not been detected yet. One could be an intermediate to felsic crystalline rock or sediments derived from such a rock (low Sm/Nd, high Nd), the other a mafic rock (highly radiogenic Nd composition). The following rock types may match the required mafic component: Oceanic crust, sub-continental mantle, or basic to intermediate orthogneiss. Current tectonic models for the evolution of the Caribbean seem to exclude the presence of oceanic crust at the impact site in end-Cretaceous times (Ross and Scott, 1988). On the other hand, impact mechanical models for the Chicxulub event do not favour a contribution of the contemporaneous sub-continental mantle to impact melt products. Hence, the most plausible mafic to intermediate component may be gneisses, similar to those reported by (Patchett and Ruiz 1987). It should be a goal of further investigations of Chicxulub core samples to identify additional basement clasts, especially such with a more mafic composition.

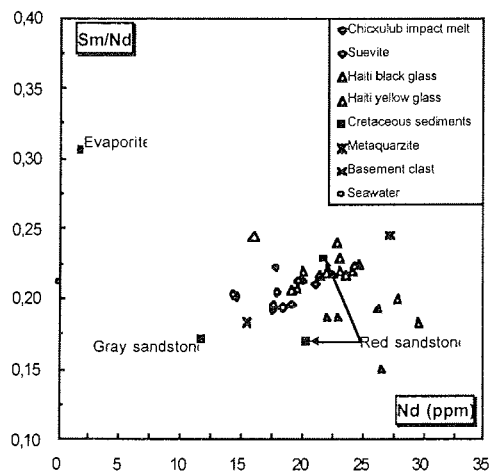


Figure 3 Data sources: Haiti tektites (Premo and Izett., 1992; Koeberl and Sigurdsson, 1992), impact melt lithologies and basement clast (Dißmann et al., 1998; Kettrup and Deutsch 1998; Blum et al., 1993), seawater (Faure, 1986), Cretaceous sediments and metaquartzite (Koeberl, 1993).

### Acknowledgments

This work is supported by a DFG grant DE 401/13-1. Y-6 and C-1 samples are from P. Claeys (HU Berlin), the Beloc material was generously provided by E. Robin (Gif-s-Yvette).

### References

- Blum, J.D., Chamberlain, C.P., Hingston, M.P., Koeberl, C., Marin, L.E., Schuraytz, B.C. and Sharpton, V.L. (1993) Isotopic comparison of K/T boundary impact glass with melt rock from the Chicxulub and Manson impact structures. *Nature* **364**: 325-327.
- DePaolo, D.J., Kyte, F.T., Marshall, B.D., O'Neil, J.R. and Smit, J. (1983) Rb-Sr, Sm-Nd, K-Ca, O, and H isotopic study of Cretaceous-Tertiary boundary sediments, Caravaca, Spain: evidence for an oceanic impact site. *EPSL* **64**: 356-373.
- Dißmann, B., Agrinier, P., Ostermann, M. and Deutsch, A. (1998) Chicxulub-PEMEX well Y-6: Geochemistry (REE,  $e_{Nd}$ ,  $e_{Sr}$ ,  $d^{18}O$ ,  $d^{13}C$ ) of impact melt breccias and suevites. *LPSC XXIX*: 1610.
- Faure, G. (1986) Principles of isotope Geology. John Wiley, New York: 589pp.
- Hildebrand, A.R., Penfield, G.T., Kring, D.A., Pilkington, M., Camargo Z, A., Jacobsen, S.B. and Boynton, W.V. (1991) Chicxulub Crater: A possible Cretaceous/Tertiary boundary impact crater on the Yucatán Peninsula, Mexico. *Geology* **19**: 867-871.
- Kettrup B. and Deutsch A. (1998) Chicxulub impactites: Sr, Nd isotope composition of melt rocks and basement clasts. *LPSC XXX*: 1184.
- Koeberl, C. (1993) Chicxulub Crater, Yucatan, Tektites, impact glasses, and the geochemistry of target rocks and breccias. *Geology* **21**: 211-214.
- Koeberl, C. and Sigurdsson, H. (1992) Geochemistry of impact glasses from the K/T boundary in Haiti: Relation to smectites and new type of glass. *GCA* **56**: 2113-2129.
- Krogh, T.E., Kamo, S.L. and Bohor B.F. (1993) Fingerprinting the K/T impact site and determining the time of impact by U-Pb dating of single shocked zircons from distal ejecta. *EPSL* **119**: 425-429.
- Lopes Ramos, E. (1975) Geological summary of the Yucatán Peninsula. The gulf of Mexico and the Caribbean: 257-282.
- Morgan, J., Warner, M. and the Chicxulub Working Group, Brittan, J., Buffler, R., Camargo Z., A., Christeson, G., Denton, P., Hildebrand, A.R., Hobbs, R., Macintyre, H., Mackenzie, G., Maguire, P., Marin, L.E., Nakamura, Y., Pilkington, M., Sharpton, V.L., Snyder, D., Suarez, G. and Trejo, A. (1997) Size and morphology of the Chicxulub impact crater. *Nature* **390**: 472-476.
- Patchett P.J. and Ruiz J. (1987) Nd isotopic ages of crust formation and metamorphism in the Precambrian of eastern and southern Mexico. *Contrib. Mineral. Petrol.* **96**: 523-528.
- Premo, W.R. and Izett, G.A. (1992) Isotopic signatures of black tektites from the K-T boundary on Haiti: Implications for the age and type of source material. *Meteoritics* **27**: 413-423.
- Ross, M.I. and Scott C.R. (1988) A hierarchical tectonic model of the Gulf of Mexico and Caribbean region. *Tectonophysics* **155**: 139-168.

- Sharpton, V.L., Dalrymple, G.R., Marin, L.E., Ryder, G., Schuraytz, B.C. and Urrutia-Fucugauchi, J. (1992) New links between the Chicxulub impact structure and the Cretaceous/Tertiary boundary. *Nature* **359**: 819-821.
- Vonhof, H.B. (1998) The strontium isotope stratigraphic record of selected geologic events. Ph. D. thesis, Vrije Univ. Amsterdam: 200pp.
- Ward, W.C., Keller, G., Stinnesbeck, W. and Adatte, T. (1995) Yucatán subsurface stratigraphy: Implications and constraints for the Chicxulub impact. *Geology* **23**: 873-876.

## **Large Meteoroid Impact into Oceanic Site: Impact on Ozone Layer.**

B.A. Klumov.

Institute for Geospheres Dynamics, Moscow, Russia.

The impact of a large cosmic body into an oceanic site results in ejecta of a huge amount of ocean water into the upper atmosphere. In the present paper we investigated subsequent evolution of the impact-disturbed region in the atmosphere: we have determined time-spatial characteristics of the region and chemical composition as well.

The mass of the impact-produced ejecta is calculated by using strong explosion model. This mass is believed being distributed in the disc-shaped region in the stratosphere at the altitudes determined by a floating of a water vapour. The spatial distribution of the water vapour is determined by using the calculation of the ejecta processes.

Subsequent evolution of the disturbed region which transforms quickly into a vortex is determined by local atmospheric turbulence and zonal wind distribution. The chemical composition is controlled by photochemistry processes.

We used 2D model of the horizontal baroclinic atmosphere based on the Kadomtsev-Petviashvili equations to evaluate the time-space characteristics of the artificial atmospheric spot. To estimate the chemical impact of the ejected sea water vapour on the stratosphere we used the advanced stratospheric photochemistry model.

Our results show that impact of a 1 km body creates in the stratosphere a long-living disturbance of the ozone concentration with the diameter of the order of a few thousands kilometers. A significant (about 50%) depletion of the ozone concentration is occur in the region. Characteristic time life of the disturbance drastically depends of the altitude. The time is about of a few days in upper stratosphere and about a few years at lower stratosphere.

## Significance of Large Ocean Impact Craters

J. Koulouris, P. Janle, B. Milkereit, and S. Werner.

Institut für Geophysik der Christian-Albrechts-Universität, Kiel, Otto-Hahn-Platz 1, 24118 Kiel, Germany.

About 150 terrestrial impact craters are known until now. Among these, five are located in marine shelf areas, possibly only one (Southern Ocean) in the deep ocean. In this investigation two topics will be addressed:

- (1) The frequency of large impact craters in the deep ocean.
- (2) Expected signature of large oceanic impact craters.

### The frequency of large impact craters in the deep ocean

The frequency of impact craters on the oceanic crust can be derived from crater production functions of the structure  $N_{cum} = a \cdot D^{-c}$  (cumulative number of craters larger of diameter  $D$ ,  $a$  and  $c$  are constants from measured crater frequencies). We considered functions derived from the terrestrial data base (McKinnon, 1982; Grieve, 1987), from the frequency of Earth orbit crossing objects (Shoemaker, 1983) and a more detailed polynomial function based on lunar craters from Neukum and Ivanov (1994). The oldest relation of McKinnon (1982) results in maximum numbers and the Shoemaker (1983) relation in minimum numbers for  $N_{cum}$ . The Grieve relation is close to Shoemaker and the Neukum and Ivanov relation gives numbers below but not far from McKinnon. As the relations are valid for subaerial impacts, only craters with  $D \geq 30$  km are considered. The water cover plays only a minor role for these large impacts (McKinnon, 1981). Figure 1 shows the size-frequency distribution of impact craters for the whole deep oceanic crust ( $273.9 \cdot 10^6 \text{ km}^2$ ) and Table 1 the cumulative numbers  $N$  for diameters of 30, 50, 100 and 200 km for the whole deep ocean and for the age province with the highest numbers i. e. from 45-90  $10^6 \text{ y}$  with  $91.2 \cdot 10^6 \text{ km}^2$ .

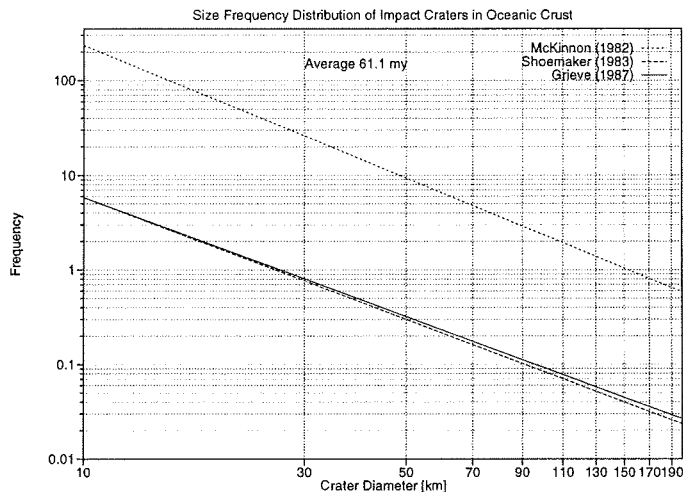


Figure 1 Size-frequency distribution of impact craters for the whole deep oceanic crust and average age of 61.1 m.y..

D [km]	≥30	≥50	≥100	≥200
N <sub>deep</sub>	0.7-30	0.3-9.4	0.1-2.3	0-0.6
N <sub>max</sub>	0.3-10	0.1-3.5	0-0.9	0-0.2

Table 1 N<sub>deep</sub>: whole deep ocean, N<sub>max</sub>: age province with the highest numbers, i.e. 45-90 10<sup>6</sup> years and 91.2 10<sup>6</sup>km<sup>2</sup>.

In summary in the whole deep ocean a few ten craters with D≥30 km, a few with D≥50 km and about one with D≥100 km can be expected. The discrimination of the cumulative numbers for different age provinces yields only significant numbers for the crust of 45-90 10<sup>6</sup>y age with an area of 91.2 10<sup>6</sup>km<sup>2</sup>.

Expected signature of large oceanic impact craters

A signature of larger impact craters at the ocean surface can only be expected from potential fields, i. e. gravity (geoid) and magnetics. In contrast to continental, subaerial craters oceanic craters should be less tectonized and eroded besides backwash effects during the late phase of the impact process. Thus the Chicxulub crater with a diameter from 180 to 300 km is a good analogue for a larger deep sea crater. Because the impact occurred in shallow water, backwash shaped the original topography. The resulting topography is preserved under a tertiary sedimentary cover. Figure 2 shows the gravity

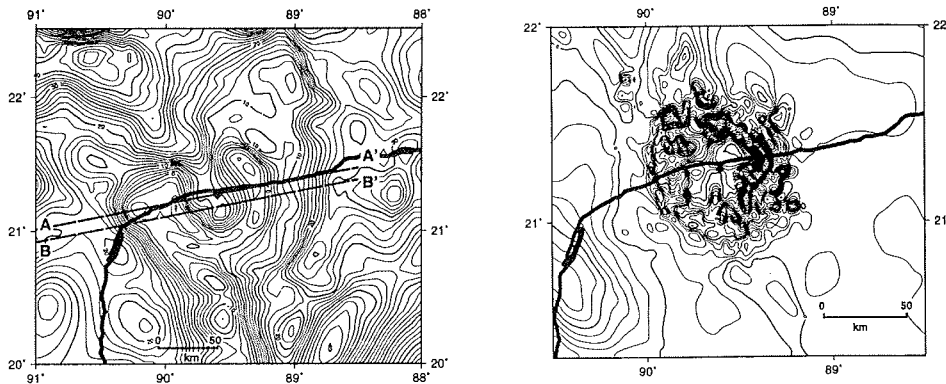


Figure 2 Potential fields of northwest Yucatan Peninsula. a) Bouguer gravity data show a U-shaped long wave-length anomaly with ca. 180 km. b) Aeromagnetic data reduced to the pole. Note the higher resolution of the magnetic anomalies. The innermost central zone is indicative of the melt body. Flight height is 500 m (Pilkington et al, 1994).

anomalies amount up to a few 10 mGal with a horizontal extent down to about 10 km. The magnetic anomalies amount up to a few 100 nT with a horizontal extent down to a few kilometers, i. e. they have shorter wavelengths. The flight height of the survey was 500 m. Outgoing from potential field anomalies of the size of the example of Chicxulub crater, large oceanic impact craters deeper than 1000 m should not give any significant signal in the potential fields. But there is a chance for receiving a signal in the magnetic field, considering a higher magnetic remanence for oceanic crustal material. In principle seismic surveys can by chance discover oceanic impact craters as has been demonstrated by the Mjølner structure with 40 km diameter (Tsikalas et al., 1998). Characteristic seismic signatures of impact craters are disturbances of horizontal layering, terracing (slumped blocks) in the crater areas and the central uplift.

#### References

- McKinnon, W. B. (1982) Impact into the Earth's ocean floor: preliminary experiments, a planetary model, and possibilities for detection. *GSA Spec. Paper* **190**:129-142.
- Grieve, R.A.F. (1987) Terrestrial Impact Structures. *Ann. Rev. Earth Planet. Science* **15**: 245-270.
- Neukum, G. and Ivanov, B. A. (1994) Crater size distribution and impact probabilities on Earth from lunar, terrestrial-planet, and asteroid cratering data. In: *Hazards due to Comets and Asteroids*, T. Gehrels (ed.), *The Univ. of Arizona Press*, Tucson, pp. 359-416.
- Pilkington, M. et al. (1994) Gravity and magnetic field modeling and structure of the Chicxulub crater, Mexico. *JRG* **99**:13147-13162.
- Shoemaker, E. (1983) Asteroid and comet bombardment of Earth. *Ann. Rev. Earth Planet. Science* **11**:461-494.
- Tsikalas, F. et al. (1998) Integrated geophysical analysis supporting the impact origin of the Mjølner structure, Barents Sea. *Tectonophysics* **289**:257-280.

## **Meteoritic Ejecta Deposits from the Late Pliocene Impact of the Eltanin Asteroid**

F.T. Kyte<sup>1</sup> and R. Gersonde<sup>2</sup>.

1) Institute of Geophysics and Planetary Physics, University of California, Los Angeles, 90095-1567 USA, (kyte@igpp.ucla.edu); 2) Alfred Wegener Institut für Polar- und Meeresforschung, D-27568 Bremerhaven, Germany.

The first evidence of the impact of the Eltanin asteroid was the discovery in 1981 of an Ir anomaly (Kyte et al., 1981) in sediments from piston core E13-3, collected in the Bellingshausen Sea by the *USNS Eltanin* in 1964. Kyte and Brownlee (1985) showed that the Ir was contained largely in mm-sized, vesicular impact melt that formed by shock-melting of the asteroid during oceanic impact. This melt was found to be a simple mixture of pure asteroidal

materials with a few percent seawater salts. Several mm-sized unmelted meteorite fragments were also identified and named the Eltanin meteorite, an anomalous mesosiderite. Subsequent work located Ir anomalies and impact debris in Eltanin cores E13-4 and E10-2 and a possible small Ir anomaly in E13-1, extending the ejecta strewnfield across 500 km of ocean floor (Kyte et al., 1988). Margolis et al. (1991) identified an additional trace component in these deposits - glassy spherules that contain magnesioferrite spinel. Interestingly, the spinel has compositions similar to those found in spherules produced by the Cretaceous-Tertiary (KT) boundary impact event.

In 1995 an expedition by the *FS Polarstern* collected several new piston cores from the ocean floor near the suspected site of the Eltanin impact. Gersonde et al. (1997), described three cores with well-preserved impact deposits that could be interpreted in much greater detail than the old, incomplete, Eltanin cores. These cores provided a depth profile from a basin near the top of local seamounts at 2700 m depth (core PS2709-1), to one at 4000 m depth (PS2708-1), and one in the deeper basin north of the seamounts (5000 m, PS2704-1). In the early stages of the impact event, sediments as old as mid Eocene were excavated and possibly ejected from nearby seamounts and surrounding basins. Initial deposits of coarse rubble were succeeded by turbidite-like laminated sands, some of which transported calcareous microfossils from the top of the seamounts into deeper basins. A final, graded unit formed by settling of meteoritic ejecta and dispersed fine-grained sediments through the 5 km water column.

Unfortunately, most deposits produced by the impact lay just beyond the reach of our 20-m-long piston core and we were forced to sample around edges of sedimentary basins where echosounding indicated that sediments were thinned. This resulted in some cores being interrupted by an erosional hiatus that affected some sediments in the early Pleistocene. Nonetheless we examined several cores that do not contain well-preserved impact deposits and three of these have produced positive results. In core PS2702-1, ~50 km to east of the well-preserved sections, we have found abundant impact melt particles within a slump that was deposited during the Pleistocene. In core PS2710-1, ~50 to the north, a small Ir anomaly (~0.3 ng/g above background) coincides with a few heavily corroded 5 mm melt particles separated in sieved fractions. Presumably, these represent lag deposits remaining after erosion of the impact horizon. In core PS2706-1, ~50 km SE of the best sites, analyses indicate a small Ir anomaly (~1 ng/g above background) in sediments of approximately the correct age. Including the older cores collected by the *USNS Eltanin*, there are now 8 sites across 600 km of ocean floor with recoverable ejecta and another two with possible meteoritic Ir anomalies.

The magnitudes of the Ir anomalies in the three well-preserved *FS Polarstern* cores are similar to the highest levels reported in *USNS Eltanin* cores. Kyte et al. (1998) estimated that 190 ng Ir/cm<sup>2</sup> was deposited at site E14-4. Comparable estimates for the new cores are 190, 330, and 180 ng Ir/cm<sup>2</sup> deposited at sites PS2704, PS2708, and PS2709, respectively. The high concentrations of debris found in the slump at site PS2702 lead us to suspect that similarly high amounts of Ir-rich ejecta were deposited at this site and we

conclude that the most concentrated ejecta deposits were formed over a region at least 50 km in diameter.

To date, about 7.9 g of impact debris has been separated from the >500  $\mu\text{m}$  fraction of these sediments. Most of this is Ir-rich, vesicular impact melt. About 400 mg, or 5% of the total is unmelted meteorite fragments, up to 5 mm in size. This is a lower limit, however, of the proportion of the coarse debris that remains unmelted. About 10% of the melt particles that have been sectioned have been found to contain inclusions of unmelted mineral grains and lithic fragments. The above estimate also does not include a 1.2 g meteorite (1.5 cm long) that was picked directly from core PS2704-1. Including this specimen would raise the fraction of the coarse debris that is unmelted to at least 18%. The largest debris was recovered from site PS2708, in the basin north of the seamounts. Three large melt particles ranging from 7 to 10 mm and the 1.5 cm meteorite were all recovered from this site. Although larger sample volumes were processed from sites PS2708 and PS2709, maximum sizes of the debris recovered were 5 to 6 mm. It is tempting to speculate that this size distribution may indicate that site PS2708 was closest to the actual impact site.

Virtually all of the unmelted meteorite fragments are basaltic. The inference by Kyte and Brownlee (1985) that the precursor asteroid was a mesosiderite with a significant fraction of Ni-Fe metal, was based on a number of observations including bulk chemical compositions of the impact melt, mineral chemistry of unmelted lithic fragments, and Sr-isotopic data (Papanastassiou et al., 1983). Although the high Ir concentrations of the impact melt require that the asteroid contained at least several percent metal, actual metallic particles have been impossible to find in the sediment deposits. It is conceivable that metal phases were more efficiently shocked and incorporated into the impact melt than silicate phases. However, it is also likely that any metal that survived the impact has subsequently been oxidized during sediment diagenesis. Only trace ( $\sim 10 \mu\text{m}$ ) inclusions of metal are observed in meteorite fragments. Patches of rusty sediments and occasional Ni-bearing oxide inclusions in the melt debris are likely residues of preexisting metal.

A portion of the large (1.5 cm) meteorite recovered has been used to make the first thin section of the Eltanin meteorite. As with other sectioned lithic fragments, this rock appears to remain largely unaltered after residing in these sediments for 2.15 Ma. However, some minor alteration is present. Fe-oxides are found along cracks, possibly reflecting transport of Fe-rich water along fractures in the rock. Also several pyroxene grains appear to be partially altered to clay minerals. Evidence of pervasive shock is evident throughout the entire section. All plagioclase is isotropic, confirming earlier interpretations that the plagioclase was converted to maskelynite (Kyte and Brownlee, 1985). Nearly all pyroxenes are extensively fractured and exsolution lamellae in pigeonites are invariable offset and/or distorted. Two incipient melt pockets have been observed within this piece. One is up to 1 mm long and contains zoned orthopyroxene in a matrix of feldspathic glass.

About 40 melt particles from the 1 to 2 mm size fraction have been examined in polished section. While the unmelted lithic fragments are relatively pristine,

the vesicular impact melt is pervasively altered. Invariably the outer portions of these particles are heavily corroded and only the central cores contain a fresh assemblage of olivine, chromite and glass. We estimate that at least 50% of the mass of vesicular debris has been pervasively altered. This makes analyses of the bulk composition of the debris difficult at best using whole-rock methods like neutron activation. Major element chemistry of the unaltered cores of these particles can be approximated by averaging numerous broad-beam (~20  $\mu\text{m}$  spot) electron microprobe analyses, but this is complicated by abundant vesicles and the relatively large size of olivine grains (~10  $\mu\text{m}$ ). Nonetheless, analyses do appear to indicate a significant variability between samples that may reflect a true heterogeneity in the source materials. Lithophile elements such as Si, Mg, and Ca vary by as much as several percent and may reflect variations in the proportions of preexisting plagioclase and pyroxene in the melt. Chromium which must originate mostly from chromite in the asteroid varies by as much as a factor of 2. Concentrations of Ir, Ni and Au vary by factors of 2 to 10, indicating that the siderophile precursor, presumably Ni-Fe metal, has been poorly mixed in the impact melt. Together, these observations indicate the likelihood that melting was all on a local scale and that bulk chemistry of individual melt particles may be representative of only small-scale mixtures of adjacent mineral grains from the precursor asteroid.

Despite all we have learned, much remains unknown. An unfortunate result of the 1995 *Polarstern* expedition was that the impact deposit was typically beyond the reach of our piston cores and we were unable to sample it as it occurred within most sedimentary basins in the study area. Hopefully this can be remedied with a return to the impact site with better sampling tools. Also, very little can be said of the fraction of the ejecta that was not coarse-grained and that was not deposited locally. Presumably, a large fraction of the mass of the Eltanin asteroid was launched as ballistic ejecta and dispersed over a large portion of the Earth's surface. Until we can successfully detect evidence of this impact deposit at some great distance from the Bellingshausen Sea we can only speculate as to the nature of this portion of the deposit.

#### References

- Gersonde, R., Kyte, F.T., Bleil, U., Diekmann, B., Flores, J.A., Gohl, K., Grahl, G., Hagen, R., Kuhn, K., Sierro, F.J., Völker, D., Abelmann, A. and Bostwick, J.A. (1997) Geological record and reconstruction of the late Pliocene impact of the Eltanin asteroid in the Southern Ocean. *Nature* **390**: 357-363.
- Kyte, F.T. and Brownlee, D.E. (1985) Unmelted meteoritic debris in the Late Pliocene Ir anomaly: evidence for the impact of a nonchondritic asteroid. *Geochim. Cosmochim. Acta* **49**: 1095-1108.
- Kyte, F.T., Zhou, L. and Wasson, J.T. (1988) New evidence on the size and possible effects of a late Pliocene oceanic impact. *Science* **241**: 63-65.
- Kyte, F.T., Zhou, Z. and Wasson, J.T. (1981) High noble metal concentrations in a late Pliocene sediment. *Nature* **292**: 417-420.
- Margolis S.V., Claeys P. and Kyte F.T. (1991) Microtektites, microkrystites and spinels from a Late Pliocene asteroid impact in the Southern Ocean. *Science* **251**: 1594-1597.

Papanastassiou, D.A., Wasserburg, G.J. and Brownlee, D.E. (1983) Chemical and isotopic study of extraterrestrial particles from the ocean floor. *Earth Plan. Sci. Lett.* **64**: 341-355.

## **The Present Status of the Lockne Marine Impact Structure (Ordovician, Sweden)**

M. Lindström.

Department of Geology and Geochemistry, Stockholm University, S-106 91 Stockholm, Sweden.

The Lockne crater (63°00' N, 14°49' E) is about 12 km wide. It formed at sea in the Middle Ordovician.

Several perceptive observations of Simon (1987) prompted Wickman (1988) to suggest that an impact structure existed at Lockne. The impact was identified by Lindström et al. (1991). Experience that was decisive for the interpretation was gained through the study of the roughly co-eval Tvären crater (Lindström et al., 1994).

A data base with over 2,000 outcrops and 6 drill-cores could be used for drawing the geological map of Lockne. Critical features are frequently well exposed. Geophysical data include gravimetry, magnetometry, resistivity, and shallow seismics from the reconnaissance phase. The regional biostratigraphy was well-known through the work of Thorslund (1940). For precise dating we relied on conodonts and chitinozoans (Grahn and Nölvak, 1993). Quartz grains with PDF were identified by Therriault and Lindström (1995).

Middle Ordovician Dalby Limestone was deposited at the site immediately before and after the impact. The crystalline basement formed a practically horizontal surface that is commonly called the Subcambrian peneplain. The sediment cover was 80 m thick, the upper 50 m consisting of lithified, bedded limestone of Early and Middle Ordovician age, whereas the lower part was Cambrian bituminous mud. A 12 km wide crater was excavated in the basement. A 2.5 km wide outer zone of this crater is raised 50-80 m above the Subcambrian peneplain. This zone has a small-scale topography of hillocks and hollows, and numerous outcrops of shattered crystalline bedrock and monomictic breccia. Inside of this zone the crater deepens rapidly. The deepest drilling met with monomictic breccia at 313 m, which is 370-400 m below the level of the present crater margin (Lindström et al., 1996). The existence of a central uplift is inferred from geophysical modelling (Sturkell and Ormö, 1998; Sturkell et al., 1998) and the report on a percussion-drilled water-well.

Sturkell (1998) pointed out what appears to be a roughly 5 km wide, surrounding zone in which successively deeper levels of the cover sediments are eliminated as one proceeds toward the crater. The crystalline basement of the Subcambrian peneplain of this zone is apparently unaffected by the impact.

No coherent melt rock has been identified, but ejected, sand-sized melt fragments form 5-20% of the uppermost resurge deposit (Simon, 1987). The fragments are strongly vesicular. One can conclude that much melt did form, but it was ejected and comminuted by explosive force that was probably connected with the watery environment.

No polymictic impact breccia or fall-back deposit has been identified.

The first sediment to enter the newly formed crater was a slurry of bituminous mud that must have come from the crater margin (the term "rim" is intentionally avoided). This happened so early (Sturkell, 1998) that modification of the crater would still have been going on. Isolated occurrences of bituminous mudstone, some with basal conglomerate and substratum basement, occur in the outer crater zone. They are suggested to have been introduced through collapse of the crater margin early in the modification stage, before the outer zone was raised above the level of the Subcambrian peneplain.

The resurge of the sea after impact carried ejecta together with sediment eroded from the surrounding sea-bed. The resurge deposits include bouldery breccias and, at an upper level, sandy to silty, turbidite-like beds ("Loftarsten"). Their total thickness in the deepest part of the crater is at least 100 m (excluding bituminous mudstone breccia). The bouldery breccias are dominated by limestone clasts. The matrix is argillaceous and apparently derived from mud intercalated between the limestone beds. The clasts contain microfossils, such as conodonts (Simon, 1987). Resurge deposits occur extensively in areas that surround the crater, but they are much thinner there.

The 2.5 km wide outer zone of the crater is cut through by radially arranged resurge gullies that deepen towards the central crater. These gullies reach depths of tens of m and widths about 1 km. They are expected to be a significant feature of craters formed in water that is at least 100 m deep but might be absent from craters formed at depths of 50 m and less. The reason for this distinction is that the rim wall of craters formed in shallow water is expected to protect against the assault of moderate resurge. The Middle Ordovician Ames crater (Carpenter and Carlson, 1992) might illustrate this principle.

Deposition of the Dalby Limestone recommenced after the resurge and ultimately filled most of the crater. The Lockne crater had become entirely covered by Ordovician and probably also by Silurian sediments by the time in the Silurian to Devonian, when Caledonian eastward overthrusting covered the region with nappes. An outlier of the lower-most local overthrust unit is preserved within the crater. The rest of the nappe cover has been removed from the crater by erosion, but overthrusts occur throughout the sedimentary

cover to the west of the crater. The nappes have travelled only short distances and contain excellent outcrops of resurge deposits and some ejecta evidently too large to be moved by the resurge (Sturkell, 1998). The crater itself was not much affected by the Caledonian orogeny. It was slightly tilted westwards, so that the eastern margin became eroded. Two minor, northeast-verging thrust-faults affect the outer zone of the crater without, however, modifying its gross outline.

To sum up, Lockne provides one of the finest areas to look for Swedish nature, Lower Paleozoic sediments and fossils, Caledonian marginal thrust tectonics, and a reasonably exposed case of impact cratering at sea.

#### References

- Carpenter, B.N. and Carlson, R. (1992) The Ames impact crater. *Oklahoma Geology Notes, Oklahoma Geological Survey* **52**: 208-223.
- Grahn, Y. and Nölvak, J. (1993) Chitinozoan dating of Ordovician impact events in Sweden and Estonia. A preliminary note. *Geologiska Föreningens i Stockholm Förhandlingar* **115**: 263-264.
- Lindström, M., Ekvall, J., Hagenfeldt, S.E., Säwe, B. and Sturkell, E.F.F. (1991) A well-preserved Cambrian impact exposed in Central Sweden. *Geologische Rundschau* **80**: 201-204.
- Lindström, M., Flodén, T., Grahn, Y. and Kathol, B. (1994) Post-impact deposits in Tvären, a marine Ordovician crater south of Stockholm, Sweden. *Geological Magazine* **131**: 91-103.
- Lindström, M., Sturkell, E.F.F., Törnberg, R. and Ormö, J. (1996) The marine impact crater at Lockne, central Sweden. *Geologiska Föreningens i Stockholm Förhandlingar* **118**: 193-206.
- Simon, S. (1987) Stratigraphie, Petrographie und Entstehungsbedingungen von Grobklastika in der autochthonen, ordovizischen Schichtenfolge Jämtlands (Schweden). *Sveriges Geologiska Undersökning C* **815**: 1-156.
- Sturkell, E.F.F. (1998) The origin of the marine Lockne impact structure, Jämtland. *Meddelanden från Stockholms Universitets Institution för Geologi och Geokemi* **296**: 1-32.
- Sturkell, E.F.F. and Ormö, J. (1998) Magnetometry of the marine, Ordovician Lockne impact structure, Jämtland, Sweden. *Journal of Applied Geophysics* **38**: 195-207.
- Sturkell, E.F.F., Ekelund, A. and Törnberg, R. (1998) Gravity modelling of Lockne, a marine impact structure in Jämtland, central Sweden. *Tectonophysics* **296**: 421-435.
- Therriault, A. and Lindström, M. (1995) Planar deformation features in quartz grains from the resurge deposits of the Lockne structure, Sweden. *Meteoritics* **30**: 700-703.
- Thorslund, P. (1940) On the Chasmops Series of Jemtland and Södermanland (Tvären). *Sveriges Geologiska Undersökning C* **436**: 1-191.
- Wickman, F.E. (1988) Possible impact structures in Sweden. In: *Deep Drilling in Crystalline Bedrock, I. The Deep Gas Drilling in the Siljan Impact Structure, Sweden and Astroblemes*, A. Bodén and K.G. Eriksson (eds.), Springer, Berlin, pp. 298-327.

## **The Cretaceous-Tertiary Event: Impact Spherules and Geochemical Signatures from Areas of SE Spain and Site 1049 (ODP Leg 171B)**

F. Martinez-Ruiz<sup>1</sup>, M. Ortega Huertas<sup>2</sup>, and I. Palomo<sup>2</sup>.

1) Instituto Andaluz de Ciencias de la Tierra. Facultad de Ciencias. Campus Fuentenueva. 18002, Granada, Spain. (fmrui@goliat.ugr.es); 2) Dpto. Mineralogía y Petrología. Facultad de Ciencias. Campus Fuentenueva. 18002, Granada, Spain.

Since Alvarez et al. (1980) proposed a meteorite impact as the cause of the mass extinction at the end of the Cretaceous, such an event has been one of the most discussed topics in the Earth Sciences. Many scientists now accept the existence of an impact in the Yucatan Peninsula, Mexico, which had a global effect and was responsible for the massive extinction. However, the global role of the K/T impact is still subject to debate (e.g. Glasby and Kunzendorf, 1996). We have compared geochemical signatures from the K/T boundary layer in distal and proximal locations to the Chicxulub structure in the Yucatan Peninsula to evaluate extraterrestrial contamination and the worldwide distribution of impact signatures. The studied sections were at Agost and Caravaca (SE Spain), and the K/T boundary section recovered by ODP Leg 171B at Blake Nose (NW Atlantic).

The Agost and Caravaca sections are located in SE Spain in the Betic Cordillera, which is part of the peri-Mediterranean Alpine orogenic belt. Cretaceous material here comprises light-green marly limestones mainly composed of calcite, quartz and clay minerals (smectite, illite and kaolinite). These materials are capped by a sharp contact with a smectite layer 2-3 mm thick marking the boundary. On top of the K/T boundary layer, greenish marly clays were deposited that gradually increase in carbonate content to marl and marly limestones of lighter color. The boundary layer material is diagenetically altered, with the alteration being more intense at the Caravaca section, where this layer appears with typical brownish-red color. At Agost, in contrast, this layer is dark green with red shades. Abundant spherules confined to the boundary layer are diagenetically altered to Fe-oxides and K-feldspar at Agost and to K-feldspar at Caravaca (Martinez-Ruiz et al., 1997). At Blake Nose a biostratigraphically complete K/T boundary interval was recovered at Site 1049 consisting of green spherical and oval-shaped spherules altered to smectite. This layer sharply overlies slumped uppermost Cretaceous foraminiferal-nannofossil ooze and is overlain by a Tertiary clay-rich ooze with planktonic foraminiferal assemblages indicative of the Early Danian (Norris et al., 1998).

Sediments from the K/T boundary layers and sediments above and below were sampled for mineralogical and geochemical analyses using X-ray diffraction (XRD), scanning electron microscopy (SEM), transmission electron microscopy (TEM), atomic absorption (AA), inductively coupled plasma-mass spectrometry (ICP-MS) -at Scientific Instrumental Centre of the University of Granada- and neutron activation (NA). Spherules were separated by sieving

and hand-picking at Agost and Caravaca and cleaned ultrasonically, then prepared for morphological studies and SEM-EDS/EMPA analyses. A representative amount was also ground for chemical analyses by ICP-MS. Geochemical and mineralogical studies focused on the impact-related material and the elements that could support extraterrestrial contamination. Geochemical analyses results from the K/T boundary and background sediments are shown in Table 1.

Samples	Fe <sub>2</sub> O <sub>3</sub>	Cr	Co	Ni	Cu	Zn	Au	Ru	Rh	Pd	Os	Ir	Pt
T Caravaca	1.99	55	6	39	16	58	<1	<1	<1	<1	<1	<0.1	<1
K/T Caravaca	13.00	851	427	1527	203	1480	19.9	37.9	9.6	35.9	27	35.2	76.9
C Caravaca	1.76	44	9	47	12	58	<1	<1	<1	<1	<1	<0.1	<1
K-fs spherules		220	136	518	225	1043							
T Agost	2.34	65	4	35	11	75	<1	<1	<1	<1	<1	<0.1	<1
K/T Agost	11.18	737	212	804	379	927	23	43	12	27	5	24.4	26
C Agost	1.66	45	4	31	8	37	<1	<1	<1	<1	<1	<0.1	<1
Fe-ox spherules		144	334	3672	1856	3483							
T Blake Nose	1.36	73	11	23	<5								
K/T Blake Nose:													
1-3 below top K/T	3.06	64	155	246	23								
3-5 below top K/T	3.04	75	206	292	15								
9-11 below top K/T	3.63	76	34	48	20								
C Blake Nose	1.50	42	34	44	6								

Fe<sub>2</sub>O<sub>3</sub> in %, Au and PGE in ppb and others in ppm. T: Tertiary background, C: Cretaceous background.

Table 1. Geochemical data from the K/T boundary, Cretaceous and Tertiary sediments.

K-feldspar and Fe-oxides spherules from the Agost and Caravaca sections show similar morphologies and textures. Their size usually ranges from 100 to 500 μm. Morphologies are similar to microtektites. Spheres and droplet shapes are common. They present crystalline textures and crystals are arranged with fibroradial and dendritic textures similar to quench-crystal textures (Martinez-Ruiz et al., 1997). The Blake Nose spherules are usually 100-1000 μm and no internal textures are observed. TEM observation show smectites forming from amorphous precursor.

The presence of impact-related spherules in the K/T boundary layers is one of the strongest pieces of evidence for the K/T impact event. Spherules from sections around the Gulf of Mexico have been reported and studied by many authors (e.g. Izett, 1991; Koeberl and Sigurdsson, 1992) since the early nineties, when Chicxulub was identified as the K/T impact crater. In this area the K/T boundary interval mostly represents the ejecta curtain while at distal locations there are major contributions of the warm fireball with the vaporized

bolide (Alvarez et al., 1995). Thus, glassy spherules altered to smectite at Blake Nose indicate the rapid cooling of the ejecta curtain, while the crystalline nature of the spherules and their textures at Agost and Caravaca suggest they derive from the more energetic part of the ejecta with significant extraterrestrial contribution. Such a contribution is also supported by the PGE and Ni enrichment in K-fs-spherule cores (Martinez-Ruiz et al., 1997).

Different geochemical compositions at proximal and distal locations also support the different nature of the impact-generated material. At Blake Nose no significant extraterrestrial element enrichment is observed. Ir content reaches 1.3 ppb in the upper part of the boundary layer (Smit et al., 1997), and even with low concentrations higher Cr, Co and Ni contents are also observed in the upper 4 cm of this layer at Hole 1049A, suggesting that the extraterrestrial elements are concentrated in the upper interval. On the other hand, PGE concentrations at Agost and Caravaca (Kyte et al., 1985; Smit, 1990; Martinez-Ruiz et al., 1992) suggest a more important bolide contribution. Fe, Ni, Co and Cr are also enriched in the boundary layer. Fe-oxides spherules are enriched in both terrestrial and extraterrestrial trace metals, indicating scavenging and adsorption of these elements during diagenetic alteration. However, Cr is not enriched in these spherules in relation to the boundary layer, indicating that the fine fraction is an effective carrier for extraterrestrial elements as has also been suggested for Ir (Alvarez et al., 1995). Trace-element concentration at Caravaca shows an enrichment of extraterrestrial elements in the boundary layer relative to the spherules. If Fe-oxides spherules originated they were altered and such elements are concentrated in the alteration phases. At Agost the original spherule material would have been enriched in extraterrestrial elements although concentrations would have been enhanced by Fe-oxide precipitation.

#### Acknowledgements

This work was supported by Project PB96-1429 (DGES, Spain) and Research Group RNM0179 (P.A.I.).

#### References

- Alvarez, L.W., Alvarez, W., Asaro, F. and Michel, H.V. (1980) Extraterrestrial cause for the Cretaceous/Tertiary extinctions. *Science* **208**: 1095-1108.
- Alvarez, W., Claeys, P. and Kieffer, S. (1995) Emplacement of Cretaceous-Tertiary boundary shocked quartz from Chicxulub crater. *Science* **269**: 930-935.
- Glasby, G.P. and Kunzendorf, H. (1996) Multiple factors in the origin of the Cretaceous/Tertiary boundary: the role of the environmental stress and deccan trap volcanism. *Geol. Rundschau* **85**: 191-210.
- Izzet, G.A. (1991) Tektites in Cretaceous-Tertiary boundary rocks on Haiti and their bearing on the Alvarez impact extinction hypothesis. *J. Geophys. Res.* **96**: 20,879-20,905.
- Koeberl, C. and Sigurdsson, H. (1992) Geochemistry of impact glasses from the K/T boundary in Haiti: Relation to smectites and a new type of glass. *Geochim. Cosmochimica Acta* **56**: 2113-2129.

- Kyte, F.T., Smit, J. and Wasson, J.T. (1985) Siderophile interelement variations in Cretaceous-Tertiary boundary sediments from Caravaca, Spain. *Earth Planet. Sci. Letters* **73**: 183-195.
- Martinez-Ruiz, F., Ortega-Huertas, M., Palomo, I. and Acquafredda, P. (1997) Quech textures in altered spherules from the Cretaceous-Tertiary boundary layer at Agost and Caravaca, SE Spain. *Sedimentary Geology* **113**: 137-147.
- Martinez-Ruiz, F., Ortega-Huertas, M., Palomo, I. and Barbieri, M. (1992) The geochemistry and mineralogy of the Cretaceous-tertiary boundary at Agost (southeast Spain). *Chemical Geology* **95**: 265-281.
- Norris, R.D., Kroon, D., Klaus, A. et al. (1998) *Proc. ODP, Init. Repts.*, 171B: College Station, TX (Ocean Drilling Program).
- Smit, J. (1990) Meteorite impact, extinction and the Cretaceous-Tertiary boundary. *Geol. Mijnbouw* **69**: 187-204.
- Smit, J., Rocchia, R., Robin, E. and ODP Leg 171B shipboard party. (1997) Preliminary Iridium analyses from a graded spherule layer at the KT boundary and late Eocene ejecta from ODP Sites 1049, 1052, 1053, Blake Nose, Florida. *Geol. Soc. Amer. Ann. Meet.* **29**: A-141.

## **The Kaluga Impact Event and its Proven and Possible Geological Consequences**

V.L. Masaitis.

Karpinsky Geological Institute, Sredny prospekt 74 St.-Petersburg, 199106, Russia  
(vcmsts@duxnet.spb.ru).

### Introduction

The about 380 Ma (Harris, 1962) Kaluga impact crater is located in the central part of the East European plain. This crater gives the opportunity to study proven proximate and probable distant geological consequences of asteroid impacts in a marine setting. The present analysis is based on published drilling data (Kazman and Tikhomirov, 1962) and other materials obtained in former time, as well as on the examination of the thin sections from the core. The Kaluga ring structure was discovered by geophysical observations and drilling, and originally considered as volcano-tectonic (Petrov, 1969) and only later recognized as impact crater (Masaitis, 1973; Masaitis et al., 1980).

### Buried crater

The inner depression is surrounded by a rim and filled with an allogenic polymict breccia and impactites (suevites and minor tagamites). The target consists of Archean and Lower Proterozoic crystalline rocks (schists, gneisses, granites), which are covered by sedimentary sequence of Upper Proterozoic argillites and siltstones (125 m) and Middle Devonian (lower horizon) clays, siltstones, sandstones and clayey sulfate-carbonate rocks (50 m). This lower horizon of Middle Devonian was in the vicinity of impact site already entirely

disturbed and redeposited at the time of impact event. The crater is buried under the Middle (upper horizon), Upper Devonian and Lower Carboniferous beds with a total thickness of about 800 m. These beds reach a higher thickness within the circular depression and outside it, yet are thinner above the buried rim. According to seismic data the crater depression with a rim to rim diameter of 15 km has a true depth about of 450-500 m. Drilling data show that the well preserved rim has the true height of about 250-300 m and a width about of 6 km. Its inner slope is partly subsided due to slumping along series of arcuate faults. Thus, the diameter of the structure originally was smaller (about of 12-13 km) and the rim was higher. A shallow annular subsidence of the bedrock with a diameter about of 23 km and an amplitude of about 50-80 m is traced outside the rim. The latter is composed of imbricated and overthrust rocks of crystalline basement and Upper Proterozoic and Middle Devonian sedimentary cover. The uplifted blocks are overlain by polymict (mostly crystalline) breccia, containing in places admixtures of impact glass fragments. The thickness of this allogenic breccia varies from some tens to 100 m. In turn this breccia is covered by a resurgent sequence, mostly a sedimentary breccia. This breccia may be absent on the rim crest, but usually its thickness increases on the outer and inner slopes of the rim, reaching up to 150-170 m.

The crater filling has been drilled only nearby the rim. In the upper part, it consists of the resurgent breccia (175 m) carrying mostly fragments of the Middle Devonian sediments, on top of suevites (85 m), containing lenses of tagamites (up to 10-20 m thick). The suevites grade into a monomict crystalline allogenic breccia, where drilling was stopped. All these rocks display numerous shock features such as diaplectic minerals and glasses. Fragments of impact melt glass in the suevites are altered by secondary processes. Remnants of polymict allogenic breccia (including suevite lenses) are also found in the annular subsidence up to a distance of about 12 km from the rim. Outside the crater, this breccia is underlain by disturbed Middle Devonian sediments and reach a thickness from 155 to 40 m's correspondingly. In the studied area around the crater, this polymict impact breccia and the disturbed bedrock are covered by a resurgent sedimentary breccia similar to that found in the crater interior. Its thickness is about of 100-130 m at the distance of 7-8 km from the rim and 50 m at the distance of 12 km. Disturbance and brecciation of the Middle Devonian bedrock sandstones may be traced up to the distance of 15-20 km from the rim crest. This resurgent breccia is composed of reworked and re-deposited sedimentary material and of distant ejecta with admixture of fragments and particles of crystalline rocks and impact glass. A significant part of this breccia originated by reworking of non-solidified clayey and limy mud, derived from the surrounding shallow sea bottom at the time of impact. The breccia grades upward into layers of claystones; the maximal thickness of these layers is about 130 m

#### Transient crater

Well bedded sedimentary target rocks in blocks adjacent to the crater rim permit reconstruction of the sequential displacements in opposite directions: At first displacement was centrifugal, accompanied by ejection and deposition of the polymict allogenic breccia, and second centripetal, caused by slumping

and formation of secondary terraces on the inner slope of the rim. The initial height of the structural uplift of the target rocks is evaluated to be on the order of about 500 m, but this uplift was built up by ejected material with an original thickness about of 150-200 m. Thus the transient rim had a height close to 700 m, but this feature was destroyed in a moment by slumping and by action of the resurgent wave. The maximum amplitude of this slumping was about 400 m causing an increase in the apparent crater diameter.

It is probable, that the Kaluga crater is a complex impact structure as a central uplift is suspected, but not revealed. The irregularities in the thickness of the uppermost Devonian and Carboniferous layers show that slow subsidence of the crater floor in the annular trough may have continued during 30-40 Ma years probably due to compaction of loose and brecciated basement rocks.

#### Probable distant effects

According to biostratigraphic data of the age of youngest disturbed beds in the vicinity (Kazman and Tikhomirov, 1962; Petrov, 1969; Tikhomirov, 1995), the Kaluga impact event occurred in the Middle or Upper Eifelian (the end of so called Mosolovo time). Isotopic dating on melt rock indicate an age of 380 Ma (Harris, 1962). At this time, the extensive areas of East European craton were occupied by epicontinental sea, which in places were of high salinity (Tikhomirov, 1995; Kruchek, 1974; Kurss, 1992; Utekhin, 1972). About twenty years ago Dr. Motuza has suggested (pers. communication) that the sedimentary sequences of this sea may contain some distant traces of the Kaluga impact event.

In the Baltic countries (Estonia, Latvia, Lithuania) and adjacent areas of northwestern Russia and Belarus, the so-called Narva breccia is widely distributed in the Middle Devonian sections, which were studied by drilling (Kurss, 1975, 1992; Narbutas et al. 1964). This breccia is composed of angular or partly rounded, up to 10 cm large fragments of solid gypsum-containing dolomites, marls and rare sandstones submerged into dolomite clay. The fragments are irregularly dispersed, some of them are coated by banded clay and marl. Rock fragments with bedding display small faults or are corrugated in places. Small faults and folds disturb also the sandstone layer at the breccia base. The thickness of the breccia varies from tens of cm up to several meters, the brecciation and disturbances attenuate upward.

Stratigraphic correlations (Kruchek, 1974; Kurss, 1975, 1992; Narbutas, et al., 1964) indicate that the Narva breccia corresponds to the so-called Morsovo-Mosolovo formation in the vicinity of the Kaluga crater, where it is strongly disturbed. The fragments of composing sedimentary rocks (clays, marls, dolomites, gypsum etc.) are included in the allogenic breccia and made the predominant part of the resurgent breccia in the crater vicinity.

Most authors have supposed that the Narva breccia originated due to subaqueous slumping of slurry mud on the sea bottom caused by earthquakes especially there, where the bottom gradient was steeper. In fact, the impact event may cause seismic shock and tsunami waves, that affected areas at a distance of some hundred km from the point of the impact. The Kaluga impact

event with an energy release of about  $10^{27}$  J have had a seismic magnitude about of  $M=7.5$ . Despite the attenuation at a distance of some hundred km, the shock may have been sufficient to induce slumping of non-consolidated sediments. Some other consequences of the Kaluga event may probably be found in the Middle Eifelian sections at this stratigraphic level in this part of the East European plain. For example, an erosional unconformity at the corresponding level is established in Upper Eifelian sections in the central Russia. These sections, however, have not been studied under this aspect so far.

#### Conclusion

At present, several synchronous formations related or probably related to the Kaluga impact event may be distinguished. They are located within the crater depression, on the rim crest, in the vicinity of the crater, at a distance of about 10-15 km from the crater rim, and at a distance of some hundred km. The absence of any visible traces of impact in between the last two areas may be caused by peculiarities of the propagation of seismic waves, by marine erosion or simply by insufficient study of the corresponding stratigraphic level. Each section is clearly distinct from the other and the respective lithologies reflect different processes (deposition of ejecta and disturbances of the base, shock induced slumping of mud, rewashing and redeposition of ejecta by resurgent wave, settling of small clasts and glass particles from dust cloud etc.). In fact, the examination of the Narva breccia recently leads to the discovery of shocked quartz which was recovered from a drillcore by the Lithuanian student A. Rimša (pers. comm.). It is probable, that a careful study of the appropriate core sections in the vicinity of the crater, and especially at long distances by stratigraphic, sedimentological and geochemical methods will give more evidences for the relation of the respective formations to the Kaluga impact event.

#### References (in Russian)

- Harris, M. A. (1962) The experience of using the K-Ar method for age measurement of iron pyrite ores of the South Ural. In: *Trans. X session Commission of measurement of absolute age of geological formations*, pp. 184-185.
- Kazman, A.V. and Tikhomirov, S.V. (1962) The results of prospecting drilling on the Kaluga area. *Trans. of SGPK 3*: 47-66.
- Kruchek, S.A. (1974) On the structure and correlation of the Narova horizon of the Middle Devonian (northeastern Belarus). In: *Problems of the geochemical and geophysical study of the Earth crust*, RISO Ac. Sci. BSSR Press, Minsk, pp. 155-160.
- Kurss, V.M. (1975) Lithology and mineral resources of the terrigenous Devonian of the Main Devonian Field. *"Zinantne" Press*, Riga, p 223.
- Kurss, V.M. (1992) The Devonian terrigenous sedimentation on the Main Devonian Field. *"Zinantne" Press*, Riga, p. 208.
- Masaitis, V.L. (1973) Geological consequences of the impacts of crateriforming meteorites. *"Nedra" Press*, Leningrad, p. 18.
- Masaitis, V.L., Danilin, A.N., Mashchak, M.S. et al. (1980) The geology of astroblemes. *"Nedra" Press*, Leningrad, p. 231.

- Narbutas, V.V., Vasiljauskas, V.M and Korkutis, V.A. (1964) New data on the knowledge of paleogeography and tectonics of the South Baltic region at the Early and Middle Devonian. In: *Questions of stratigraphy and paleogeography of the Devonian Baltics*, "Mintis" Press, Vilnius, pp. 113-123.
- Petrov, V.G. (1969) The peculiarities of the interior of the Kaluga structure. *Bull. Moscow Explor. Soc.* **6**: 36-42.
- Tikhomirov, S.V. (1995) The stages of the Devonian sedimentation at the Russian platform and general questions of the evolution and structure of the stratisphere. "Nedra" Press, Moscow, p. 445.
- Utekhin, D.N. (1972) New data on the Devonian lithology and paleogeography of the Voronezh uplift. In: *Lithology and paleogeography of the Paleozoic deposits of the Russian platform*, "Nauka" Press, Moscow, pp. 93-103.

## **The Tore "Sea-Mount": A possible Megaimpact Crater in the Deep Ocean**

J.F. Monteiro, A Ribeiro, and J. Munha.

Departamento de Geologia FCUL, Universidade de Lisboa Portugal (jfmonte@fc.ul.pt).

The Tore "Sea-Mount" (Laughton et al., 1975) is considered to be an impact crater due to its peculiar morphology; it has an elliptical shape (122 km long by 86 km wide), with a central depression (5 km deep) and an elevated rim at about 2 km deep. The major axis (N22°E) is oblique to magnetic anomaly MO, but parallel to younger magnetic anomalies to the West.

Other possible origins may be excluded by the following reasons: a giant caldera origin seems unlikely because the "Sea-Mount" is located in oceanic crust of basaltic composition; an origin by the intersection of regional tectonic trends doesn't explain the scarp in the SW rim of the "Sea-Mount"; thus, the alternative to impact is an unknown mechanism (cryptoexplosion?) that remains to be proven. Recent studies (Monteiro et al., 1998) do indeed support the megaimpact origin.

Ejecta was found in a coastal site (10 km N of Nazaré), 300 km to the East of the Tore "Sea-Mount" (Monteiro et al., 1997). The ejecta occurs on top of brecciated limestone of Cenomanian age (Callapez, 1998) and consists of polymitic breccia that includes suevite-type clasts, diaplectic glasses, microscopic spherules and irregular shard-like structures; some spherules preserve the dumbbell shape typical of microtektites and shocked quartz occur in the matrix of polymitic breccia. All these are textural features diagnostic of impact. The main mineralogy of the breccia consists of pyrite, hematite, devitrified glass, quartz and calcite; solid hydrocarbons also occur as surface accumulations and impregnations occupying the pore spaces of the breccia.

The ejecta occurs along a corridor aligned N80°E, pointing to the Tore "Sea-Mount".

Besides these structural and textural features, a geochemical anomaly was detected both in the ejecta and in a green mudstone layer (0 to 50 cm thick) occurring on top of it (Monteiro et al., 1998); the anomalous elemental concentrations are about 5 to 10 times the average continental crustal abundances and include iridium as well as other PGE.

At Nazaré there is a complete section of Cenomanian-Turonian age (Soares, 1966; Pena dos Reis et al., 1997; Callapez, 1998). Significantly, a sharp stratigraphic discontinuity is observed at the Cenomanian-Turonian boundary, between highly brecciated (Cenomanian) limestones and siliciclastic sandstones (Lousões Formation of Turonian age). We propose that the Lousões Formation reflects a series of complex events resulting from tsunamic activity, related to the disruptive impact event at the end of the Cenomanian. Indeed, the sandstones display several characteristics that are typical of tempestite deposits (lamination and parallel laminated sediments, cross bedding, sand with fossil debris and collapse structures as skin slump blocks).

The genetic link between the Tore "Sea-Mount" and the megaimpact event near the Cenomanian-Turonian boundary (91 My) responsible for the Nazaré ejecta layer and tsunami deposits remain to be established by direct evidence for an impact at the Tore "Sea-Mount". However, the existing chronological constraints are not at all incompatible with this link; indeed, the Tore "Sea-Mount" must be younger than anomaly Mo (118 My), making the impact origin not only possible but probable.

According to scaling crater dimensions the Tore "Sea-Mount" could represent an unique example of a megaimpact structure in the deep ocean. The elliptical shape was not due to very oblique impact, because it would be too much of a coincidence that its long axis would be parallel to younger magnetic anomalies to the West of the "Sea-Mount"; we suggest instead that the original shape was circular and that the actual elliptical morphology was due to subsequent deformation related to compression by ridge push (perpendicular to younger magnetic lineations), in accordance with significant strain within the oceanic lithosphere (Ribeiro et al., 1997).

#### Acknowledgements

This research was supported by FCT grant PRAXIS XXI/BD/9542/96 to J.F. Monteiro.

#### References

- Callapez, P.M. (1998) Estratigrafia e Paleobiologia do Cenomaniano-Turoniano. O Significado do Eixo da Nazaré-Leiria-Pombal. *PhD thesis*, Universidade de Coimbra.
- Laughton, A. et al. (1975) Bathymetry of the Northeast Atlantic: Mid Atlantic Ridge to Southwest Europe. *Deep Sea Research*, pp. 791-810.

- Monteiro, J.F. et al. (1997) Ejecta from Meteorite Impact Near the Cenomanian-Turonian Boundary found North of Nazaré, Portugal. *Papers to 29<sup>th</sup> Lunar Plan. Sci. Conference*, II, p.967.
- Monteiro, J.F., Munhá, J. and Ribeiro, A. (1998) Impact Ejecta Horizon Near the Cenomanian-Turonian Boundary, North of Nazaré, Portugal. *Com. do Inst. Geol. Min.* **84**, Fac. 1, pp. 111-114.
- Pena dos Reis, R. et al. (1997) El paleokars de Nazaré (Cretácico Superior de la Cuenca Lusitana, Portugal). *Geogaceta* **22**, pp. 149-152.
- Ribeiro, A. et al. (1997) The "Tore Sea-Mount": an Elliptic Megaimpact Crater as a Strain Marker in Oceanic Lithosphere. *Abstracts Pres. to the EUG 9*, Strasbourg.
- Soares, A. (1966) Estudo das Formações pós-Jurássicas da região entre Sargento Mor e Montemor-o-Velho (Margem direita do Rio Mondego). *Rev. Fac. Cienc. Univ. de Coimbra* **XL**, 343 p.

## **Recognition of Mid-Frasnian (Early Late Devonian) Oceanic Impacts: Alamo, Nevada, Usa, and Amönau, Hessen, Germany**

J. R. Morrow<sup>1</sup>, C. A. Sandberg<sup>2</sup>, and W. Ziegler<sup>3</sup>.

1) Department of Earth Sciences, University of Northern Colorado, Greeley, Colorado 80639, USA, (jrmorro@bentley.unco.edu); 2) US Geological Survey, Box 25046, MS 939, Federal Center, Denver, Colorado 80225-0046, USA; 3) Forschungsinstitut Senckenberg, D-60325 Frankfurt a.M., Germany.

The oceanic, sub-critical Alamo Impact occurred at, or offshore from, the distal margin of a carbonate platform that fringed the western North American craton during early Late Devonian (middle Frasnian) time. Megabreccia and related deposits resulting from this impact are termed the Alamo Breccia from their location near the present town of Alamo, north of Las Vegas, in southern Nevada. These deposits span several paleotectonic settings ranging from the shallow-water middle shelf to the deeper water outer shelf, slope, and basin. The phenomena related to this possible comet impact are termed the Alamo Impact Event, which is dated by conodonts found below, within, and above the breccia to have occurred during the *punctata* conodont Zone (~370 Ma). Post-Devonian tectonism, erosion, and volcanic cover have largely obscured the original Alamo crater site. Consequently, initial recognition of the Alamo Impact Event and interpretation of its magnitude and extent were based largely on the catastrophic effects of the impact on the nearby carbonate platform. These huge-scale effects include fracturing and delamination of the upper part of the carbonate platform by shock waves prior to its collapse and deposition of the thick (up to 130 m) Alamo Breccia, consisting of a lower carbonate megabreccia (debrite) capped by graded tsunami (turbidite) deposits. Additionally, close to the crater rim, dikes and sills of sandstone containing

fragments of Middle Devonian carbonate and sandstone were injected upward by transitory fluid pressures into at least 300 m of the Middle Devonian carbonate sequence underlying the Alamo breccia (Warme and Sandberg, 1995, 1996; Warme and Kuehner, 1998).

Recently, smaller scale evidence of the impact has been found in deeper water foreslope to basin settings (Sandberg et al., 1997; Morrow et al., 1998). At some localities, isolated exposures of possibly channelized, poorly graded, off-platform, impact debris-flow carbonate breccia, as thick as 35 m, rest disconformably on much older Middle Devonian rocks. These deposits give closure to the three incomplete rings of deposits located on the adjacent carbonate platform and help constrain the possible size of the impact crater. At other deeper water localities, where the breccia is absent, a widespread, regional stratigraphic gap, representing a duration as long as ~8 m.y., separates pre-event Middle Devonian strata from overlying post-event Upper Devonian strata. This widespread gap could be the result of post-impact rebound.

An off-platform location for the impact site was interpreted on the basis of deep-water biofacies (Ziegler and Sandberg, 1990) conodonts and lithoclasts transported into the matrix of the Alamo Breccia on the shallow-water platform (Warme and Sandberg, 1995, 1996). It is important to emphasize that, in the absence of a well-preserved crater, initial recognition of the impact event was based primarily on its shallow-water effects.

Exotic conodont faunas recovered from carbonate-spherule-bearing impact ejecta masses in the upper part of the Alamo Breccia provide a possible constraint on the minimum stratigraphic depth of crater excavation. These faunas, which are Silurian, Ordovician, and possibly as old as Late Cambrian, indicate an impact excavation depth of ~1.5 km. Crater scaling calculations based on this inferred excavation depth indicate that the original Alamo Impact structure may have been 75 km or more in diameter (Morrow et al., 1998). In addition to the huge (as long as 500 m) megabreccia blocks and overlying tsunami deposits that compose the Alamo Breccia, the shattered rock units below it, the carbonate ejecta spherules and ejected conodonts within it, and the stratigraphic gap in laterally adjacent strata, interpretation of the Alamo Impact Event is supported by the occurrence of shocked quartz grains and an iridium anomaly (Laroux et al., 1995; Warme and Sandberg, 1995, 1996; Sandberg et al., 1997; Warme and Kuehner, 1998).

Recent stratigraphic and conodont biostratigraphic work (Ziegler and Sandberg, unpublished data) on an anomalous Frasnian megabreccia near Amönau, Hessen, Germany, suggests an origin similar to that of the Alamo Impact Breccia.

Timing of the Amönau Breccia, which is dated by conodonts as *punctata* Zone or the slightly older *transitans* Zone, is also closely similar to that of the Alamo Breccia. Heretofore, the Amönau Breccia, which contains large blocks derived from a Devonian carbonate reef, mixed with basalt clasts and glass shards, was interpreted to have resulted from carbonate-platform collapse produced

by a volcanic explosion (Bender et al., 1984). Now, additional investigations are being conducted to determine whether this collapse could have been produced by a nearby oceanic impact.

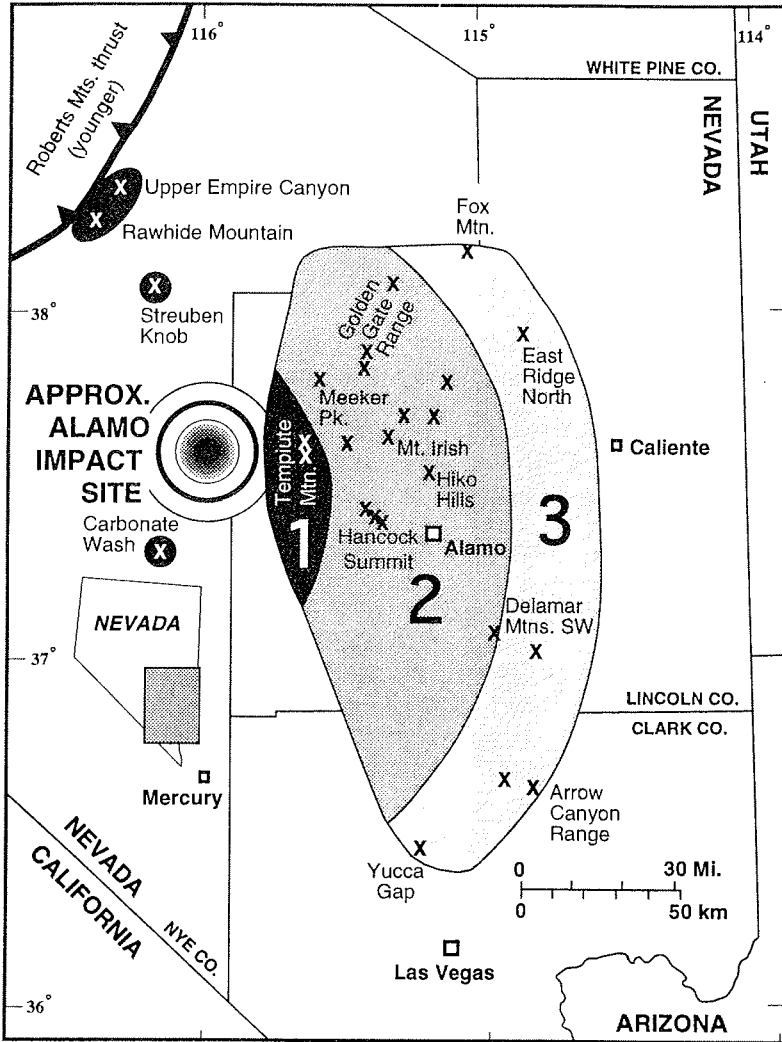


**Figure 1.** -- Alamo Breccia localities in southern Nevada and approximate early Late Devonian (~370 Ma) Alamo Impact site in Proto-Pacific Ocean. Six known deep-water localities shown by black areas. Numbered semicircular rings of Alamo Breccia had these paleotectonic settings: (1) slope to deep basin, (2) deep to middle shelf, and (3) inner shelf (mainly tidal flat). Post-impact Roberts Mountains thrust was emplaced in latest Devonian to Early Carboniferous time.

If an impact origin can be established for the Amönau Breccia, it is likely that at least two closely spaced oceanic impacts occurred adjacent to the Euramerican continent during the middle Frasnian and that these impacts represent part of a comet shower or a series of comet showers. To date, no major biotic turnover or mass extinction pulses have been directly linked with these mid-Frasnian extraterrestrial events. However, their approximate timing with onset of the late Frasnian tropical marine ecosystem collapse and stepwise extinction that culminated ~3 m.y. later at the Frasnian-Famennian (F-F, mid-Late Devonian) boundary suggests that they could have played a role in the initial environmental destabilization preceding the crisis. A similar relationship between multiple, closely spaced sub-critical impacts and onset of ecosystem collapse was proposed by Poag (1997) for the late Eocene to early Oligocene interval, where documented late Eocene impacts preceded the earliest Oligocene global biotic crisis by ~2 m.y.

#### References

- Bender, P., Hühner, G., Kupfahl, H.-G. and Voutta, U. (1984) Ein Mitteldevon/Oberdevon-Profil bei Amönau auf Bl. 5018 Wetter (Hessen). *Geologisches Jahrbuch Hessen* **112**: 31-65.
- Laroux, H., Warne, J.E. and Doukhan, J.C. (1995) Shocked quartz in the Alamo breccia, southern Nevada: Evidence for a Devonian impact event. *Geology* **23**: 1003-1006.
- Morrow, J.R., Sandberg, C.A., Warne, J.E. and Kuehner, H.-C. (1998) Regional and possible global effects of sub-critical Late Devonian Alamo impact event, southern Nevada, USA. *J. British Interplanet. Soc.* **51**: 451-460.
- Poag, C.W. (1997) Roadblocks on the kill curve: Testing the Raup hypothesis. *Palaïos* **12**: 582-590.
- Sandberg, C.A., Morrow, J.R. and Warne, J.E. (1997) Late Devonian Alamo impact event, global Kellwasser Events, and major eustatic events, eastern Great Basin, Nevada and Utah. Brigham Young University *Geology Studies* **42(1)**: 129-160.
- Warne, J.E. and Kuehner, H.-C. (1998) Anatomy of an anomaly: The Devonian catastrophic Alamo impact breccia of southern Nevada. *Intern. Geol. Rev.* **40**: 189-216.
- Warne, J.E. and Sandberg, C.A. (1995) The catastrophic Alamo Breccia of southern Nevada: Record of a Late Devonian extraterrestrial impact. *Courier Forschungsinstitut Senckenberg* **188**: 31-57.
- Warne, J.E. and Sandberg, C.A. (1996) Alamo megabreccia: Record of a Late Devonian impact in southern Nevada. *GSA Today* **6(1)**: 1-7.
- Ziegler, W. and Sandberg, C.A. (1990) The Late Devonian standard conodont zonation. *Courier Forschungsinstitut Senckenberg* **121**: 1-115.

## Geological Characteristics of Marine-Target Craters

J. Ormö<sup>1</sup> and M. Lindström<sup>2</sup>.

1) International Research School of Planetary Sciences, Università d'Annunzio, 65127 Pescara, Italy (jens.ormo@geo.su.se); 2) Dept. of Geology, Stockholm University, 10691 Stockholm, Sweden.

Cosmic impacts on Earth most often occur at sea, but knowledge about impact processes and craters is based mainly on laboratory experiments, extraterrestrial cases, and on terrestrial land impacts. An evidence for a marine-target crater is when marine sediments of the same facies were deposited at the site immediately before and after the impact. A few of the worlds craters have been known to have formed at sea, e.g. the famous Chicxulub crater in Mexico. In recent years, five craters in Baltoscandia have been understood to have formed in an epicontinental paleo-sea. They constitute about one third of the known marine-target craters on Earth. They have the advantages of being accessible to studies on land and/or with core drillings. Furthermore, together with two North American craters, they are all of about the same Ordovician age which allows paleogeographic reconstructions and, thus, comparisons of the effects of different target water depth. The increased number of documented marine-target craters make it possible for the first time to quantify their special geological characteristics. Knowledge of the correct size, morphology, and lithologies of the crater is crucial for the understanding of its formation and calculating the global effects of the event.

Table 1 lists prominent features for a number of marine-target craters. The classification is done after published target water depth in relation to apparent crater size. The Chicxulub crater was left out as its enormous size in relation to the very shallow target water depth (Morgan et al., 1997) makes this structure inadequate as a model for studying the influences of the target water depth on the morphology of craters. The Flynn Creek crater is included as the first crater to have been ascribed a marine formation (Roddy, 1977). Roddy (1977) suggested the water depth to have been shallow and any resurge effects are uncertain although he describes breaches in the rim wall and a thin breccia sequence washed back into the crater. The Brent crater formed nearshore and no resurge broke through the rim wall (Lozej and Beales, 1975). This was also the case at the Ames structure at which the wall rose above the waves and became karstified (Carpenter and Carlson, 1997). The Kamensk crater (Movshovich and Milyavsky, 1990) has been explored by over 330 drillings. There is an inner, 20 km wide crater, surrounded by a 9 km wide zone in which target rocks are crushed and the upper part of the target sedimentary succession is removed. It is crossed by radial furrows that deepen toward the central crater and widen and bifurcate outwards. They are proximally over 100 m deep and filled with allogenic breccia. The very large Chesapeake Bay (Poag, 1997), Montagnais (Jansa, 1993), and Mjølñir craters (Dypvik 1996) have in common that they are still covered by the shelf sea in which they presumably formed. They are well documented through geophysics. There are several drill cores from the Chesapeake Bay structure,

Crater	Published diameter (km)	In this work suggested diam. (km)	Character (suggested in italics)	Age (Myr.)	Resurge deposit (m thick)	Melt sheet	Resurge gullies (number)	Rim wall	Target water depth (m)
Eltanin	0?		cratering in water	2.15	50	-	?		5,000
Lockne	outer 13.5 inner 7.5	outer 24 inner 7.5	complex concentric	455	190	-	4	outer - inner -	>>200
Tvären	2	inner 2 outer? eroded	simple concentric?	457	65	-	?	? eroded	100-150
Granby	3		simple	465	90	-	?	+	50-100
Hummeln	1.2		simple	~465	0?	-	0?	?eroded	25-75
Kärdla	4	outer ~14 inner 4	complex concentric	455	200	-	2	outer - inner +	20-75
Mjölñir	40	outer? 40 (faulted) inner? 16	complex concentric?	~140	45-180?	-?	?	-	300-500
Montagnais	45		complex	50.5	~550?	+	?	-	<600
Chesapeake Bay	90	outer? 90 (faulted) inner? 27	complex concentric?	40-45	400	-	?	-	200-500
Kamensk	20	outer 38 inner 20	complex concentric	65	700	-	12	-	100-200
Ames	15		complex	450-460	0	-?	0	+	10-50
Flynn Creek	3.8		complex	360	<50 ?	-?	?	+ faulted	~10
Brent	4		simple	453	0	+	0	+ eroded	0-25

Table 1. Structures formed by cosmic impacts at sea. Classification after published target water depth in relation to apparent crater size. Eltanin (Gersonde et al., 1997), Lockne (Lindström et al., 1996a. Age: Grahn et al., 1996), Tvären (Lindström et al., 1994. Age: Grahn et al., 1996), Granby (Bruun & Dahlman, 1982. Age: Grahn et al., 1996. Water depth: Lindström et al., 1996b and this paper), Hummeln (Lindström et al., manuscript), Kärdla (Puura & Suuroja, 1992. Age: Grahn et al., 1996. Water depth: Puura & Suuroja, 1992 and Lindström et al., 1996b), Mjölñir (Dypvik et al., 1996. Melt sheet, resurge deposit, and rim wall: Tsikalas et al., 1998), Montagnais (Jansa, 1993), Chesapeake Bay (Poag, 1997), Kamensk (Movshovich & Milyavsky, 1990), Ames (Carpenter & Carlson, 1992. Age: John Repetski (pers. comm.). Water depth: Lindström et al., 1996a and this paper), Flynn Creek (Roddy, 1977), Brent (Lozej & Beales, 1975. Age: Grahn & Ormó, 1995. Water depth: this paper based on Lozej & Beales, 1975).

but there is only one published drill site, with drill-chips and no continuous core, from Montagnais. This makes the amount of melt and suevite proposed by Jansa (1993) uncertain. A 121 m short core drilling from the Mjölñir structure still awaits public documentation. Seismic sounding reveals a large central uplift surrounded by a moat and a peripheral terrain with rotated fault blocks (Dypvik *et al.*, 1996). The Lockne, Kärdla, Granby, Hummeln, and Tvären craters all had targets with sediments, 50-200 m thick, composed of hard Ordovician limestone that rested on weak Cambrian sand and mudstones on top of a crystalline basement. The impacts that formed Granby and possibly Hummeln apparently occurred at a regressive phase of the Ordovician sea (Männil, 1966; Fortey, 1984). The description of Granby, based on drill-cores (Bruun and Dahlman, 1982), contains evidence of slumping and some indication of resurge. Remnants of the rim at the Granby crater show signs of having a preserved overturned flap. The drill core from Hummeln reveals slumped sediments in a similar manner to Granby, but an absence of resurge sediments. Sedimentological and paleoecological evidences indicate that the Kärdla crater formed in a shallow, sublittoral environment (Puura and Suuroja, 1992). Outside the partly destroyed crater rim and radially to a distance about 7 km from the centre of the crater, the sedimentary target stratigraphy gets increasingly more complete. This zone is suggested by Puura and Suuroja (1992) possibly to have formed by ground surge associated with the ejecta curtain during cratering.

At the time of impact the Lockne area was situated on the western margin of an epicontinental sea (Männil, 1966). To the west, the area was transitional to a slope environment. Sedimentologic and palaeoecologic evidence favours a relatively deep shelf position, rather than shallow water for the Lockne impact site (Lindström *et al.*, 1996a). The Lockne crater is concentric with a 7.5 km wide and over 300 m deep central depression (inner crater) in the crystalline basement. The outer crater has a level, 2.5-3 km wide, zone where authigenic breccia occurs as patches and dikes in the fractured crystalline basement. This zone continues in the sedimentary target rocks as a slightly inclined, distinct discontinuity surface where resurge breccia has been deposited on increasingly higher stratigraphic levels. Impact related injections do also occur in this outer zone (Sturkell and Ormö, 1997). At a distance of 45 km from the centre of the structure there is virtually no loss of underlying beds; however an ejecta layer is present (Sturkell *et al.*, manuscript). The steepest inclination of the surface that crosscuts the pre-impact stratigraphy (about 1-2°; Sturkell, 1998) occurs within 12 km from the centre of the structure. No slumping has taken place in the way described from Mjølínir and Chesapeake Bay. We suggest this surface at Lockne to be incorporated in the final crater diameter, because we believe it is a product of the excavation stage. In Table 1 we have applied this interpretation on the other listed craters that show similarities to Lockne in morphology and lithology. The outer crater at Lockne is, like at Kamensk, radially crossed by deep resurge-excavated gullies that are up to 1 km wide, 3 km long and more than 100 m deep. Resurge deposits constitute a large part of the infill of the inner crater and the gullies, but are also widely distributed around the crater. The lower part of the resurge breccia is matrix supported, and is similar to debris flow deposits. The upper part is clast supported, appears to have been transported in suspension, and has a relatively high proportion of crystalline ejecta clasts. This stratigraphy is apparently the result of the ejecta-loaded resurge flowing towards the crater depression, picking up and dragging along material from the fractured sedimentary strata. The Eltanin event (Gersonde *et al.*, 1997) is included as the only documented deep-ocean impact. Apparently the water depth was too great for cratering in the seafloor to occur.

There are obvious differences in both the geology and morphology between impact craters formed on land and at sea. At shallow target water depths, the resulting crater shows features very much resembling those of a land-target impact. When water is present in the target (shallow marine or fluvial environment) a weak rim wall may develop with high pore water pressure. The collapse of such a wall may lead to early intrusion of the open sea. At greater target water depths the resulting crater often lacks melt sheet and a rim wall, is concentric, has a fining-up resurge sequence, and has the outer parts cut by radial gullies eroded by a resurge. The homogenous, flat outer crater zone differs from morphologic features obtained by slumping or by downfaulting of a terraced zone. The rim wall is mainly developed in the water mass. The concentric shape may be the result of the layered target in a similar way as described from small lunar craters in regolith (Quaide and Oberbeck, 1968), possibly in combination with the higher position of the explosion in relation to the preserved part of the crater in the seafloor. Future investigations of marine-target craters must take into consideration the possibilities for an outer shallow

crater when estimating the dimensions. More energy is expended in such a marine impact than revealed by the apparent, and most obvious, inner crater. How much more is a subject to be further studied.

#### References

- Bruun, Å. and Dahlman, B. (1982) Den paleozoiska berggrunden. *Sveriges Geologiska Undersökning Af* **120**: 76-109.
- Carpenter, B.N. and Carlson, R. (1992) The Ames impact structure. Oklahoma Geology Notes, Oklahoma *Geological Survey* **52**: 208-223.
- Carpenter, B.N. and Carlson, R. (1997) The Ames Meteorite-Impact Crater. Oklahoma *Geological Survey Circular* **100**: 104-119.
- Dypvik, H., et al. (1996) Mjølner structure: an impact crater in the Barents Sea. *Geology* **24**: 779-782.
- Fortey, R.A. (1984) Global earlier Ordovician transgressions and regressions and their biological implications. *Palaeont. Contrib. from the Univ. of Oslo* **295**: 37-50.
- Gersonde, R., Kyte, F.T., Bleil, U., Diekmann, B., Flores, J.A., Gohl, K., Grahl, G., Hagen, R., Kuhn, K., Sierro, F.J., Völker, D., Abelman, A. and Bostwick, J.A. (1997) Geological record and reconstruction of the late Pliocene impact of the Eltanin asteroid in the Southern Ocean. *Nature* **390**: 357-363.
- Grahn, Y. and Ormö, J. (1995) Microfossil dating of the Brent meteorite crater, southeast Ontario, Canada. *Revue de Micropaléontologie* **38**: 131-137.
- Grahn, Y., Nölvak, J. and Paris, F. (1996) Precise chitinozoan dating of Ordovician impact events in Baltoscandia. *J. of Micropalaeontology* **15**: 21-35.
- Jansa, L.F. (1993) Cometary impacts into ocean: their recognition and the threshold constraint for biological extinctions. *Palaeogeogr., Palaeoclim., Palaeoecol.* **104**: 271-286.
- Lindström, M., Flodén, T., Grahn, Y. and Kathol, B. (1994) Post-impact deposits in Tvären, a marine Ordovician crater south of Stockholm, Sweden. *Geol. Mag.* **131**: 91-103.
- Lindström, M., Sturkell, E.F.F., Törnberg, R. and Ormö, J. (1996a) The marine impact crater at Lockne, central Sweden. *GFF* **118**: 193-206.
- Lindström, M., Ormö, J., Sturkell, E.F.F. and Törnberg, R. (1996b) Geological information from Ordovician marine impact craters. *GFF* **118 A**: 99-100.
- Lindström, M., et al. The Lower Paleozoic of the probable impact crater of Hummeln, Sweden. *Submitted to GFF*.
- Lozej, G.P. and Beales, F.W. (1975) The unmetamorphosed sedimentary fill of the Brent meteorite crater, southeastern Ontario. *Canad. J. of Earth Sci.* **12**: 606-628.
- Männil, R. (1966) Evolution of the Baltic Basin during the Ordovician. *Eesti, NSV Tead. Akad. Geol. Inst.* (Summary in English), pp. 1-201.
- Morgan, J., Warner, M. and The Chicxulub Working Group (1997) Size and morphology of the Chicxulub impact crater. *Nature* **390**: 472-476.
- Movshovich, E.V. and Milyavsky, A.E. (1990) Morphology and inner structure of Kamensk and Gusev astroblemes. In: *Impact craters of the Mesozoic-Cenozoic boundary*, V.L. Masaitis (ed.), (Summary in English), pp. 110-146. Leningrad: Nauka.

- Poag, C.W. (1997) The Chesapeake Bay bolide impact: a convulsive event in Atlantic coastal plain evolution. *Sedimentary Geology* **108**: 45-90.
- Puura, V. and Suuroja, K. (1992) Ordovician impact crater at Kärddla, Hiiumaa Island, Estonia. *Tectonophysics* **216**: 143-156.
- Quaide, W.L. and Oberbeck, V.R. (1968) Thickness determinations of the lunar surface layer from lunar impact craters. *J. Geophys. Res.* **73**: 5247-5270.
- Roddy, D.J. (1977) Pre-impact conditions and cratering processes at the Flynn Creek crater, Tennessee. In: *Impact and Explosion Cratering*, D.J. Roddy and R.B. Merrill, (eds.), pp. 277-308.
- Sturkell, E.F.F. and Ormö, J. (1997) Impact-related clastic injections in the marine Ordovician Lockne impact structure, central Sweden. *Sedimentology* **44**: 793-804.
- Sturkell, E.F.F. (1998) Resurge morphology of the marine Lockne impact crater, Jämtland, central Sweden. *Geol. Mag.* **135**: 121-127.
- Sturkell, E.F.F., Ormö, J., Nölvak, J. and Wallin, Å. The Lockne marine-target impact characterised through an impact related marker bed. *Submitted to Meteoritics*.
- Tsikalas, F., Gudlaugsson, S.T. and Faleide, J.I. (1998) Collapse, infilling, and postimpact deformation at the Mjølner impact structure, Barents Sea. *Geol. Soc. of Am. Bull.* **110**: 537-552.

## **Mulkarra Impact, South Australia: A Complex Impact Structure.**

J.B. Plescia.

U. S. Geological Survey, 2255 N. Gemini Drive, Flagstaff, AZ 86001. (jplescia@usgs.gov).

### Introduction

Flynn (1989) identified a subsurface structure of the western Eromanga Basin in South Australia that he interpreted as a buried impact crater. Interpretation of an impact origin was based on seismic reflection (Figure 1) and gravity data. Seismic reflection data indicated a disturbed zone ~17 km across surrounding a bowl-shaped zone ~9 km across.

Residual gravity data showed a circular negative anomaly 6-7 km across surrounded by a positive anomaly; total gravity relief was ~ 1 mGal. Flynn's (1989) interpretation was that of a simple 9 km bowl-shaped crater. He did not discuss the nature or origin of the broader 17 km disturbed zone. However, a 9 km diameter is well above the simple-to-complex transition diameter (3 km), making it unlikely that this is a simple crater. Thus, two models may be suggested: (1) impact into unconsolidated marine sediment whose properties affected crater formation such that an unusually large simple crater formed and which disturbed the surrounding sediment to a radius of 8.5 km, or (2) formation of a 17 km structure with a peak ring.

### Geologic Context

The stratigraphic section in which the Mulkarra structure occurs consists of Jurassic and Cretaceous terrestrial and marine sediments unconformably overlying Cambrian-Ordovician age metamorphic basement. In ascending stratigraphic order (decreasing age) the section consists of fluvio-lacustrine sediments including the Hutton Sandstone, Birkhead Formation, and Mooga Formation, overlain by marine sediments of the Cadna-Owie Formation, Bulldog Shale, Coorikiana Sandstone (a shallow shoreface sand which interrupts the marine section) and the Oodnadatta Formation. Above this lies the fluvial and lacustrine Winton Formation. An unconformity separates this section from the overlying Tertiary and Recent aeolian sediments. The only post-Jurassic regional deformation in the area is the Tertiary age northeast-trending Birdsville Track Ridge anticline to the northwest. Seismic reflection data indicate that the strata outside of the structure are flat lying and undeformed. Seismic Reflection Data: A series of orthogonal seismic reflection lines over the region define the structural aspect of the Mulkarra structure (Flynn, 1989). One northeast trending profile (85-ZKM) crosses the structure almost through the center. Additional northeast and northwest trending seismic lines define the remainder of the structure. Figure 1 shows the migrated seismic line 85-ZKM along with the structural interpretation of Flynn. Within the interior, reflectors are broken up into a series of horsts and grabens (~500 m wide) and normal faults with perhaps 50-100 m of offset. The deformed zone is ~17 km across. At the center is a bowl-shaped depression 9 km across overlying incoherent reflectors. Deformation occurs below the Coorikiana Sandstone (the prominent reflector labeled Bx at 750 m depth), but extends through the remaining section and possibly into the basement (1400 m depth). The basement contact is labeled as Z. The shallow depression between shot points 1700 and 1850 was considered by Flynn to mark the bowl-shaped crater.

### Gravity Survey

To better constrain the crustal structure and understand the nature of the Mulkarra structure, gravity data were collected in September 1993 using a Lacoste Romberg meter; elevation control was established using a laser theodolite. Data were collected along eight radial profiles separated by 45° azimuth centered on the gravity anomaly defined by Flynn (1989). The new data were combined with data presented by Flynn (1989) that were collected in 1988 (Busuttil, 1988). The combined set consists of >600 stations.

The uppermost part of the stratigraphic section at Mulkarra is characterized by a seismic velocity of 2.4 km sec<sup>-1</sup>, thus a density of 2.1 g cm<sup>-3</sup> was used in the reduction. The more detailed gravity survey reported here defines a Bouguer gravity field decreasing to the west-southwest, consistent with the broader gravity field of the region defined in Williams (1975). Residual anomaly maps of the area were constructed by removing polynomial surfaces of various orders to the Bouguer gravity and then calculating residual values. These residual maps isolate the anomaly directly associated with the Mulkarra structure.

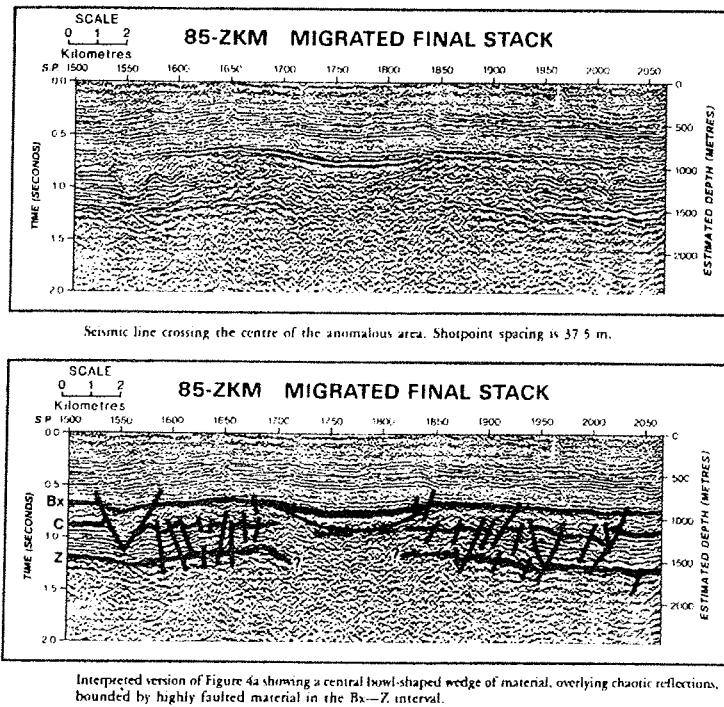


Figure 1 Northeast trending seismic reflection profile across the Mulkarra structure (from Flynn, 1989)

The residual gravity map (Fig. 2), after removing a third-order polynomial surface, shows a central low reaching  $-0.50$  mGal surrounded by an annular high about 7 km in diameter reaching  $+0.5$  mGal; total gravity relief is about 1 mGal. This central zone is then surrounded by an outer gravity low that is somewhat discontinuous. The outer zone reaches lows of  $-1.5$  mGal and has a diameter of 15-16 km (measured to the axis of the outer low) or 20 km (measured to the outer edge of the low). Several of the anomalies around the margin of the map area are probably partly artificial due to the paucity of data at the extreme edges.

#### Interpretation

Gravity and seismic data, along with a general understanding of crater formation, suggest that the Mulkarra structure is not a 9 km simple crater. Rather, the gravity and seismic reflection data indicate it is a 20 km complex crater with a 9 km central pit or peak ring.

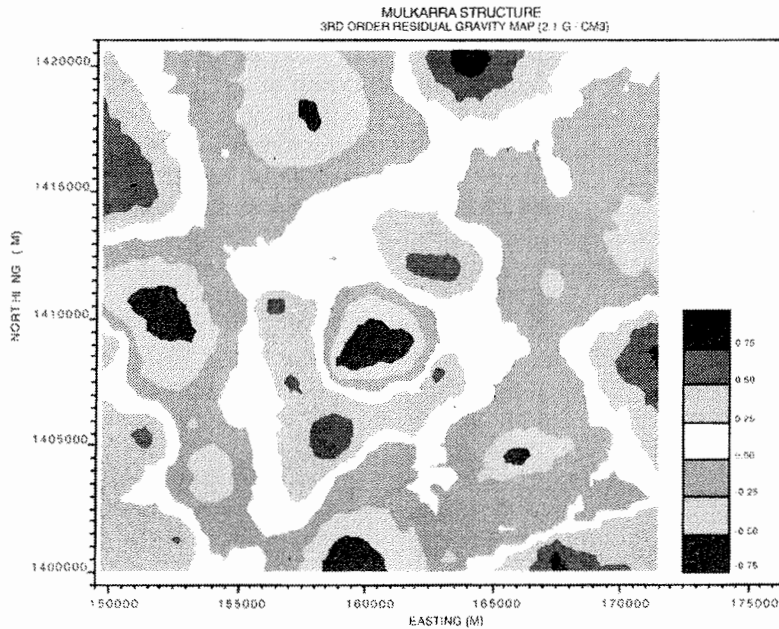


Figure 2 Third-order residual gravity anomaly map of the Mulkarra structure. Contour interval 0.25 mGal.

The stratigraphic context of the structure suggests it was formed in a shallow marine environment in unconsolidated sediments. A 20 km diameter structure is within the complex size range, although the diameter is smaller than the transition diameters for central pits (22 km) and peak rings (25 km) (Pike, 1983). However, as the final form of the crater is controlled by the strength of the material (Melosh, 1989), a low cohesion and low viscosity target (i.e., unconsolidated marine sediments) could result in the onset of a central peak ring at smaller diameters than occur in more competent material.

The Marquez structure in Texas and the Chesapeake structure along the Atlantic coast of Virginia may be analogs for some of the structural characteristics of the Mulkarra impact. Marquez is a 13 - 20 km diameter complex impact crater (Sharpton and Gibson, 1990) which shows only limited deformation in seismic reflection profiles across the structure. Seismic data (Gibson, 1990) show a central peak (characterized by chaotic and incoherent reflectors) and a surrounding annulus where the strata are only mildly deformed. Concentric inward dipping normal faults with <100 m of displacement surround the Mulkarra structure. A well-defined rim does not occur. Buchanan et al. (1998) suggest that as Marquez formed in a marine environment in unconsolidated sediments, the classic bowl-shaped structure with a central peak and well-defined rim did not form. The Chesapeake structure (Poag, 1996, 1997; Koeberl et al., 1996) is a 90 km complex impact structure with a well developed central peak ring 3-6 km in diameter. The

margins of the structure are marked by a set of concentric normal faults and slump blocks, overlain by a breccia layer; the central peak ring is composed of crystalline basement brought up from depth. Younger sediments overly the entire structure. Seismic profiles show no evidence of a topographic crater rim, and the interpretations by Poag (1996, 1997) show no evidence for structural uplift around the margin. As the Chesapeake structure also formed in a marine environment, the unlithified sediments may not have been able to propagate the stresses to form an uplifted rim, and the sediments around the margin of the structure may have simply slid along a basement decollement toward the center in response to the excavation.

Energy scaling and morphometric relations would indicate that a 20 km complex crater would have had a transient crater of about 13-15 km diameter, with a central peak ring of about 8-12 km uplifting material from 4-5 km. Assuming projectiles impacting at 15 km sec<sup>-1</sup>, the projectile would have had a diameter of 1.4 to 1.7 km (assuming densities of 3.5 and 2.5 g cm<sup>-3</sup> respectively). The total energy of the impact would have been of the order 7 x 10<sup>20</sup> J or 1.7 x 10<sup>5</sup> Megatons, and would correspond to a Richter magnitude of about 9.1.

#### References

- Buchanan, P.C., Koeberl, C. and Reid, A.M. (1998) Impact into unconsolidated, water-rich sediments at the Marquez Dome, Texas. *Meteoritics* **33**: 1053-1064.
- Busuttill, S. (1988) Data acquisition and subsequent interpretation of the gravity and magnetic survey of the Mulkarra area, Mulka block, PELs 5 and 6, South Australia. SANTOS Ltd. Unpublished Report.
- Flynn, M. (1989) The Mulkarra Structure: A possible buried impact crater in the western Eromanga Basin, Australia. In: *The Cooper and Eromanga Basins Australia*, B.J. O'Neil (ed.), *Australian Society of Exploration Geophysicists*, pp. 431-439.
- Gibson Jr., J.W. (1990) Marquez Dome - An impact feature in Leon County, Texas. *M. Sc. thesis*, University of Houston, 65 pp.
- Koeberl, C., Poag, C.W., Reimold, W.U. and Brandt, D. (1996) Impact origin of the Chesapeake Bay structure, and source of the North American tektites. *Science* **271**: 1263-1268.
- Melosh, H.J. (1989) *Impact Cratering: A Geologic Process*. Oxford University Press, 245 pp.
- Pike, R. (1983) Comment on 'A Schematic Model of Crater Modification by gravity' by H. J. Melosh. *J. Geophys. Res.* **88**: 2500-2504.
- Poag, C.W. (1996) Structural outer rim of Chesapeake Bay impact crater: Seismic and bore hole evidence. *Meteoritics and Planetary Science* **31**: 218-226.
- Poag, C.W. (1997) The Chesapeake Bay bolide impact: a convulsive event in the Atlantic Coastal Plain evolution. *Sedimentary Geology* **108**: 45-90.
- Sharpton, V.L. and Gibson Jr., J.W. (1990) The Marquez dome impact structure, Leon County, Texas. Abstracts **21st Lunar Planet. Sci. Conf.**, 1136-1137.
- Williams, A.F. (1975) Gason, South Australia, 1:250,000 Geological Series - Explanatory Notes. Geological Survey South Australia, 27 pp.

## **Chesapeake Bay Impact Structure: Geology and Geophysics.**

C. W. Poag<sup>1</sup>, J.B. Plescia<sup>2</sup> and Ph.C. Molzer<sup>1</sup>.

1) U. S. Geological Survey, Woods Hole, MA 02543 (wpoag@usgs.gov; pmolzer@usgs.gov);

2) U. S. Geological Survey, Flagstaff, AZ 86001 (jplescia@usgs.gov).

### Introduction

The Chesapeake Bay impact structure is a complex impact crater, 85 km in diameter, located in the subsurface of southeastern Virginia, USA (37°16.5'N, 76°0.7'W). The structure was identified on the basis of seismic reflection profiles, borehole data, and gravity data (Poag et al., 1994). The crater formed in the late Eocene (~35 Ma) on the inner continental shelf, a submarine environment. At 85 km diameter, this is the largest impact feature in the United States and the seventh largest in the world; it is also one of the best preserved, as it was immediately buried by younger sediments. A complex circular gravity anomaly (8-13 mGal gravity relief) occurs over the structure.

### Geology and Structure

Figure 1 illustrates a schematic cross-section of the Chesapeake Bay structure. The regional geological framework consists of eastward-dipping and thickening sedimentary formations overlying a similarly eastward-dipping crystalline basement complex. The basement consists of Piedmont granitic and metasedimentary rocks of Proterozoic to Paleozoic age. Overlying the basement are poorly lithified marine and nonmarine sediments, which are ~ 0.6 to 1.6 km thick across the structure.

The sedimentary column begins with basal nonmarine Lower Cretaceous siliciclastic units of the Potomac Formation. Above the Potomac are mostly marine units including: an unnamed Upper Cretaceous unit; Brightseat Formation (lower Paleocene); Aquia Formation (upper Paleocene); Marlboro Clay (upper Paleocene); Nanjemoy Formation (lower Eocene); Piney Point Formation (middle Eocene); Chickahominy Formation (upper Eocene); Delmarva beds (lower Oligocene); Old Church Formation (upper Oligocene); Calvert Formation (middle and lower Miocene); Choptank Formation, St. Mary's Formation, and Eastover Formation (upper Miocene); Yorktown Formation (Pliocene); and a complex series of Pleistocene and Holocene units. Impact deformation involves rock units from the crystalline basement to the basal Chickahominy Formation. The Upper Chickahominy and younger units are undeformed by the impact, but thicken and sag over the structure due to compaction of underlying units.

More than 2,000 km of seismic reflection profiles define the structural aspects of the impact. The principal components include an irregularly circular outer rim formed by a steep fault scarp surrounding: (1) an annular trough holding a series of normal-faulted and slumped megablocks; (2) a peak ring; (3) an inner basin; and (4) a central peak. All the interior features of the crater are overlain by the Exmore impact breccia, composed of fallback, fallout, resurge and washback debris. Seismic reflection profiles show that the average diameter of the outer rim is ~ 85 km and relief from outer rim to inner basin floor is ~1.3 km.

by the Exmore impact breccia, composed of fallback, fallout, resurge and washback debris. Seismic reflection profiles show that the average diameter of the outer rim is ~ 85 km and relief from outer rim to inner basin floor is ~1.3 km.

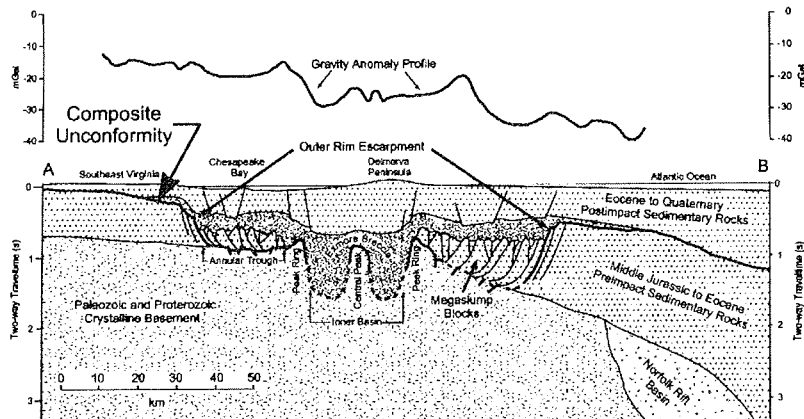


Figure 1 Schematic cross section of the Chesapeake Bay impact structure (from Poag et al. 1999).

A prominent, well-defined pair of seismic reflectors clearly define the floor of the annular trough, 600-1200 m below the sediment surface. Within the annular trough are a series of concentric normal-faulted, rotated megablocks, whose incorporated strata dip both toward and away from the center of the structure. The basement reflectors do not show evidence of rotated blocks or other displacement coincident with most normal faults in the overlying sedimentary section. Thus, we conclude the majority of the normal faults cutting the sedimentary section ramp into a decollement along the sediment / basement contact. A similar ramping and decollement are interpreted at the Upheaval Dome structure (5-km-diameter complex impact) in Canyonlands National Park, Utah (Kriens et al., 1997, 1999). At Upheaval Dome, however, the decollement occurs within a sedimentary section. In the Chesapeake Bay structure, the basement reflectors of the annular trough are deformed regionally into low anticlinal folds and are cut by normal and reverse faults. At the inner edge of the annular trough, the basement reflectors rise 100-200 m over an irregular peak ring, which averages 40 km in diameter. The basement reflectors then descend into the interior of the inner basin before rising again over a central peak of ~1-km relief.

The tilted megablocks, peak ring, inner basin, and central peak of the Chesapeake structure are overlain by the Exmore breccia, an autochthonous (and partly allochthonous?) impactite composed of sedimentary and

crystalline basement clasts. Shocked quartz and planar deformation features in quartz and feldspar grains have been identified within the upper 60 m of the Exmore breccia, confirming its impact origin (Koeberl et al., 1996). The lower part of the Exmore breccia has not yet been sampled. Overlying the impact structure is a succession of mainly marine sedimentary deposits 300-500 m thick. A structural depression over the Chesapeake Bay crater has resulted in a localized thickening of individual stratigraphic units over the structure. This local thickening is due to differential compaction of the Exmore breccia and to post-impact cooling of the crystalline basement.

Gravity

The gravity signature of the region including the Chesapeake Bay impact structure is complicated by numerous positive and negative anomalies associated with the crystalline basement which has a complex pre-Mesozoic history, particularly the intrusion of numerous low-density granitic plutons. Figure 2 illustrates the gravity map of the region constructed from data compiled by J. Costain. New gravity data collected on the Delmarva Peninsula and from a marine survey over Chesapeake Bay support the seismic evidence for a central peak.



Figure 2 Gravity anomaly map of the Chesapeake Bay impact structure. Onshore data are simple Bouguer gravity values; offshore data are free-air gravity values. Contour interval is 1 mGal. The outer rim of the structure is denoted by the heavy line.

The center of the structure is defined by a negative anomaly reaching -28 mGal surrounded by an annular high of variable width reaching about -15 to -20 mGal. Overall, this central anomaly has a diameter of ~45 km and gravity relief of 8 to 13 mGal. Several smaller relative highs occur within the central low. The relative high nearest the crater center is associated with the central peak indicated on the seismic profiles. Along the margin of the structure, the gravity field exhibits both positive and negative anomalies, including highs along the northeast and western margins and prominent lows to the north-northwest and southeast. These smaller anomalies, which have significant amplitude, are related to density contrasts in the crystalline basement (especially granitic plutons; Dysart et al., 1983) and, therefore, are unrelated to the impact structure. A simple gravity model shows that filling the inner basin with breccia having a density contrast of about -0.15-0.20 g cm<sup>-3</sup> with respect to the surrounding sediments would produce the observed central negative anomaly.

#### Discussion

Seismic reflection data show a well-defined complex impact structure with all of the classic components: outer rim, annular trough containing faulted megablocks, peak ring, inner basin, and central peak. At 85-km diameter, the structure is within the size range of complex craters having peak rings and central peaks. Assuming the observed 85 km diameter represents the collapse diameter after terrace formation, the transient crater diameter would have been ~50-54 km with an excavation depth of ~5 km (Schmidt and Housen, 1987; Cintala and Grieve, 1998). Using the energy scaling relationships defined by Schmidt and Housen (1987), the characteristics of the impactor can be approximated. Assuming an asteroidal projectile traveling at 15 km sec<sup>-1</sup>, it would have a diameter of 7-8 km depending upon the bulk density (3.5 to 2.5 g cm<sup>-3</sup> respectively). A short-period comet impacting at 25 km sec<sup>-1</sup> would have had a diameter of ~10-11 km. The total energy of the impact would amount to ~6.5 x 10<sup>22</sup> J or 1.5 x 10<sup>7</sup> Megatons. About 5000 km<sup>3</sup> of impact melt would have been produced.

A number of morphometric relations have been established relating various attributes of complex and simple craters (Pike, 1977, 1985; Melosh, 1989). The diameter of the peak ring at the Chesapeake Bay structure is about 40 km, consistent with the data for other central peak ring craters. A peak ring is also consistent with the morphology of other similar size impact structures: Vredefort (140 km diameter) and Popigai (85 km diameter) both exhibit a peak ring and central peak; whereas Puchezh-Katunki (80 km diameter) exhibits a peak with central depression. A diameter of ~7-8 km for the central peak is also consistent with other complex craters (Pike, 1985). The peak ring defines a region of uplifted basement rocks. Grieve and Pilkington (1996) present a relation between the diameter of a structure and the amount of structural uplift in the central peak. That relation would indicate uplift of about 8.4 km. However, the relatively flat floor of the annular trough does not seem consistent with 8-9 km of uplift.

### References

- Cintala, M. and Grieve, R. (1998) Scaling impact melting and crater dimensions: Implications for the lunar cratering record. *Meteoritics and Planetary Science* **33**: 889-912.
- Dysart, P., Coruh, S. and Costain, J. (1983) Seismic responses of major regional unconformities in Atlantic Coastal Plain sediments at Smith Point, Virginia. *Geol. Soc. of America Bull.* **94**: 305-311.
- Grieve, R. and Pilkington, M. (1996) The signature of terrestrial impact. *AGSO J. Aus. Geol. and Geophys.* **16**: 399-420.
- Koeberl, C., Poag, C., Reimold, W. and Brandt, D. (1996) Impact origin of the Chesapeake Bay structure, and source of the North American tektites. *Science* **271**: 1263-1268.
- Kriens, B., Shoemaker, E. and Herkenhoff, K. (1997) Structure and kinematics of a complex impact crater, Upheaval Dome, southeast Utah. In: *Geological Society of America Field Trip Guidebook, 1997 Annual Meeting, Salt Lake City, Utah*, Link, P.K., and Kowalis, B.J., (eds.), *Brigham Young University Geology Studies*, **42**: 19-31.
- Kriens, B., Shoemaker, E. and Herkenhoff, K. (1999) Geology of the Upheaval Dome impact structure. *J. Geophys. Res.*, submitted.
- Melosh, H. (1989) *Impact Cratering: A Geologic Process*. Oxford University Press, 245 pp.
- Pike, R. (1977) Size dependence in the shape of fresh impact craters on the Moon. In: *Impact and Explosion Cratering*, Roddy, D., Pepin, R. and Merrill, R. (eds.), Pergamon Press, pp. 489-509.
- Pike, R. (1983) Comment on 'A Schematic Model of Crater Modification by gravity' by H.J. Melosh. *J. Geophys. Res.* **88**: 2500-2504.
- Pike, R. (1985) Some morphologic systematics of complex impact structures. *Meteoritics* **20**: 49-68.
- Poag, C. (1996) Structural outer rim of Chesapeake Bay impact crater: Seismic and bore hole evidence. *Meteoritics and Planetary Science* **31**: 218-226.
- Poag, C. (1997) The Chesapeake Bay bolide impact: a convulsive event in the Atlantic Coastal Plain evolution. *Sedimentary Geology* **108**: 45-90.
- Poag, C., Powars, D., Poppe, L. and Mixon, R. (1994) Meteoroid mayhem in Ole Virginny: Source of the North American tektite strewn field. *Geology* **22**: 691-694.
- Poag, C., Hutchinson, D., Colman, S. and Lee, M. (1999) Seismic expression of the Chesapeake Bay impact crater: Structural and morphological refinements based on new seismic data. *Geol. Soc. Amer. Spec. Pap.* (in press).
- Schmidt, R. and Housen, K. (1987) Some recent advances in the scaling of impact and explosion cratering. *Intern. J. Impact Engineering* **5**: 543-560.

## **5 Million Years of Milankovitch Cycles in Marine Sediments across the K/T Boundary at the Black Sea Coast near Bjala, Bulgaria.**

A. Preisinger<sup>1</sup>, S. Aslanian<sup>1,2</sup>, H. Summesberger<sup>3</sup>, and H. Stradner<sup>4</sup>.

1) Institute of Mineralogy, Crystallography and Structural Chemistry, Techn. Univ. of Vienna, Austria, 1060 Wien, Getreidemarkt 9 (apreisin@mail.zserv.tuwien.ac.at); 2) Permanent address: Geological Institute BAS, Sofia, Bulgaria; 3) Museum of Natural History, Vienna; 4) Geological Survey of Austria, Vienna

Worldwide the Cretaceous/Tertiary (K/T) impact at Chicxulub, Yucatan, Mexico, marks an extremely precise reference point in the geological timescale. An age of 65.0 million years was assigned to this event (Swisher et al., 1992).

In this report marine sediments from the continuous K/T section at the Black Sea coast near Bjala, Bulgaria, longitude 27°53'58"E, latitude 42°52'40"N are dealt with (Preisinger et al., 1993). Rhythmic sedimentation over a vertical range of 100 m was taking place there and resulted in the deposition of limestones with intercalated marls under hemipelagic conditions from Late Cretaceous (C-30 m) to Early Tertiary (T+70 m) (Fig. 1). More than 850 analyses by means of a "carbonate bomb" were done to determine the CO<sub>2</sub> contents of the sediment samples. The accumulation rate at Bjala is about twice as high in the Cretaceous as it is in the Tertiary section (Rögl et al., 1996). This is in good agreement with the change of the accumulation rate across the K/T boundary at other sites elsewhere (Herbert and D'Hondt, 1990).

In the Tertiary sediments (70 m) of Bjala 172 cycles of CaCO<sub>3</sub> beds could be identified within the magnetic polarity zones from Chron 29R to Chron 27N. The levels of magnetic polarity turnover lie for C29R/C29N at T+630 cm; for C29N/C28R at T+1960 cm; for C28R/C28N at T+2330 cm; for C28N/C27R at T+4460 cm; for C27R/C27N at T+6080 cm; for C27N/C26R at T+6440 cm, respectively, above the K/T boundary level (T+0 cm) (Preisinger et al., 1993).

The time-span of a magnetic polarity zone is characterised by the number of the limestone beds with high CaCO<sub>3</sub> contents. Figure 2 compares our data with the timescale of Harland et al. (1990), which was rectified by Mussett and McCormack (Mussett and McCormack, 1993). In our study the timescale for the Bjala section is calibrated by means of precessional Milankovitch cycles of an average duration of 22.5 kyr each over a time-span of 5 million years.

The changes of magnetic polarity in sediment layers (Chron R→N and Chron N→R) were found to correspond to minima of CaCO<sub>3</sub> contents. Conclusions to this observation will be discussed at the meeting.

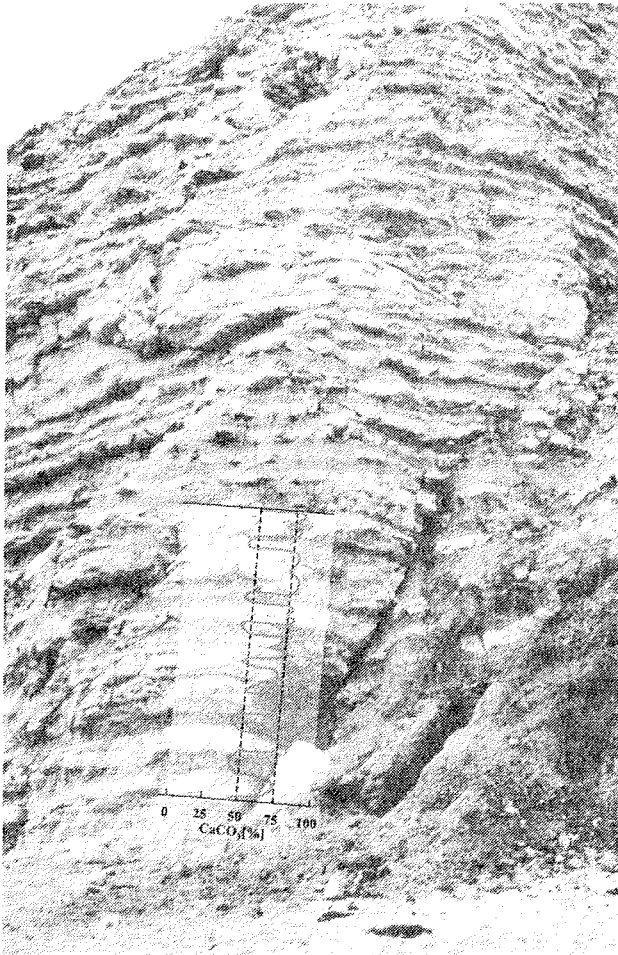


Figure 1 The  $\text{CaCO}_3$  beds of the K/T boundary section of Bjala, Bulgaria. The magnetic polarity zone of Chron 28N and the  $\text{CaCO}_3$  content of some limestones with intercalated marls are shown.

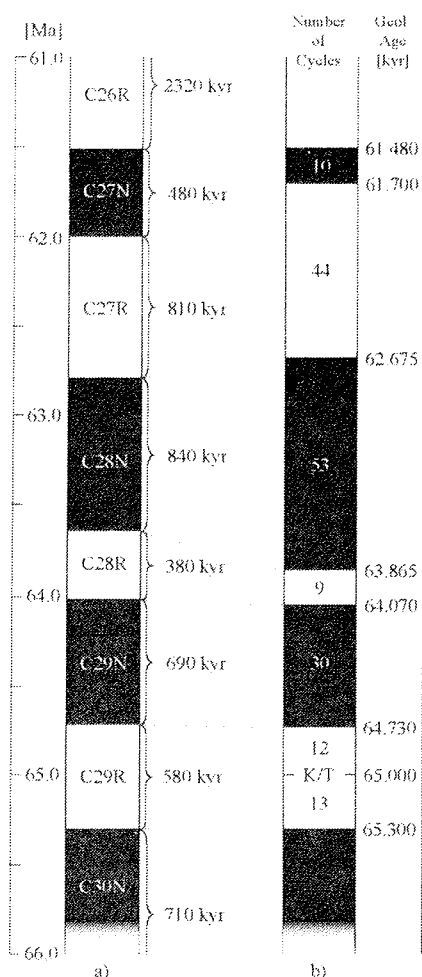


Figure 2 Five Million years of magnetic polarity timescale across the K/T boundary.  
a) Harland et al. (1990), rectified scale (-0.15 Ma) after Mussett and McCormack (1993).  
b) our study at the Bjala boundary section.

#### References

- Harland, W.B., Armstrong, R. L., Cox, A. V., Craig, L. E., Smith, A. G. and Smith, D. C. (1990) *A geologic time-scale*, 1989, Cambridge Univ. Press.
- Herbert, T.D. and D'Hondt, S.L. (1990) Precessional climate cyclicity in Late Cretaceous-Early Tertiary marine sediments: a high resolution chronometer of Cretaceous-Tertiary boundary events. *Earth Planet. Sci. Lett.* **99**: 263-275.
- Mussett, A.E. and McCormack, A.G. (1993) Magnetic polarity time scales; a new test in high resolution stratigraphy. In: *High Resolution Stratigraphy*, Hailwood E.A. and Kidd R.B. (eds) *Geol. Soc. Spec. Publ.*, pp. 27-37.

- Preisinger, A., Aslanian, S., Stoykova, K., Grass, F., Mauritsch, H.-J. and Scholger, R. (1993) Cretaceous/Tertiary boundary section on the coast of the Black Sea near Bjala, Bulgaria. *Paleogeog. Paleoclimat. Paleoecol.* **104**: 219-228.
- Rögl, F., von Salis, K. Preisinger, A., Aslanian, S. und Summersberger, A. (1996) Stratigraphy across the Cretaceous/Paleogene boundary near Bjala, Bulgaria. In: *Geologie de l'Afrique et de l'Atlantique sud*, Jardine, S., Klasz, J., de Delonay, J.P. (eds) *Elf Aquitaine Edition*, pp. 673-683.
- Swisher, C.C. and 11 others (1992) Coeval  $^{40}\text{Ar}/^{39}\text{Ar}$  ages of 65.0 million years ago from Chicxulub crater melt and Cretaceous/Tertiary boundary tectites. *Science* **257**: 954-958.

## Ejecta Deposits of the Chicxulub Impact

J. Smit

Dept. of Paleontology, Institute of Earth Sciences, Vrije Universiteit, de Boelelaan 1085, 1081HV Amsterdam, Netherlands (<smit@geo.vu.nl>)

The ejecta deposits of the Chicxulub impact can be regionally grouped, depending on distance from the impact and the depositional environment.

Distal ejecta layers occur globally, > 6000 km from the crater center. The distal ejecta layer has a consistent thickness of 2-3 mm, is strongly enriched in PGE and contains abundant microkrystites ( $20000/\text{cm}^2$ ), usually altered to clay, except for the abundant skeletal crystals of nickel-rich spinels. There is no observed trend in the thickness as function of distance from the crater, although the concentration of PGE and concentration of shocked minerals and their shock intensity increases towards sites antipodal to Chicxulub (southwest Pacific).

Intermediate ejecta layers occur mostly in continental coal-swamp deposits, 2000-4000 km from the crater. The ejecta layer is typically 1-2 cm thick, dual layered, consisting of a lower, thicker spherule-rich layer, amalgamated to an upper, PGE and shocked minerals enriched layer.

The proximal Chicxulub ejecta deposits (<2500 km from the crater) are invariably reworked, outside the crater by tsunami waves and gravity flows, and by seawater rushback in- and just outside the crater. The ejecta-tsunami deposits occur in outer shelf water depths (100-500 m) around the Gulf-coast (e.g. Moscow Landing, Brazos, Mulato, Lajilla, Mimbral, and La Ceiba). Mass-flows are encountered at deep-water sites (ODP 536/540, 1049, Beloc, Coxquihui) or near steep carbonate platform edges (Bochil, el Guayal, el Caribe, Sta Theresa). The only exception are the ejecta blanket deposits near Chetumal - la Union and Northern Belize (Albion Island). The typical sequence of tsunami or gravity influenced ejecta deposit is from bottom to top as follows:

- A) Coarse grained, large-scale cross-bedded, tektite and limestone ejecta-rich, channel deposits.
- B) A stack of sheet-like, ejecta-poor graded and small-scale cross-bedded sandstone deposits, containing ample evidence for oscillating, wave induced currents. The sandstones are rich in near-shore detrital clasts, plant debris, and reworked foraminifers from the local sea floor.
- C) Flaser-like, thin-bedded and cross-bedded sandstone layers alternating with fine silt layers enriched in PGE and Ni-rich spinels.
- D) A graded siltstone layer, enriched in PGE, resulting from settling of fine detritus from the watercolumn.

This sequence is typical for the Brazos river, Mimbral and Lajilla sites, but at shallower depths, like in the Parras basin, or in Alabama (Mussell Creek, Moscow Landing), it may be wholly or partly eroded by a subsequent lower Paleocene sea-level fall. It is remarkable that the coarse ejecta (tektites, clasts) at the bottom are stratigraphically separated from the (very fine-grained) PGE enriched ejecta, as also observed in intermediate sites. The first normal, background deposits on top of the sequence are invariably strongly impoverished in oceanic biota (nannofossils, foraminifers)

Just outside the rim of the Chiapas-Yucatan carbonate platform, the ejecta deposits occur mostly in the top of thick (<70m) conglomeratic gravity flow deposits, that may have been triggered by the earthquakes caused by the impact at Chicxulub.

Ejecta-blanket deposits have been traced in the Ticul-1, Unam-5 and Yuc-2 wells, and in Northern Belize and near Chetumal. The basal ejecta blanket deposits near Chetumal are represented by a >30 m thick breccia/diamictite, separated from the autochthonous bedrock by a 1m cataclastic breccia, pulverized by friction between bedrock and shifting ejecta-blanket. The basal diamictite consist of dolomite boulders and altered bubbly glass fragments floating in a matrix of pulverized dolomite. The top of the blanket deposits near Chetumal is eroded off and covered by a lower Paleocene calcrete soil (caliche). In the drill holes Y-2 and Unam-5, the basal dolomite/anhydrite clast rich ejecta blanket ('bunte breccia type')(>600 m) is overlain by a melt-rich suevitic polymict breccia (>200 m) with basement blocks, followed by graded >40 m suevitic glass clast dominated breccia, with cross-bedding structures. The latter is probably due to water rushing back to the crater. Inside the crater the sequence is poorly known. Inferred is a sequence of graded breccias on top of the holocrystalline meltsheet, terminating in a suevitic sandstone with traces of crossbedding, representing the water rush-back deposits. Those are overlain just outside the crater by fine-grained deepwater deposits of basal Paleocene age.

## **Kärdla Crater (Hiiumaa Island, Estonia) - The Result of an Impact in a Shallow Epicontinental Sea**

K. Suuroja<sup>1</sup>, V. Puura<sup>2</sup>, and S. Suuroja<sup>1</sup>.

1) Geological Survey of Estonia, Kadaka tee 80/82, Tallinn, Estonia (s.suuroja@egk.ee); 2) University of Tartu, Vanemuise 46, Tartu, Estonia

The Kärdla marine impact crater was formed in Middle Ordovician, earliest Caradoc time (ca 455 Ma) in a shallow epicontinental sea, not far (ca 10 km) from the nearshore non-deposition area. At that time the impact site on the Baltica Continent located in Southern Hemisphere between 40-50°latitudes. The projectile (impactor) of unknown composition penetrated the thin (less than 100 m) water layer and sedimentary cover (ca 140 m) consisting of water-saturated friable mainly siliciclastic sediments and exploded in the uppermost part of the Precambrian crystalline basement. The impact generated more than 500 m deep complex crater, rim-to-rim diameter of which was 4 km, and an elliptical ring fault, up to 15 km in diameter (Fig. 1). Within the ring fault the sedimentary target rocks are considerably disturbed. Due to the marine environments, almost all impact-related deposits have preserved both in the crater proper and in the surrounding area. 52 drill holes penetrate this succession. Marine environments were responsible for the formation of up to 60 m thick resurge breccia unit in the crater and erosion of the surrounding ring wall and ejecta layer. Resurge deposits formed in the crater proper when the resurging mudflow violently rushed back into a newly formed deep. The intensity of erosion exalaterated from the ring fault towards the rim wall. Initially the seafloor (sedimentary rocks and a thin (<1m) layer of unlithified mud) was crushed and partly removed by the impact. Up to 20 m thick layer of sedimentary target deposits (considerably hard limestones and poorly lithified sands) was relocated from the outer slope of the ring wall. The erosional cut on the ring wall occasionally reached some 200 m. The erosion was areally different as well as was different the height of the rim wall left. Resurge deposits in the crater proper consist of clast-supported breccias in which apparent sorting and bedding, as well as evidence of shockmetamorphism are absent. Clast size ranges from less than a centimetre up to tens of metres. In the composition of clasts the whole succession of target rocks is represented, but the rocks of the uppermost part of the sedimentary cover, especially limestones, prevail. Limestones form only ca 10% of the sedimentary target succession, but their content in the composition of the resurge breccias reaches in places 50%. The contact of the resurge breccias and the underlying slump deposits in the crater proper is quite sharp.

Resurge breccias differentiate from slump breccias by their position in the section as well as by lithological composition. Up to 90 m thick pile of slump breccias are made up mainly of blocks of Cambrian terrigenous rocks (sandstones, siltstones, claystones) with some admixture of other sedimentary target rocks. The textures of different breccias are different: the resurge breccias bear clear traces of flow, but the slump breccias, that formed in relatively waterless environment, lack these textures. After the formation of the

coarse-grained resurge breccias, up to 25 m thick succession of clastic deposits (gravel, sand, silt clay) have been precipitated in the crater proper. Major part (up to 20 m) of this succession is represented by silty deposits. Close to the ring wall, the thickness of this layer decreases and more coarse-grained deposits (gravel, sand) dominate.

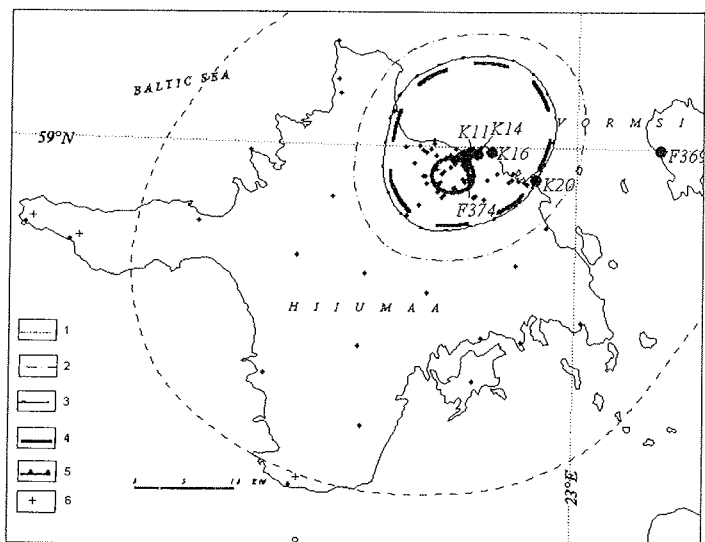


Figure 1 Structural zones and distribution of ejected and partly redeposited material in the vicinity of the Kärđla structure. 1=contour of fine-grained ejected and redeposited material, 2=contour of coarse-clastic ejecta layer, 3=contour of post-impact erosion, 4=ring-fault, 5= crater rim, 6=impact-related clastic admixture in limestones. Large black dots mark drillholes presented in Fig. 2, small dots mark additional drillholes.

From the ejected clastic material around the crater in radius up to 20 km 0.01-0.8 m thick layer of the distal ejecta and redeposited material was formed. In the limestone layer of surrounding area that was formed during the impact, the admixture of ejected clasts up to distance of 80 km from the impact site can be observed. On the outer slope of the ring wall the ejecta layer has been demolished by resurging wave and subsequent marine erosion. In the distal successions of these deposits two layers can be observed. The lower ejecta layer with coarse (>1mm) clastic fragments of carbonate rocks, sand-, silt-, and claystones and crystalline rocks of the target is cemented by carbonate material. Its preserved thickness ranges from 1 cm to 2m. It has a sharp, slightly undulating contact with the pre-impact soft un lithified bottom sediments, partly (up to 50 cm) removed by the impact processes. In the normal stratigraphic sequence in distal parts of ejecta, this contact is transitional.

The upper part of the impact-related layer composed of sandy or silty clasts within the clayey carbonate matrix, often thin-bedded. Its maximal thickness at

about 5 km from the wall is up to 0.8 m (Fig. 2). It covers the lower ejecta layer or, in distal parts (over 30km from the crater wall) overlies the target rocks having transitional contacts with the underlying sediments. The influence of the impact to the sea was expressed in transformation of the sea floor morphology: formation of the crater deep, arising the central uplift, crater ring wall and surroundings. The whole area surrounded by the ring fault was elevated 5-10 m. Other processes evoked by the impact (crushing of sea floor, resurge erosion, precipitation ejecta layer) also influenced sea floor morphology. In the immediate vicinity of the crater rim the thickness of the survived ejecta layer reached 2 m (Fig. 2), while in the distal part it is remarkably thinner (some millimetres, Figs. 1 and 2). The layer can be followed for up to 80 km to the north-east and ca 40 km to the south-west of the crater. Outside the crater rim, at the distance of ca 1 km, huge ejected blocks (up to 50 m in diameter) are found.

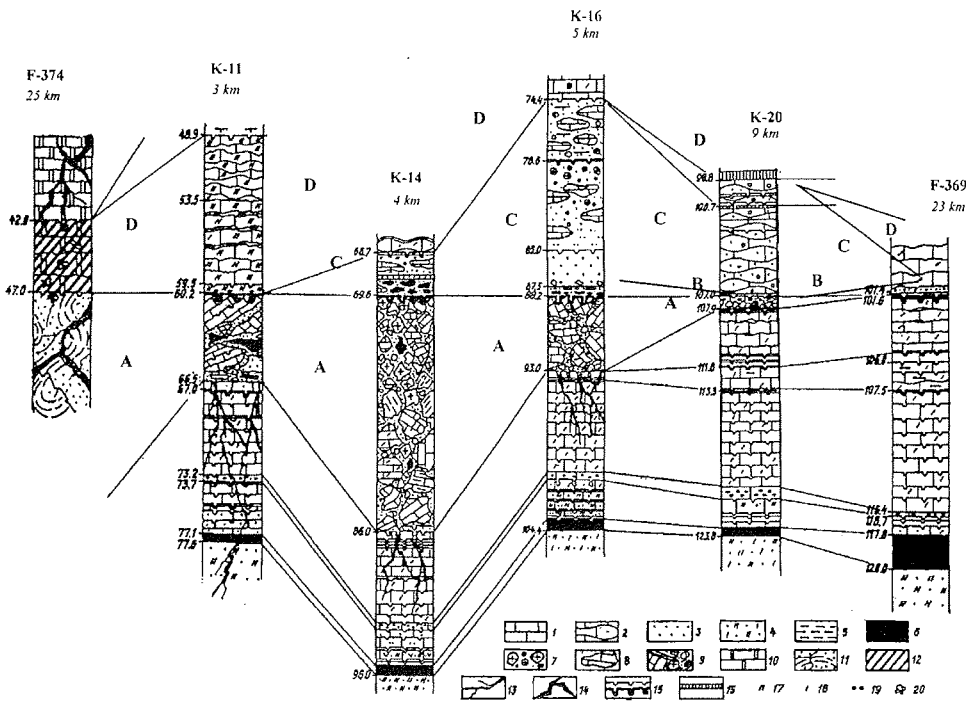


Figure 2 (A)-(C): Drill core logs of the impact-related and country rocks east of the crater rim. For location of the drill sites see Figure 1 (large black dots). On top of logs: drill hole designation and distance of drill site from crater center. A=paraautochthonous breccia, B=ejecta layer, C=redeposited material, D=covering limestone. Lithologies: 1-2= limestone, 3-4=sandstones, 5=Cambrian sandstones, 6=*Dictyonema* shale (lower Ordovician), 7=gravel and pebbles of sedimentary and crystalline target rocks, 8=limestone nodules, 9=block breccia, 10=dolomite, 11=dislocated Cambrian terrigenous rocks, 12=lead and zinc mineralizations, 13=fractures, 14=sulphide veins, 15=discontinuity surfaces (above) and hardgrounds (below), 16=K-bentonite, 17=coarse grained bioclastic admixture, 18=fine grained bioclastic admixture, 19=goethite ooliths, 20=caverns.

## **Atmospheric Perturbations and Tsunamis caused by an Impact of a Cosmic Body into an Ocean**

A.V. Teterev and L.V. Rudak.

Department of Applied Mathematics and Computer Science, Belarus State University, 4 F. Skorina avenue, Minsk, 220050, Belarus (teterev@fpm.bsu.unibel.by).

### Introduction

A large number of publications are devoted to numerical simulation of impacts of asteroids and comets into water basins of the Earth and formation of tsunamis. However, one cannot say that all aspects of this complicated phenomenon are studied thoroughly. This is mostly due to a large number of factors such as size of a body, its composition, impact velocity, impact angle, depth of a water basin, which determine the consequences of a catastrophe. At modeling of impacts it is often important to know prehistory of movement of an object through the atmosphere. It is the case when small, large or high-velocity bodies are under consideration, because small bodies suffer fragmentation and movement of high-velocity or large ones causes significant perturbations of the atmosphere.

### Brief description of the model

Parameters of a formed destructive wave depend very much on an initial stage of an impact, when formation of a water crater, ejection of large water masses into the atmosphere and rise of water around the crater occur. In this paper the initial stage of an impact is a primary subject of interest. A water kernel of a comet was considered as a cosmic object falling into the ocean. The surface of the bottom of the ocean was considered as a rigid impenetrable wall. A special algorithm of computation of contact boundaries in the Eulerian coordinates was used for more precise determination of their location. At modeling of the water crater being formed after an impact the approach with the transparent contact boundary was used together with the traditional gas-dynamic approach. In this approach the boundary being calculated becomes a boundary between different phases (liquid and mixture of vapor and liquid) of one substance rather than a boundary between two different substances. The condition of transition of substance from one phase to another is violation of its continuity.

### Initial data and outcomes of computational experiments

The calculations were carried out according to two scenarios. In the first of them modeling was started at the moment when the comet touched the surface of the ocean. In the second one the movement of the comet through the dense layers of the Earth's atmosphere was also calculated. In calculations the depth of the ocean was 2-4 km. The range of impact velocities was from 15 to 25 km/s. Sizes of the comet kernel varied from 250 m to 5 km, densities - from 10 to 1000 kg/m<sup>3</sup>. Kinetic energy of the impactor was from 10<sup>3</sup> to 10<sup>5</sup> Mt TNT. The obtained results make possible to reveal dynamics of water crater and ejecta cloud formation. The data related to the movement of water masses near the place of impact can be used as the initial data for solution of a

problem of transformation of formed water currents into tsunamis. The results obtained from a series of computational experiments demonstrate universality and flexibility of the developed approach to impacts of cosmic bodies into oceans, which can be simulated using modern personal computers.

#### Acknowledgments

This research was supported by the International Science and Technology Center within project B-23/96.

#### References

- Gault, D.E., Sonett, C.P. and Wedekind, J.A. (1979) Tsunami generation by planetoid impact. *LPSC X*: 422-424.
- Hills, J.G. and Mader, C.L. (1995) Tsunami produced by the impacts of small asteroids. *Proceedings of the Planetary Defense Workshop Lawrence Livermore National Laboratory, Livermore, California.*: 67-76.
- Nemtchinov, I.V., Popov, S.P. and Teterev, A.V. (1994) Estimates of the characteristics of waves and tsunami produced by asteroid and comets falling into oceans and seas. *Solar System Research*. **28**: no. 3: 260-274.
- Teterev, A.V., Misychenko, N.I., Rudak, L.V., Nemchinov, I.V., Romanov, G.S. and Smetannikov, A.S. (1993) Atmospheric breakup of a small comet in the Earth's atmosphere. *LPSC XXIV*: 1417-1418.
- Teterev, A.V. (1998). A model of interaction of a vaporous jet and high-velocity condensed fragments at the giant impact. *Origin of the Earth and Moon Meeting. Monterey, California*, pp. 45-46.

## **Underwater Cratering at Impacts into Oceans**

A.V. Teterev.

Department of Applied Mathematics and Computer Science, Belarus State University, 4 F.Skorina avenue, Minsk, 220050, Belarus (teterev@fpm.bsu.unibel.by).

#### Introduction

A larger part of the Earth's surface is covered by water, so the possibility of falling of asteroids into oceans are higher than onto the land. However, only one underwater crater is known. It is connected both with difficulties in detection of such a phenomenon, which is impossible to discover by usual observation, and with the fact that a water layer of thickness 4-5 km is a much more reliable shield of the bottom surface than the Earth's atmosphere, the only defense for the land. The water column can take over an essential part of energy of an impact of an asteroid of medium size and convert it into the destructive force of generated tsunamis and into giant ejection of water masses into the atmosphere. However, with time, these consequences of a catastrophic impact are being forgotten. Decisive evidences of the past cataclysm are an underwater crater and the asteroid substance dispersed over large underwater territories. Numerical modeling of underwater cratering is a

subject of many papers, but their number is smaller than the number of works dealing with cratering on the land.

#### Description of computational experiments

In numerical modeling of this phenomenon, due to its large scale, the calculation of the flight of a cosmic body through the Earth's atmosphere is not needed. The simulation can be started at the moment when the body is already on the surface of an ocean. Moreover, in this case the computation of a contact boundary between the ocean surface and the atmosphere is not so important as the determination of a boundary between water and the ocean bottom. Calculations of impacts of water and granite bodies were carried out to examine the influence of the impactor density on parameters of the underwater crater.

Along with the process of pressing out of the bottom rock as a continuous medium, ejection of rock in the form of discrete formations of solid phase of substance was also considered. A similar technique was used for calculation of dispersion of asteroid substance. This approach allows one to examine the fallout trajectories of ejected rock and asteroid debris. The dynamics of distribution of released energy on substances and on kinetic and thermal components was investigated.

A subject of special interest is the study of an oblique impact into an ocean, i.e. 3D modeling. Performed 3D calculations were based on a gas-dynamic code without computation of contact boundaries. At the moment a program complex on 3D modeling of the phenomenon under consideration taking into account contact boundaries is being tested.

#### Acknowledgments

This research was supported by the International Science and Technology Center within project B-23/96.

#### References

- Ahrens, T.J. and O'Keefe, J. (1987) Impact on the Earth, ocean and atmosphere. *Int. J. Impact Eng.* **5**: 13-32.
- Gersonde, R., Kyte, F.T., Bleil, U., Diekmann, B., Flores, J.A., Gohl, K., Grahl, G., Hagen, R., Kuhn, G., Sierro, F.J., Völker, D., Abelman, A. and Bostwick, J.A. (1997) Geological record and reconstruction of the late Pliocene impact of the Eltanin asteroid in the Southern Ocean. *Nature* **390**, no. 27: 357-363.
- Nemtchinov, I.V., Loseva, T.V and Teterev, A.V. (1996) Impacts into oceans and seas. *Earth, Moon, and Planets* **72**: 405-418.
- Roddy, D.J., Shuster, S., Rosenblatt, M., Grant, L., Hassig, P. and Kreyenhagen, K. (1987) Computer simulations of large asteroid impacts into oceanic and continental sites - preliminary results on atmospheric, cratering and ejecta dynamics. *Int. J. Impact Eng.* **5**: 123-135.
- Teterev, A.V. (1998) Cratering model of asteroid and comet impact on a planetary surface. *Hypervelocity Impact Symposium*. Huntsville, Alabama.: 33-34.

## **Component Analysis of the Resurge Deposits in the Marine Lockne and Tvären Impact Structures**

R. Törnberg.

Dept. of Geology and Geochemistry, Stockholm University, S-106 91 Stockholm, Sweden  
(tornberg@geo.su.se).

This study is based on component analysis of thin-sections made of samples from outcrops and drill-cores from the Swedish Lockne and Tvären structures. It aims at widening the understanding the distribution of shock features and in general impact-related target rocks in marine craters. The Tvären and Lockne structures have both been determined to be the results of impacts which occurred at sea. They are of Caradocian (Middle Ordovician) age and the target surfaces were all covered by Cambrian and Ordovician sedimentary deposits.

The fractured bedrock, the authigenic breccia, and the secular sediments, are much like the same units in craters formed on land. However, the crater wall surroundings are more prone to collapse due to water saturation. Shock features in the authigenic (predominantly crystalline) breccias are only rarely found and even more seldom in abundance (Lindström and Sturkell, 1992; Törnberg, 1994; Lindqvist, 1998). The only exception to this would be the authigenic breccias outlining the central part of the crater floor. Unfortunately, there are no such drill-cores from the Lockne and Tvären structures yet.

The largest differences between craters formed on land and at sea are found among the allogenic units. The allogenic units consist of the ballistically emplaced ejecta and the water transported resurge deposits. The resurge deposits are derived from erosion by the returning sea water of ejecta and target surface material. Hence, like the ejecta deposits, the resurge deposits are mainly derived from the upper parts of the target. As a result, it is often impossible to differentiate between ejecta and resurge deposits in practice.

The resurge deposit commonly consists of a lower, poorly sorted, matrix supported part and an upper relatively well, but still poorly sorted, clast supported part. The upper part was deposited from watery suspension. The lower part is probably a mix between locally formed breccias, ejecta and material deposited from a debris flows prior to the return of the resurge waves. The resurge deposits reach a thickness of almost 200 m in the central part of the Lockne structure (Lindström et al., 1996).

The sandy to gravely part of the resurge deposit is the unit richest in shock features such as planar deformation features and melt. Preliminary data from the Lockne and Tvären structures show that the resurge arenites in general contain about 1-2% grains with PDF's. More fine or coarse grained varieties of the resurge deposits most often have less than 0.5%. Planar deformation features occur in almost all of the 31 thin-section of the resurge deposits in the Tvären and Lockne structures studied until now.

The major reason for this is that greater shock leads to finer crushing and that water has the capacity to sort granular material. Hence, the most likely grain size where to find shocked minerals is among the most finely crushed and well sorted, sandy to gravelly deposits. Shock features in these deposits never reach as great abundancies as in the most shocked parts of craters formed on land. They are, however, thanks to the sorting capacity of water much more wide spread and easy to find than in craters formed on land.

Impact-related pyroclastics are also abundant in most thin-sections. Up to 20% of partly or totally molten fragments occur (Simon, 1987). The average abundance is in the order of 5-10%.

In spite years of field work combined with drillings and geophysical modelling, no impact melt sheets or melt pockets have been found in any of the 3 craters discussed. The most likely explanation is that there aren't any. Melt has been found as small aggregates and droplets in the resurge deposits of the Lockne and Tvären. Tvären is a fairly small structure and can not be expected to contain much melt. The Lockne structure on the other hand is some 12 km in diameter and would most likely contain a melt pockets or a melt sheet if it had been created on land in a crystalline target (Grieve et al., 1977).

I suggest that the melt in marine craters mainly occurs in the arenitic resurge deposits and that it is a less important feature than in craters formed on land. I also suggest that the explanations for this can be linked to the presence of sea water and sediments in the target. Whether water has a significant shock absorbing affect in the initial stage of the impact can be argued about. Kieffer and Simonds (1980) imply that, although significantly more melt is produced in sedimentary targets, the melt will be strongly dispersed by explosively expanding pore water and CO<sub>2</sub>. As even more water is present in marine impact events it is likely that such events will result in even greater dispersion of melt. Contact with the comparatively cold water and the abrasion of resurge wave will further disintegrate the melt particles and make them more vulnerable to alteration. The sea water in turn causes increased metasomatism.

#### References

- Grieve, R.A.F., Dence, M.R. and Robertson, P.B. (1977) Cratering process: As interpreted from the occurrence of impact melts. In: *Impact and Explosion Cratering*, D.J. Roddy, R.O. Pepin and R.B. Merrill (eds.) Pergamon Press: 791-814.
- Kieffer, S.W. and Simonds, C.H. (1980) The role of volatiles and lithology in the impact cratering process. *Rev. Geophys. Space Physics* **18**: 143-181.
- Lindqvist, A. (1998) Geology of the southwestern part of the Lockne impact crater, Jämtland. *Master thesis*, Department of Geology and Geochemistry. 38 p.
- Lindström, M. and Sturkell, E.F.F. (1992) Geology of the Early Palaeozoic Lockne impact structure, central Sweden. *Tectonophysics* **216**: 169-185.
- Lindström, M., Sturkell, E.F.F., Törnberg, R. and Örmö, J. (1996) The marine impact crater at Lockne, central Sweden. *GFF* **118**: 193-206.

Törnberg, R. (1994) Frequency distribution of shock metamorphic effects and dimensioning of the marine impact crater of the Tvären Bay, Sweden. *Master thesis*, Department of Geology and Geochemistry, 23 p.

## **Porosity Variation, Seismic-Amplitude Anomalies and Hydrocarbon Potential of the Mjølner Impact Crater**

F. Tsikalas, J. I. Faleide, O. Eldholm, and S. T. Gudlaugsson<sup>1</sup>.

Department of Geology, University of Oslo, P.O. Box 1047 Blindern, N-0316 Oslo, Norway (filippos.tsikalas@geologi.uio.no). 1) Now at Orkustofnun, Geoscience Division, Reykjavik, Iceland.

The 40-km-diameter Mjølner Structure, one of the few well-preserved marine impact craters on Earth, has been extensively studied geologically and geophysically (Gudlaugsson, 1993; Dypvik et al., 1996; Tsikalas et al., 1998a, b, c). The impact origin of the structure has been convincingly confirmed by two shallow drillholes, one close to its center and another ~30 km away from its periphery. The drillholes show sedimentological (brecciated and mass-/fluid-flow sediments), geochemical (strong iridium enrichment), and mineralogical (shock quartz grains) evidence that are typical of impact craters. Detailed geophysical analysis of the structure also provides new and important constraints on meteorite impacts into water-covered areas. In particular, the low-strength sedimentary target rocks and the presence of water have led to increased gravitational collapse and infilling resulting in a shallow apparent crater depth. The observed geophysical anomalies closely correspond to the structural crater expression and to the laterally-varying physical properties induced by the impact in a shallow marine sedimentary basin.

A quantitative model of the porosity change is developed on the basis of the previously determined density and seismic traveltime distributions, and the post-impact sediment deformation (Fig. 1). Compared with the surrounding undisturbed platform sediments the porosity increases by 3% to 7% at the periphery of the structure, while it decreases by 2% to 5% at the central crater. The present porosity distribution (Fig. 1) is the result of several counteracting impact cratering processes. In particular, the primary effect of impact is a porosity increase caused by extensive fracturing and brecciation. However, less pervasive brecciation in the relatively soft sediments may explain a lower-than-expected gravity signature, accounting also for the lateral porosity change. The impact left a peripheral region where porosity-increasing processes such as fracturing, brecciation, and gravitational collapse prevailed over density-increasing ones, while the opposite is the case at the central crater where higher densities and lower porosities are related to structural uplift of deeper rocks. The interrelation of porosity and density within the large, 850-1400 km<sup>3</sup>, mushroom-shaped volume of impact-deformed strata (Fig. 2)

was essential for the post-impact development of the structure. Indeed, the extensive post-impact burial resulted in a setting where the periphery of the structure and the surrounding platform compacted considerably more than the denser central core, giving the impression of an uplifted central high relative to the surrounding areas.

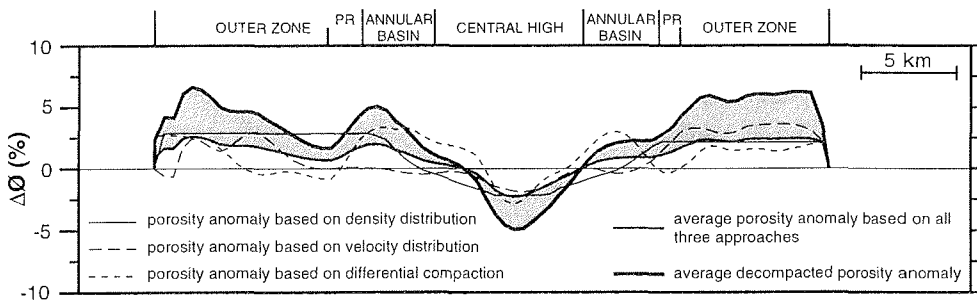


Figure 1 Relative porosity anomaly models for the Mjølnir impact crater. PR: peak ring.

High-resolution single-channel seismic profiles reveal several intra-sedimentary features considered as classical gas indicators. These include: (1) enhanced reflectors and smearing, appearing as a distinct local increase in amplitude of individual reflectors (Fig. 3), (2) restricted columnar disturbances, exhibiting a "chimney form" in which no reflections are apparent (Fig. 3a), and (3) acoustic blanketing, appearing as a loss of coherence partially obliterating all seismic reflections below (Fig. 3b). All these seismic-amplitude footprints are concentrated at the periphery of the structure where they are underlain by tilted fault-blocks and largely brecciated strata. Thus, the seismic-amplitude anomalies are spatially related to the mushroom-shaped volume (Fig. 2) of impact-deformed strata and may be indicative of gas occurrence in sediments within and above the structure.

The Mjølnir crater is located in the southwestern Barents Sea which for the last two decades have experienced extensive hydrocarbon exploration. In particular, the structure lies in a platform area adjacent to deep basins that are considered to have produced hydrocarbons at some stage of their geological history. We believe that the most likely potential plays in the Mjølnir area are Lower to Middle Jurassic sands structurally trapped within the impact-generated tilted fault-blocks, and the syn-impact, extensively fractured, allochthonous breccia. Nevertheless, the porosity and permeability of the sandstones and breccia may have been modified by several complex diagenetic processes, such as mechanical compaction, silicification, and dissolution. In addition, the consequences of the Cenozoic uplift and erosion provide a major regional risk factor in most of the western Barents Sea.

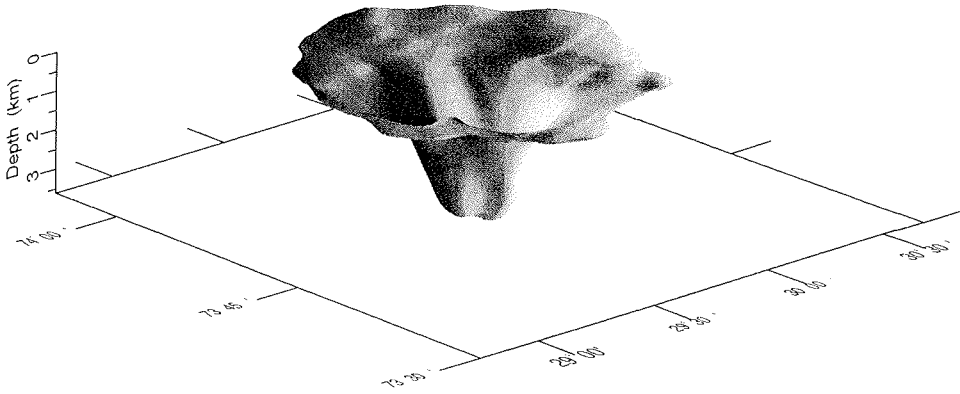


Figure 2 Illuminated perspective diagram of the impact-deformed strata at Mjølneur. Vertical scale exaggeration ca. 5.5x.

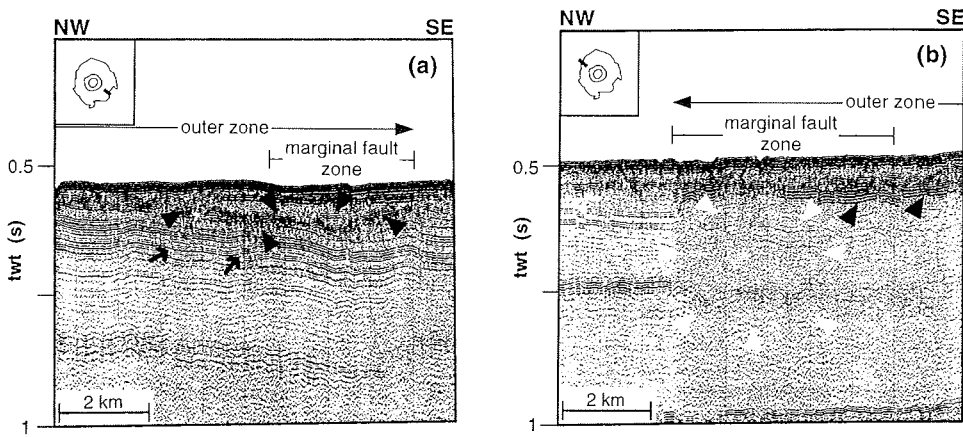


Figure 3 High-resolution single-channel seismic profiles across the crater rim exhibiting gas related seismic-amplitude anomalies. Black triangles: enhanced reflectors and smearing; white triangles: acoustic blanketing; black arrows: restricted columnar disturbances („chimneys“).

### References

- Dypvik, H., Gudlaugsson, S.T., Tsikalas, F., Attrep, M. Jr., Ferrell, R.E. Jr., Krinsley, D.H., Mørk, A., Faleide, J.I. and Nagy, J. (1996) Mjølñir structure: An impact crater in the Barents Sea. *Geology* **24**: 779-782
- Gudlaugsson, S.T. (1993) Large impact crater in the Barents Sea. *Geology* **21**: 291-294.
- Tsikalas, F., Gudlaugsson, S.T. and Faleide, J.I. (1998a) Collapse, infilling, and post-impact deformation at the Mjølñir impact structure, Barents Sea. *Geol. Soc. Am. Bull.* **110**: 537-552.
- Tsikalas, F., Gudlaugsson, S.T. and Faleide, J.I. (1998b) The anatomy of a buried complex impact structure: the Mjølñir Structure, Barents Sea. *J. Geophys. Res.* **103**: 30,469-30,484.
- Tsikalas, F., Gudlaugsson, S.T., Eldholm, O. and Faleide, J.I. (1998c) Integrated geophysical analysis supporting the impact origin of the Mjølñir Structure, Barents Sea. *Tectonophysics* **289**: 257-280.

## **Marine Impact Site Shiyli: Origin of Central Uplift due to elastic Response of Target Rocks**

S.A.Vishnevsky<sup>1</sup>, and V.F. Korobkov<sup>2</sup>.

1) Institute of Mineralogy and Petrology, Novosibirsk-90, 630090, RUSSIA (svish@math.nsc.ru); 2) Kereev str. 6, apt.25, Aktubinsk-22, 463022, Kazakhstan.

The origin of central uplift in complex craters is still a matter of debates. A number of hypotheses is proposed here: post-impact isostasy relaxation (Dabizha et al., 1976), gravity collapse (Dence et al., 1977; Melosh, 1989), strength response of target rock (Head, 1976), elastic response of target (Baldwin, 1963), and others. Geologic structure of central uplift of the Shiyli marine astrobleme in the Western Kazakhstan is of a definite concern to the problem discussed.

The Shiyli astrobleme, of ~3.2 km in diameter, with center co-ordinates 49°10'N, 57°51'E, and age of origin ~45 ±5 Ma (Vishnevsky and Korobkov, 1989) was originated in shallow, ~ 300 m deep, Eocenian marine basin on a target with two-stage structure. The target includes a basement (dislocated Paleozoic and Triassic terrigenous rocks) and a sedimentary cover (loose Cretaceous and Paleogenian marine and continental deposits, including marine members of Middle-Eocenian age, with a total thickness of the cover ~260 m). The astrobleme is heavily eroded now, and the central uplift of ~1200 m in diameter, surrounded by ring syncline can only be observed here. Clear traces of weak shock metamorphism are found in the structure rocks: "gries" breccia, shatter cones, shock slickensides, and PDFs in quartz, with evident {1013} maximum of their orientation distribution. Low level of regional post-impact erosion (<100 m of target rocks) indicates that during the Shiyli impact

event all the bottom sediments of the Eocenian Sea had experienced a weak impulse of shock energy.

Examined by boring holes, the non-root geologic structure of the central uplift was formed in the sedimentary cover rocks exclusively, and no structural uplift is observed in buried plane surface of the basement. In particular, the basal member of the cover (Low Cretaceous clays) is the first one demonstrating the structure of the central uplift. Comparing to its usual, ~55-60 m, thickness around the astrobleme, the member increases strongly (up to 120 m in thickness) on the axis of the central uplift, but is thinning down to 20-30 m around the uplift. All other members of the cover confirm this structure, which seems to be a result of ground centripetal flow to the axis of the central uplift. At this, the replacement was accompanied by the ring subsidence of cover rocks around the central uplift. As a result, the present collar of Paleogenic rocks was preserved in the ring syncline around the central uplift, being protected from erosion.

Due to a presence of non-dislocated rigid basement, such a structure of the central uplift was not possible to be formed by means of crater's gravity collapse or by isostasy relaxation. At the same time, the origin of the central uplift can be explained by elastic response of the target rocks. Following to the model of cratering after (Gault et al., 1968), this process is supposed to be limited geometrically by any spherical sector of target rock compression zone under the center of impact "explosion". Within the sector, isobars of rarefaction wave were approximately parallel to each other and to the surface of shock wave front. Ground centripetal movement within this sector was resulted from summation of shock-wave-induced particle velocity (centrifugal vector) and rarefaction-wave-induced elastic expansion velocities of the ground (centripetal vector), with the resulting dominating of the last one.

The example of Shiyli astrobleme shows that elastic response is one of the principal mechanisms of the central uplift origin in the complex craters. Another mechanisms (gravity collapse, explosive expansion of superheated porous water, and so on) may have the supporting significance only. The clear evidence of target elastic response in Shiyli astrobleme may be the result of marine kind of the impact event (more deep, then usual, shape of growing crater cavity and a strong dissipation of excavation energy in water). The presence of rigid basement in target may play an important role also (limitation of the process by loose cover sediments). Comparing to continental impact structures, the marine astroblemes of Shiyli type (low-pressure shock impulse into non-water members of the target) may be characterised by reduced development of the crater structure, limited, probably, by the origin of central uplift and sub-bottom displacement of sediments around it only.

#### References

- Baldwin, R.B. (1963) *The measure of the Moon*. Chicago, University of Chicago Press, 488 p.
- Dabizha, A.M., Krass, M.S. and Fedynsky, VV. (1976) Evolution of meteoritic craters as the structures of the Earth crust. *Astronomichesky vestnik* **10**: 6-17 (in Russian).

- Dence, M.R., Grieve, R.A.F. and Robertson, P.B. (1977) Terrestrial impact structures: principal characteristics and energy considerations. In: *Impact and explosion cratering*. New York, Pergamon Press, pp. 247-275.
- Gault, D.E., Quaide, W.L. and Oberbeck, V.R. (1968) Impact cratering mechanics and structures. In: *Shock metamorphism of natural materials*. Baltimore: Mono Book Corp., pp. 87-99.
- Head, J.W. (1976) The significance of substrate characteristics in determining morphology and morphometry of Lunar craters. *Proc. 7th Lunar Sci. Conf.* **3**: 2913-2929.
- Melosh, H.J. (1989) *Impact cratering: a geologic process*. New York, Oxford University Press, 245 p.
- Vishnevsky, S.A. and Korobkov, V.F. (1989) Shiyli Dome: heavily-eroded astrobleme in the Werstern Cis-Mugojarian. Novosibirsk: *Inst. of Geology and Geophysics Press, preprint*, **13**: 51 p. (in Russian).

### **The Seismic Fingerprint of the Eltanin Impact**

D. Völker\* and V. Spiess

Dept. of Earth Science, University of Bremen, Klagenfurter Straße, D-28359 Bremen (a13g@mtu.uni-bremen.de) \*present address: Geological Institute, University of Tübingen, Sigwartstrasse 10, D-72076 Tübingen

During Polarstern Cruise ANT XII/4 in spring 1995 a detailed study was carried out in the area between 58°S, 92°W and 57°S, 89°W to identify the potential impact area of the Eltanin meteorite with geological and geophysical methods. A narrow grid of acoustic survey lines was measured with the digital Parasound/ParaDigMA echosounder system and the Hydrosweep swath sounder to map topography and to image surface sediment structures.

The objective of this study was to get a complete information about the surface sediment distribution and their variation with depth from the working area. To identify the impact area, disturbed sediment structures were expected, which are characterized by mass movements or re-sedimentation or the loss of internal structures due to the massive pressure waves and extreme currents during the event. However, no example is known from oceanic areas as an analog, and therefore a mapping of sedimentary features in conjunction with sediment sampling was the focus during the cruise. Since the overall influence on the sea bed sediment cover can not be predicted, the availability of the narrow beam digital sediment echosounder Parasound is most advantageous, since further data processing, an improved lateral and vertical resolution due to the parametric sound generation, and an analysis of specific acoustic characteristics can be carried out onshore, in contrast to conventional 3.5 kHz analog recording devices.

In general, reflection patterns were similar both on elevated areas of the seamount group and in deeper parts of the surrounding basins. They are characterized by numerous densely spaced reflectors, which reveal some local variation in sediment accumulation. Beneath this surface layer a diffusely

reflective zone of up to 10 m thickness was observed, which grades into a acoustically transparent zone of 10 to 60 m thickness. The base of this transparent unit is highly reflective, but appears patchy and reveals pronounced local variability (Reflector EL). In most places it represents the deepest reflection, which could be imaged by the 4 kHz signal due to sound attenuation with depth.

We propose that Reflector EL in conjunction with the overlying transparent unit represents the time and material, which had suffered major dislocation and resedimentation due to the impact, and which reveals a strong local variability probably due to chaotic physical disturbance. Reflector EL seems to be either in contact with older sediments or basement, indicating the non-pelagic origin of this interface. The sequence of acoustic units is widely found in the area, both on elevated areas and in basins from 3000 m to 5200 m water depth, which would not be explained by local mass movement events, but only by a more regional cause. In few locations sediments of this unit were cored and impact material was found (Gersonde et al., 1997), which constrained the tentative assignments.

#### References

Gersonde, R., Kyte, F.T., Bleil, U., Diekmann, B., Flores, J.A., Gohl, K., Grahl, G., Hagen, R., Kuhn, K., Sierro, F.J., Völker, D., Abelman, A. and Bostwick, J.A. (1997) Geological record and reconstruction of the late Pliocene impact of the Eltanin asteroid in the Southern Ocean. *Nature* **390**: 357-363.

## **Middle Ordovician Acritarchs from Impact Structures in Sweden**

Å. Wallin.

Department of Geology and Geochemistry, University of Stockholm, 106 91 Stockholm, Sweden, (asa.wallin@geo.su.se).

#### Introduction

Impact structures are important geologically, among other things for the stratigraphic and paleo-ecologic information that they can host. Three impact structures formed on Baltica in the Lower Caradoc (Baltoscandian stages Kukrusean and Haljalan) are discovered. The Tvären crater (SE Sweden) was formed about 460 Ma (Ormö, pers.comm. 1998) in the *Nemagraptus gracilis* graptolite Chron and the *Baltoniodus variabilis* conodont Subchron. The Lockne crater (W central Sweden) and the Kärddla crater (Estonia) were formed about 455 Ma (Sturkell, 1998; Puura and Suuroja, 1992) in the *Diplograptus multidens* graptolite Chron and the *Baltoniodus gerdae* Subchron. All craters were created in an epicontinental sea.

A project has been initiated to study acritarchs in the secular (infilling) sediments from the Tvären and the Lockne structures. Both successions consist of Dalby Limestone, and the thickness is 65 m and 88 m respectively. The Dalby Limestone was deposited during the Kukrusean Age and the Idaverean Subage, and the total thickness outside the craters is 10-22 meters. Secular sediments give the opportunity to study sediments formed under controlled conditions from a relatively short time interval. By comparing secular sections with coeval assemblages not from impact structures, it is possible to investigate if the impacts affected the diversity of the floras, to study short time variability and evolutionary trends and possibly improve the current age estimations of the impacts and the infillings. Furthermore, a high resolution biostratigraphy can be established of the intervals represented as secular deposits. These investigations will lead to a definition of regional acritarch biozones.

#### The Tvären structure

The crater constitutes a circular depression, 2 km wide, filled with sediment, in an area dominated by Precambrian crystalline rocks. Substantial information has been gathered from a complete core sequence drilled in the depression. The succession consists of a subautochthonous, crystalline breccia, 60 m of a fining upwards resurge deposit and 80 m secular sediments of grey, carbonatic mudstone (Lindström et al., 1994). By examination of fragments in the resurge material, it has been possible to identify the pre-impact stratigraphy of Cambrian and Ordovician deposits in the area (Ormö, 1994). The age of the event is the late Kukrusean, based on conodonts and chitinozoans, which also indicate that infilling of the structure was completed before the end of Kukrusean (Grahm et al., 1996). The crater rim may have hosted reef-like structures, according to fragments found in slumps in the sequence, containing skeletons of echinoderms, bryozoans, brachiopods, trilobites, ostracods and calcareous algae, which suggest a warm water environment for the area. A changing bottom environment within the structure, to successively shallower, has made it possible to study the habitat of bottom living organisms (Lindström et al., 1994).

#### The Lockne structure

The crater consist of a 7.5 km wide inner crater, developed in the crystalline basement, surrounded by a 3 km wide outer crater. It is situated at the Caledonian erosional front, and parts are still covered by a thin nappe outlier. Resurge of the sea after the impact eroded gullies radially through the outer crater. The resurge deposits are more than 200 meters thick, and the secular post-impact Dalby Limestone nearly 100 meters. The Dalby Limestone is characterized by massive, light grey, hard calcilutite that occurs as ellipsoidal to irregularly rounded nodules in a grey argillaceous matrix (Lindström et al., 1996).

#### Palynology

Baltica was positioned at southerly latitudes during the Ordovician. Middle Ordovician acritarch assemblages in Swedish sequences show similarities with warm water assemblages found in Canada, USA, northern China and Australia. Earlier work on Swedish Middle Ordovician acritarchs were made by

Kjellström (1971a, 1971b, 1972, 1976) and Gorkà (1987). Standard palynological preparation is carried out on 50 g sediment samples, using a 20 µm sieve.

In the Lockne section, only few samples have been investigated so far. They exhibit black coloured acritarchs that have been carbonized and fragmented because of the overburden from the Caledonides. The TAI-value is 4-5, and dominating genera are *Baltisphaeridium* and *Goniosphaeridium*. Further data await comparison with the Tvären investigation.

In the Tvären section, samples were analyzed from every second meter. The acritarchs are very well preserved, abundant and diverse with a TAI-value of 1+. The flora contains acanthomorphs, sphaeromorphs and polygonomorphs. Chitinozoans and scolecodonts are also present. The absolute abundance is about 5000 specimens per gram and the species richness about 50 species per sample. The dominance of the genera *Baltisphaeridium*, *Ordovicidium*, *Peteinosphaeridium* and *Goniosphaeridium* exhibits the characteristics for Baltic assemblages.

#### References

- Gorkà, H. (1987) Acritarches et prasinophyceae de l'Ordovicien Moyen (Viruen) du sondage de Smedsby Gård No. 1 (Gotland, Suède). *Rev. Palaeobotany and Palynology* **52**: 257-297.
- Grahn, Y., Nölvak, J. and Paris, F. (1996) Precise chitinozoan dating of Ordovician events in Baltoscandia. *J. Micropalaeont.* **15**: 21-35.
- Kjellström, G. (1971a) Ordovician microplankton (Baltisphaerids) from the Grötlingbo borehole No. 1 in Gotland, Sweden. *Sveriges Geologiska Undersökning, serie C* **655**: 1-75.
- Kjellström, G. (1971b) Middle Ordovician microplankton from the Grötlingbo borehole No. 1 in Gotland, Sweden. *Sveriges Geologiska Undersökning, serie C* **669**: 1-35.
- Kjellström, G. (1972) Lower Viruan microplankton from a boring in Öland, Sweden. *Neues Jahrbuch für Geologie und Paläontologie, Monatshefte*: 713-719.
- Kjellström, G. (1976) Lower Viruan (Middle Ordovician) microplankton from the Ekön borehole No. 1 in Östergötland, Sweden. *Sveriges Geologiska Undersökning, serie C* **724**: 1-44.
- Lindström, M., Flodén, T., Grahn, Y. and Kathol, B. (1994) Post-impact deposits in Tvären, a marine Middle Ordovician crater south of Stockholm, Sweden. *Geol. Mag.* **131**(1): 91-103.
- Lindström, M., Sturkell, E.F.F., Törnberg, R. and Ormö, J. (1996) The marine impact crater at Lockne, central Sweden. *Geologiska Föreningen i Stockholm Förhandlingar* **118**: 193-206.
- Ormö, J. (1994) The pre-impact Ordovician stratigraphy of the Tvären Bay impact structure, SE Sweden. *Geologiska Föreningens i Stockholm Förhandlingar* **116**: 139-144.
- Puura, V. and Suuroja, K. (1992) Ordovician impact crater at Kärđla, Hiiumaa Island, Estonia. *Tectonophysics* **216**: 143-156.
- Sturkell, E.F.F. (1998) The Origin of the Marine Lockne Impact Structure, Jämtland. *Unpublished Ph.D. thesis*, University of Stockholm, Sweden.

## Numerical Modeling of Oceanic Impact Events

K. Wünnemann<sup>1,2</sup> and M. A. Lange<sup>2</sup>.

1) Inst. f. Planetologie, D-48149 Münster, Germany; 2) Inst. f. Geophysik, D-48149 Münster, Germany, (wunnema@uni-muenster.de).

Although 70% of the Earth's surface is covered by oceans so far only one deep sea impact, the ~2.15 Myr old Eltanin crater in the Bellingshausen Sea, has been discovered and investigated (Gersonde et al., 1997). The apparent lack of oceanic impact structures is due to (i) the relatively young age of the oceanic crust, (ii) its renewal by subduction and seafloor spreading, (iii) the fact that not all projectiles hitting the ocean's surface will leave traces at the sea floor, and (iv) the inaccessibility of the ocean bottom. The interaction of the impacting body and the water column causes loss of kinetic energy both from oceanic drag and from mass loss due to hydrodynamic heating, prior to hitting the ocean bottom. This process is accompanied by significant compressive stresses, which may exceed the yield strength of the asteroid's material and result in fragmentation of the impacting body. A first order estimate of the kinetic energy loss of the asteroid during its passage through the water column can be obtained by solving the one-dimensional equation of motion (O'Keefe and Ahrens, 1982). Moreover, the planar impact approximation provides a good estimate of maximum shock pressures in the early stages of an impact (Melosh, 1982). Both estimates can be improved through numerical modeling. This paper presents numerical computer simulations aimed to describe impacts onto a water covered target. The kinetic energy loss and the maximum pressures at the top of the ocean crust are calculated based on boundary conditions such as the initial kinetic energy of the asteroid and the water depth at the impact site. In some cases the mass and the velocity of the asteroid does not suffice to produce a crater at the seafloor. However, the shock wave which is induced in the water column causes unique traces that are observable in marine sediments. This evidence enables the localization of such impact sites, an estimate of the size of the impact event and an assessment of possible environmental effects caused by such an event.

### Acknowledgement

This work is supported by DFG Graduiertenkolleg.

### References

- Gersonde, R., et al. (1997) Geological record and reconstruction of the late Pliocene impact of the Eltanin asteroid in the southern ocean. *Nature* **390**: 357-363.
- Melosh, H.J. (1982) The mechanics of large meteorid impacts in the earth's oceans. *Geol. Soci. Amer. Spec. Pap.* **190**: 121-127.
- O'Keefe, J.D. and Ahrens, T.J. (1982) The interaction of the cretaceous/tertiary extinction bolide with the atmosphere, ocean and solid earth. *Geol. Soc. Amer. Spec. Pap.* **190**: 103-120.

**Participants**

<b>Name</b>	<b>Address</b>	<b>Phone</b>	<b>Fax</b>	<b>e-mail</b>
Abelmann, Andrea	Alfred Wegener Inst., P.O. box 120161, 27515 Bremerhaven, Germany	00 49-471-4831-205	00 49-471-4831-149	aabelmann@awi- bremerhaven.de
Abels, Andreas	Inst.f.Planetologie, WWU Münster, Wilhelm-Klemm- Str. 10, 48149 Münster, Germany	00 49-251-833-3937	00 49-251-833-3968	abels@uni-muenster.de
Agrinier, Pierre	Lab. Geochimie des Isotopes Stables, IPGP, 75252 Paris Cedex 05, France	00 33-1 44 27 28 11	00 33-1 44 27 28 30	piag@ccr.jussieu.fr
Ainsaar, Leho	Institute of Geology, University of Tartu, Vanemuise 46 Tartu 51014, Estonia	00 37-27375829	00 37-27375836	lainsaar@math.ut.ee
Apel, Markus	Museum f. Naturkunde, Abt. f. Paläontologie, Invalidenstr. 43, 10155 Berlin, Germany	00 49-(0)30-2093-8658	00 49-(0)30-2093-8868	marcus.apel@rz-hu-berlin.de
Arkonsuo, Anja	Väinämöisenkatu, 5 A 8, 00100 Helsinki, Finland	00 358-9-4546-047	00 358-9-447-389	anjaarkonsuo@online. tietokone.fi
Artemieva, Natalia	Inst. for Dynamics of Geospheres, RAS, Leninsky pr., 38, bld.6, Moscow, Russia, 117979	00 7-095-1376511	00 7-095-1376511	art@idg.chph.ras.ru
Aslanian, S.	Geological Institute BAS, Sofia, Bulgaria			
Bahlburg, Heinrich	Geol.-Paläont. Inst., WWU Münster, Corrensstraße 24, 48149 Münster, Germany	00 49-251-833 3935	00 49-251-833 3968	bahlbur@uni-muenster.de
Beaudoin, Bernard	Ecole des Mines de Paris, CGES-Sedimentologie, 35 rue Saint-Honore, 77305 Fontainebleau, France			beaudoin@cges.ensmp.fr
Becquey, Sabine	Alfred Wegener Inst., P.O. box 120161, 27515 Bremerhaven, Germany	00 49-471-4831-207	00 49-471-4831-149	sbecquey@awi- bremerhaven.de
Bleil, Ulrich	Universität Bremen, Fachbereich Geowissen- schaften, P.O. box 330440, 28334 Bremen	00 49-(0)421-218-3366	00 49-(0)421-218-7008	bleil@zfn.uni-bremen.de
Bischoff, Lutz	Geol.-Paläont. Inst., WWU Münster, Corrensstraße 24, 48149 Münster, Germany	00 49-251-833-3964	00 49-251-833-3968	bischol@uni-muenster.de

**Participants**

<b>Name</b>	<b>Address</b>	<b>Phone</b>	<b>Fax</b>	<b>e-mail</b>
Censarek, Bernd	Alfred Wegener Inst., P.O. box 120161, 27515 Bremerhaven, Germany	00 49-471-4831-341	00 49-471-4831-149	bcensarek@awi- bremerhaven.de
Claeys, Philippe	Inst.f.Mineralogie, Museum f. Naturkunde, 10099 Berlin, Germany	00 49-30-2093-8857	00 49-30-2093-8565	philippe.claeys@rz.hu- berlin.de
von Dalwigk, Ilka	Dept of Geology and Geochemistry, Stockholm Univ., 10691 Stockholm, Sweden	00 46-8-164-757	00 46-8-674-7879	ilka@geo.su.se
Deutsch, Alexander	Inst. f. Planetologie, WWU Münster, Wilhelm-Klemm- Str. 10, 48149 Münster, Germany	00 49-251-83-33484	00 49-251-83-39083	deutsca@uni-muenster.de
Diekmann, Bernhard	Alfred Wegener Inst., P.O. box 120161, 27515 Bremerhaven, Germany	00 49-471-4831-202	00 49-471-4831-149	bdiekmann@awi- bremerhaven.de
Ebbing, Jörg	Inst. f. Geowissenschaften, Geophysik, Uni. Kiel, Otto-Hahn-Platz 1, 24118 Kiel, Germany	00 49-431-880-1918	00 49-431-880-4432	jebbing@geophysik.uni- kiel.de
Flores, Jose-Abel	Depart. de Geologia, Univ. de Salamanca, 37008 Salamanca, Spain	00 34-923-29449	00 34-923-294514	flores@gugu.usal.es
Galeotti, Simone	Inst.di Geologia, Uni. di Urbino, Campus Scientifico, Loc.Crocicchia, 61029 Urbino, Italy	0039-722-304273	0039-722-304220	s.galeotti@uniurb.it
Gerasimov, Mikhail	Russ. Acad. Sci., 1 Space Research Inst., Profsoyuznaya st., 84/32, Moscow, 117810 Russia			mgerasim@mx.iki.rssi.ru
Gersonde, Rainer	Alfred Wegener Inst., P.O. box 120161, 27515 Bremerhaven, Germany	00 49-471-4831-203	00 49-471-4831-149	rgersonde@awi- bremerhaven.de
Gilmour, Ian	Planetary Sci. Research Inst., The Open University Milton Keynes, MK7 6AA. UK	00 44-190-865-5140	00 44-190-865-5910	i.gilmour@open.ac.uk
Hass, Christian	Alfred Wegener Inst., P.O. box 120161, 27515 Bremerhaven, Germany	00 49-(0)471-4831-128	00 49-(0)471-4831-149	chass@awi-bremerhaven.de

**Participants**

<b>Name</b>	<b>Address</b>	<b>Phone</b>	<b>Fax</b>	<b>e-mail</b>
Hillenbrand, Claus-Dieter	Alfred Wegener Inst., P.O. box 120161, 27515 Bremerhaven, Germany	00 49-(0)471-4831-238	00 49-(0)471-4831-149	chillebrand@awi- bremerhaven.de
Ivanov, Boris A.	Inst. f. Dynamics of Geospheres, Russ. Acad. Sci., Leninsky Prospect 38-6, Moscow, Russia 117321	00 7-095-338-17-13	00 7-095-137-6511	baivanov@glasnet.ru
Jones, Adrian P.	Depart. of Geological Sci., Uni. College London, Gower Street, London WC1E 6BT, U.K.	00 44-171-5042415	00 44-171-3887614	adrian.jones@ucl.ac.uk
Kettrup, Bianca	Inst. f. Planetologie, WWU Münster, Wilhelm-Klemm- Str. 10, 48149 Münster, Germany	00 49-(0)251-83-33689	00 49-(0)251-83-36301	kettrup@uni-muenster
Kettrup, Dirk	Inst. f. Planetologie, WWU Münster, Wilhelm-Klemm- Str. 10, 48149 Münster, Germany	00 49-(0)251-83-39113	00 49-(0)251-83-36301	kettrupd@uni-muenster.de
Klumov, Boris	Institute for Dynamics of Geospheres, RAS, Leninsky pr. 38, Bldg. 6, Moscow, Russia, 117321	0	007-095-1376511	klumov@idg.chph.ras.ru
Koeberl, Christian	Inst. of Geochemistry, Univ. of Vienna, Althanstrasse 14, 1090 Vienna, Austria	00 43-1-31336 1714	00 43-1-31336 781	christian.koeberl@univie. ac.at
Koulouris, Jannis	Inst. f. Geowissenschaften, Geophysik, Uni. Kiel., Otto-Hahn-Platz 1, 24118 Kiel, Germany	00 49-(0)431-880-1518	00 49-(0)431-880-4432	pla02@geophysik.uni-kiel.de
Kuhn, Gerhard	Alfred Wegener Inst., P.O. box 120161, 27515 Bremerhaven, Germany	0049-(0)471-4831-204	00 49-(0)471-4831-149	gkuhn@awi-bremerhaven.de
Kyte, Frank	Inst.of Geophysics and Planetary Physics, UCLA, Los Angeles,CA 90095-1567, USA	00 1-310-825-2015	00 1-310-206-3051	kyte@igpp.ucla.edu
Lange, Manfred	Inst. f. Geophysik, WWU Münster, Corrensstraße 24, 48149 Münster, Germany	00 49-(0)251-833-3591	00 49-(0)251-833-6100	langema@uni-muenster.de
Leosson, Markus M.	Institute of Petrography und Geochemistry, University of Karlsruhe (TH), Kaiserstrasse 12, 76128 Karlsruhe	00 49-(0)721-608-7581	00 49-(0)721-697-328	Markus.Leosson@bio- geo.uni-karlsruhe.de
Leng, Claudia	Alfred Wegener Inst., P.O. box 120161, 27515 Bremerhaven, Germany	00 49-(0)471-4831-231	00 49-(0)471-4831-149	-

**Participants**

<b>Name</b>	<b>Address</b>	<b>Phone</b>	<b>Fax</b>	<b>e-mail</b>
Lindström, Maurits	Dept. of Geology and Geochemistry, Stockholm Uni., 10691 Stockholm, Sweden	0046-8-164724	00 46-8-6747897	-
Martinez-Ruiz, Francisca C.	Inst. Andaluz de Ciencias de la Tierra, Fac. Ciencias, Fuentenuevas/n., 18002 Granada, Spain	00 34-958-246228	00 34-958-243384	fmruiz@goliat.ugr.es
Masaitis, Victor L.	Karpinsky Geological Inst., Sredny prospekt 74, St.- Petersburg, 199106 Russia	007-812-218-9206	007-812-213-5738	vsegei@mail.wplus.net
Milkereit, Bernd	Inst. f. Geowissenschaften, Geophysik, Uni. Kiel, Otto-Hahn-Platz 1, 24118 Kiel, Germany	00 49-(0)431-880-3914	00 49-(0)431-880-4432	geo40@physik.uni-kiel.de
Miller, Heinz	Alfred Wegener Inst., P.O. box 120161, 27515 Bremerhaven, Germany	00 49-471-4831-210	00 49-471-4831-149	hmiller@awi-bremerhaven.de
Monteiro, Jose F.	Depart. de Geologia FCUL - Univ. de Lisboa, Edificio C-2, Campo Grande, 1700 Lisboa, Portugal		00 351-1-7500064	jf.monteiro@mail.teleweb.pt
Müller, Christian	Alfred Wegener Inst., P.O. box 120161, 27515 Bremerhaven, Germany	00 49-(0)471-4831-267	00 49-(0)471-4831-149	cmueller@awi- bremerhaven.de
Ormö, Jens	Dept. of Geology and Geochemistry, Stockholm Uni., 10691 Stockholm, Sweden	00 46-70-6974052	00 46-8-6747897	jens.ormo@geo.su.se
Plescia, Jeff	U.S. Geological Survey, Astrogeology Program, 2255 N.Gemini Drive, Flagstaff, AZ 8600, USA	00 1-520-556-7341	00 1-520-556-7014	jplescia@flagmail.wr.usgs. gov
Pohl, Jean-Paul	Institut für Allgemeine und Angewandte Geophysik, Theresienstrasse 41, 80333 München, Germany	0049-(0)89-23944230	0049-(0)89-23944205	pohl@alice.geophysik.uni- muenchen.de
Preisinger, A.	Inst. f. Mineralogie und Kristallographie, TU Wien, Getreidemarkt 6, 1060 Wien, Austria	00 43-1-406-6050	00 43-1-586-8136	lpetras@fbch.tuwien.ac.at
Salge, Tobias	Inst.f.Mineralogie, Museum f.Naturkunde, 10099 Berlin, Germany	00 49-(0)30-2093-8570	00 49-(0)30-2093-8565	Tobias.Salge@rz.hu- berlin.de
Schultze, Arnold	Univ. Lüneburg, 21332 Lüneburg, Germany	00 49-(0)4131-32966	00 49-(0)4131-32966	-

**Participants**

<b>Name</b>	<b>Address</b>	<b>Phone</b>	<b>Fax</b>	<b>e-mail</b>
Smit, Jan	Dept.of Paleontology, Vrije Univ., de Boelelaan 1085, 1081HV Amsterdam, Netherlands	00 31-20-4447384	00 31-20-6462457	smit@geo.vu.nl
Spiess, Volkhard	Universität Bremen,Fachbereich Geowissenschaften, P.O. box 330440 28, 28334 Bremen, Germany	00 49-(0)421-218-7167	00 49-(0)421-218-7179	a13g@mtu.uni-bremen.de
Suuroja,Sten	Geological Survey of Estonia, Kadaka tee 80/82, Tallinn 12618, Estonia	00 372-2-6720092	00 372-2-6720091	s.suuroja@egk.ee
Teterev, Alexander	Dep.of Applied Mathematics & Computer Sciences Belarus State Univ., 4F.Skorina ave., Minsk, 220050 Belarus	00 375-17-226 55 48	00 375 -17-226 55 48	Teterev@fpm.bsu.unibel.by
Törnberg, Roger	Dept. of Geology and Geochemistry, Stockholm Uni., 10691 Stockholm, Sweden	00 46-8-674-7818	00 46-8-674-7897	tornberg@geo.su.se
Tsikalas, Filippos	Dept.of Geology, Uni. of Oslo, P.O.Box 1047, Blindern, 0316 Oslo, Norway	00 47-22-856678	00 47-22-854215	filippos.tsikalas@geologi.uio.no
Vernackelen, Jutta	Alfred Wegener Inst., P.O. box 120161, 27515 Bremerhaven, Germany	00 49 -(0)471-4831-231	00 49- (0)471- 4831 - 149	-
Vishnevsky, Sergei A.	Inst. of Mineralogy and Petrology, Novosibirsk-90, 630090 Russia	00 7 -3832-33-36-08	00 7-3832-33-27-92	svish @math.nsc.ru
Werner, Stephanie	Inst. f. Geowissenschaften, Geophysik, Uni. Kiel, Otto-Hahn-Platz 1, 24118 Kiel, Germany	00 49-(0)431-8804562		swerner@geophysik.uni-kiel.de
Wünnemann, Kai	Inst. f. Geophysik, WWU Münster, Corrensstrasse 24, 48149 Münster, Germany	00 49-(0)251-8333597		wunnema@uni-muenster.de
Ziegler, Willi	Palisadenweg 6, 35419 Hungen, Germany	00 49-(0)6402-1421		WilliZiegler@t-online.de
Zielinski, Ulrich	Alfred Wegener Inst., P.O. box 120161, 27515 Bremerhaven, Germany	00 49-471-4831-221	00 49-471-4831-149	uzielinski@awi-bremerhaven.de

## Folgende Hefte der Reihe „Berichte zur Polarforschung“ sind bisher erschienen:

- \* **Sonderheft Nr. 1/1981** – „Die Antarktis und ihr Lebensraum“  
Eine Einführung für Besucher – Herausgegeben im Auftrag von SCAR
- \* **Heft Nr. 1/1982** – „Die Filchner-Schelfeis-Expedition 1980/81“  
zusammengestellt von Heinz Kohnen
- \* **Heft Nr. 2/1982** – „Deutsche Antarktis-Expedition 1980/81 mit FS ‚Meteor‘“  
First International BIOMASS Experiment (FIBEX) – Liste der Zooplankton- und Mikronektonnetzänge  
zusammengestellt von Norbert Klages
- \* **Heft Nr. 3/1982** – „Digitale und analoge Krill-Echolot-Rohdatenerfassung an Bord des Forschungsschiffes ‚Meteor‘“ (im Rahmen von FIBEX 1980/81, Fahrtrabschnitt ANT III), von Bodo Morgenstern
- \* **Heft Nr. 4/1982** – „Filchner-Schelfeis-Expedition 1980/81“  
Liste der Planktonfänge und Lichtstärkemessungen  
zusammengestellt von Gerd Hubold und H. Eberhard Drescher
- \* **Heft Nr. 5/1982** – „Joint Biological Expedition on RRS ‚John Biscoe‘, February 1982“  
by G. Hempel and R. B. Heywood
- \* **Heft Nr. 6/1982** – „Antarktis-Expedition 1981/82 (Unternehmen ‚Eiswarte‘)“  
zusammengestellt von Gode Gravenhorst
- \* **Heft Nr. 7/1982** – „Marin-Biologisches Begleitprogramm zur Standorterkundung 1979/80 mit MS ‚Polarstern‘ (Pre-Site Survey)“ – Stationslisten der Mikronekton- und Zooplanktonfänge sowie der Bodenfischerei  
zusammengestellt von R. Schneppenheim
- \* **Heft Nr. 8/1983** – „The Post-Fibex Data Interpretation Workshop“  
by D. L. Cram and J.-C. Freytag with the collaboration of J. W. Schmidt, M. Mall, R. Kresse, T. Schwinghammer
- \* **Heft Nr. 9/1983** – „Distribution of some groups of zooplankton in the inner Weddell Sea in summer 1979/80“  
by I. Hempel, G. Hubold, B. Kaczmaruk, R. Keller, R. Weigmann-Haass
- \* **Heft Nr. 10/1983** – „Fluor im antarktischen Ökosystem“ – DFG-Symposium November 1982  
zusammengestellt von Dieter Adelung
- \* **Heft Nr. 11/1983** – „Joint Biological Expedition on RRS ‚John Biscoe‘, February 1982 (II)“  
Data of micronekton and zooplankton hauls, by Uwe Piatkowski
- \* **Heft Nr. 12/1983** – „Das biologische Programm der ANTARKTIS-I-Expedition 1983 mit FS ‚Polarstern‘“  
Stationslisten der Plankton-, Benthos- und Grundsleppnetzänge und Liste der Probennahme an Robben und Vögeln, von H. E. Drescher, G. Hubold, U. Piatkowski, J. Plötz und J. Voß
- \* **Heft Nr. 13/1983** – „Die Antarktis-Expedition von MS ‚Polarbjörn‘ 1982/83“ (Sommerkampagne zur Atka-Bucht und zu den Kraul-Bergen), zusammengestellt von Heinz Kohnen
- \* **Sonderheft Nr. 2/1983** – „Die erste Antarktis-Expedition von FS ‚Polarstern‘ (Kapstadt, 20. Januar 1983 – Rio de Janeiro, 25. März 1983)“, Bericht des Fahrtleiters Prof. Dr. Gotthilf Hempel
- \* **Sonderheft Nr. 3/1983** – „Sicherheit und Überleben bei Polarexpeditionen“  
zusammengestellt von Heinz Kohnen
- \* **Heft Nr. 14/1983** – „Die erste Antarktis-Expedition (ANTARKTIS I) von FS ‚Polarstern‘ 1982/83“  
herausgegeben von Gotthilf Hempel
- \* **Sonderheft Nr. 4/1983** – „On the Biology of Krill *Euphausia superba*“ – Proceedings of the Seminar and Report of the Krill Ecology Group, Bremerhaven 12. - 16. May 1983, edited by S. B. Schnack
- \* **Heft Nr. 15/1983** – „German Antarctic Expedition 1980/81 with FRV ‚Walther Herwig‘ and RV ‚Meteor‘“ – First International BIOMASS Experiment (FIBEX) – Data of micronekton and zooplankton hauls  
by Uwe Piatkowski and Norbert Klages
- \* **Sonderheft Nr. 5/1984** – „The observatories of the Georg von Neumayer Station“, by Ernst Augstein
- \* **Heft Nr. 16/1984** – „FIBEX cruise zooplankton data“  
by U. Piatkowski, I. Hempel and S. Rakusa-Suszczewski
- \* **Heft Nr. 17/1984** – „Fahrtbericht (cruise report) der ‚Polarstern‘-Reise ARKTIS I, 1983“  
von E. Augstein, G. Hempel und J. Thiede
- \* **Heft Nr. 18/1984** – „Die Expedition ANTARKTIS II mit FS ‚Polarstern‘ 1983/84“,  
Bericht von den Fahrtrabschnitten 1, 2 und 3, herausgegeben von D. Fütterer
- \* **Heft Nr. 19/1984** – „Die Expedition ANTARKTIS II mit FS ‚Polarstern‘ 1983/84“,  
Bericht vom Fahrtrabschnitt 4, Punta Arenas-Kapstadt (Ant-II/4), herausgegeben von H. Kohnen
- \* **Heft Nr. 20/1984** – „Die Expedition ARKTIS II des FS ‚Polarstern‘ 1984, mit Beiträgen des FS ‚Valdivia‘ und des Forschungsflugzeuges ‚Falcon 20‘ zum Marginal Ice Zone Experiment 1984 (MIZEX)“  
von E. Augstein, G. Hempel, J. Schwarz, J. Thiede und W. Weigel
- \* **Heft Nr. 21/1985** – „Euphausiid larvae in plankton from the vicinity of the Antarctic Peninsula, February 1982“ by Sigrid Marschall and Elke Mizdalski
- \* **Heft Nr. 22/1985** – „Maps of the geographical distribution of macrozooplankton in the Atlantic sector of the Southern Ocean“ by Uwe Piatkowski
- \* **Heft Nr. 23/1985** – „Untersuchungen zur Funktionsmorphologie und Nahrungsaufnahme der Larven des Antarktischen Krills *Euphausia superba* Dana“ von Hans-Peter Marschall

- Heft Nr. 24/1985** – „Untersuchungen zum Periglazial auf der König-Georg-Insel Südshetlandinseln/ Antarktika. Deutsche physiogeographische Forschungen in der Antarktis. – Bericht über die Kampagne 1983/84“ von Dietrich Barsch, Wolf-Dieter Blümel, Wolfgang Flügel, Roland Mäusbacher, Gerhard Stäblein, Wolfgang Zick
- \* **Heft Nr. 25/1985** – „Die Expedition ANTARKTIS III mit FS ‚Polarstern‘ 1984/1985“ herausgegeben von Gotthilf Hempel.
  - \* **Heft Nr. 26/1985** – „The Southern Ocean“; A survey of oceanographic and marine meteorological research work by Hellmer et al.
  - \* **Heft Nr. 27/1986** – „Spätpleistozäne Sedimentationsprozesse am antarktischen Kontinentalhang vor Kapp Norvegia, östliche Weddell-See“ von Hannes Grobe  
**Heft Nr. 28/1986** – „Die Expedition ARKTIS III mit ‚Polarstern‘ 1985 mit Beiträgen der Fahrtteilnehmer, herausgegeben von Rainer Gersonde
  - \* **Heft Nr. 29/1986** – „5 Jahre Schwerpunktprogramm ‚Antarktisforschung‘ der Deutschen Forschungsgemeinschaft.“ Rückblick und Ausblick. Zusammenge stellt von Gotthilf Hempel, Sprecher des Schwerpunktprogramms  
**Heft Nr. 30/1986** – „The Meteorological Data of the Georg-von-Neumayer-Station for 1981 and 1982“ by Marianne Gube and Friedrich Obleitner
  - \* **Heft Nr. 31/1986** – „Zur Biologie der Jugendstadien der Notothenioidei (Pisces) an der Antarktischen Halbinsel“ von A. Kellermann
  - \* **Heft Nr. 32/1986** – „Die Expedition ANTARKTIS IV mit FS ‚Polarstern‘ 1985/86“ mit Beiträgen der Fahrtteilnehmer, herausgegeben von Dieter Fütterer  
**Heft Nr. 33/1987** – „Die Expedition ANTARKTIS-IV mit FS ‚Polarstern‘ 1985/86 – Bericht zu den Fahrtabschnitten ANT-IV/3-4“ von Dieter Karl Fütterer  
**Heft Nr. 34/1987** – „Zoogeographische Untersuchungen und Gemeinschaftsanalysen an antarktischen Makroplankton“ von U. Piatkowski  
**Heft Nr. 35/1987** – „Zur Verbreitung des Meso- und Makrozooplanktons in Oberflächenwasser der Weddell See (Antarktis)“ von E. Boysen-Ennen  
**Heft Nr. 36/1987** – „Zur Nahrungs- und Bewegungsphysiologie von *Salpa thompsoni* und *Salpa fusiformis*“ von M. Reinke  
**Heft Nr. 37/1987** – „The Eastern Weddell Sea Drifting Buoy Data Set of the Winter Weddell Sea Project (WWSP)“ 1986 by Heinrich Hoerber und Marianne Gube-Lehnhardt  
**Heft Nr. 38/1987** – „The Meteorological Data of the Georg von Neumayer Station for 1983 and 1984“ by M. Gube-Lehnhardt  
**Heft Nr. 39/1987** – „Die Winter-Expedition mit FS ‚Polarstern‘ in die Antarktis (ANT V/1-3)“ herausgegeben von Sigrid Schnack-Schiel  
**Heft Nr. 40/1987** – „Weather and Synoptic Situation during Winter Weddell Sea Project 1986 (ANT V/2) July 16 - September 10, 1986“ by Werner Rabe  
**Heft Nr. 41/1988** – „Zur Verbreitung und Ökologie der Seegurken im Weddellmeer (Antarktis)“ von Julian Gutt  
**Heft Nr. 42/1988** – „The zooplankton community in the deep bathyal and abyssal zones of the eastern North Atlantic“ by Werner Beckmann
  - \* **Heft Nr. 43/1988** – „Scientific cruise report of Arctic Expedition ARK IV/3“ Wissenschaftlicher Fahrtbericht der Arktis-Expedition ARK IV/3, compiled by Jörn Thiede
  - \* **Heft Nr. 44/1988** – „Data Report for FV ‚Polarstern‘ Cruise ARK IV/1, 1987 to the Arctic and Polar Fronts“ by Hans-Jürgen Hirche  
**Heft Nr. 45/1988** – „Zoogeographie und Gemeinschaftsanalyse des Makrozoobenthos des Weddellmeeres (Antarktis)“ von Joachim Volz  
**Heft Nr. 46/1988** – „Meteorological and Oceanographic Data of the Winter-Weddell-Sea Project 1986 (ANT V/3)“ by Eberhard Fahrback  
**Heft Nr. 47/1988** – „Verteilung und Herkunft glazial-mariner Gerölle am Antarktischen Kontinentalrand des östlichen Weddellmeeres“ von Wolfgang Oskierski  
**Heft Nr. 48/1988** – „Variationen des Erdmagnetfeldes an der GvN-Station“ von Arnold Brodscholl
  - \* **Heft Nr. 49/1988** – „Zur Bedeutung der Lipide im antarktischen Zooplankton“ von Wilhelm Hagen
  - \* **Heft Nr. 50/1988** – „Die gezeitenbedingte Dynamik des Ekström-Schelfeises, Antarktis“ von Wolfgang Kobarg  
**Heft Nr. 51/1988** – „Ökomorphologie nototheniider Fische aus dem Weddellmeer, Antarktis“ von Werner Ekau  
**Heft Nr. 52/1988** – „Zusammensetzung der Bodenfauna in der westlichen Fram-Straße“ von Dieter Piepenburg
  - \* **Heft Nr. 53/1988** – „Untersuchungen zur Ökologie des Phytoplanktons im südöstlichen Weddellmeer (Antarktis) im Jan./Febr. 1985“ von Eva-Maria Nöthig  
**Heft Nr. 54/1988** – „Die Fischfauna des östlichen und südlichen Weddellmeeres: geographische Verbreitung, Nahrung und trophische Stellung der Fischarten“ von Wiebke Schwarzbach  
**Heft Nr. 55/1988** – „Weight and length data of zooplankton in the Weddell Sea in austral spring 1986 (Ant. V/3)“ by Elke Mizdalski  
**Heft Nr. 56/1989** – „Scientific cruise report of Arctic expeditions ARK IV/1, 2 & 3“ by G. Krause, J. Meinke und J. Thiede

- Heft Nr. 57/1989** – „Die Expedition ANTARKTIS V mit FS ‚Polarstern‘ 1986/87“  
Bericht von den Fahrtabschnitten ANT V/4-5 von H. Miller und H. Oerter
- **Heft Nr. 58/1989** – „Die Expedition ANTARKTIS VI mit FS ‚Polarstern‘ 1987/88“  
von D. K. Fütterer
  - Heft Nr. 59/1989** – „Die Expedition ARKTIS V/1a, 1b und 2 mit FS ‚Polarstern‘ 1988“  
von M. Spindler
  - Heft Nr. 60/1989** – „Ein zweidimensionales Modell zur thermohalinen Zirkulation unter dem Schelfeis“  
von H. H. Hellmer
  - Heft Nr. 61/1989** – „Die Vulkanite im westlichen und mittleren Neuschwabenland,  
Vestfjella und Ahlmannryggen, Antarktika“ von M. Peters
  - **Heft Nr. 62/1989** – „The Expedition ANTARKTIS VII/1 and 2 (EPOS I) of RV ‚Polarstern‘  
in 1988/89“, by I. Hempel
  - Heft Nr. 63/1989** – „Die Eisalgenflora des Weddellmeeres (Antarktis): Artenzusammensetzung und Biomasse  
sowie Ökophysiologie ausgewählter Arten“ von Annette Bartsch
  - Heft Nr. 64/1989** – „Meteorological Data of the G.-v.-Neumayer-Station (Antarctica)“ by L. Helmes
  - Heft Nr. 65/1989** – „Expedition Antarktis VII/3 in 1988/89“ by I. Hempel, P. H. Schalk, V. Smetacek
  - Heft Nr. 66/1989** – „Geomorphologisch-glaziologische Detailkartierung  
des arid-hochpolaren Borgmassivet, Neuschwabenland, Antarktika“ von Karsten Brunk
  - Heft Nr. 67/1990** – „Identification key and catalogue of larval Antarctic fishes“,  
edited by Adolf Kellermann
  - Heft Nr. 68/1990** – „The Expedition Antarktis VII/4 (Epos leg 3) and VII/5 of RV ‚Polarstern‘ in 1989“,  
edited by W. Arntz, W. Ernst, I. Hempel
  - Heft Nr. 69/1990** – „Abhängigkeiten elastischer und rheologischer Eigenschaften des Meereises vom  
Eisgefüge“, von Harald Hellmann
  - **Heft Nr. 70/1990** – „Die beschalten benthischen Mollusken (Gastropoda und Bivalvia) des  
Weddellmeeres, Antarktis“, von Stefan Hain
  - Heft Nr. 71/1990** – „Sedimentologie und Paläomagnetik an Sedimenten der Maudkuppe (Nordöstliches  
Weddellmeer)“, von Dieter Cordes
  - Heft Nr. 72/1990** – „Distribution and abundance of planktonic copepods (Crustacea) in the Weddell Sea  
in summer 1980/81“, by F. Kurbjeweit and S. Ali-Khan
  - Heft Nr. 73/1990** – „Zur Frühdiagenese von organischem Kohlenstoff und Opal in Sedimenten des südlichen  
und östlichen Weddellmeeres“, von M. Schlüter
  - Heft Nr. 74/1990** – „Expeditionen ANTARKTIS-VIII/3 und VIII/4 mit FS ‚Polarstern‘ 1989“  
von Rainer Gersonde und Gotthilf Hempel
  - Heft Nr. 75/1991** – „Quartäre Sedimentationsprozesse am Kontinentalhang des Süd-Orkey-Plateaus im  
nordwestlichen Weddellmeer (Antarktis)“, von Sigrun Grünig
  - Heft Nr. 76/1990** – „Ergebnisse der faunistischen Arbeiten im Benthal von King George Island  
(Südshetlandinseln, Antarktis)“, von Martin Rauschert
  - Heft Nr. 77/1990** – „Verteilung von Mikroplankton-Organismen nordwestlich der Antarktischen Halbinsel  
unter dem Einfluß sich ändernder Umweltbedingungen im Herbst“, von Heinz Klöser
  - Heft Nr. 78/1991** – „Hochauflösende Magnetostratigraphie spätquartärer Sedimente arktischer  
Meeresgebiete“, von Norbert R. Nowaczyk
  - Heft Nr. 79/1991** – „Ökophysiologische Untersuchungen zur Salinitäts- und Temperaturtoleranz  
antarktischer Grünalgen unter besonderer Berücksichtigung des  $\beta$ -Dimethylsulfoniumpropionat  
(DMSP) - Stoffwechsels“, von Ulf Karsten
  - Heft Nr. 80/1991** – „Die Expedition ARKTIS VII/1 mit FS ‚Polarstern‘ 1990“,  
herausgegeben von Jörn Thiede und Gotthilf Hempel
  - Heft Nr. 81/1991** – „Paläoglazilogie und Paläozeanographie im Spätquartär am Kontinentalrand des  
südlichen Weddellmeeres, Antarktis“, von Martin Melles
  - Heft Nr. 82/1991** – „Quantifizierung von Meeresseigenschaften: Automatische Bildanalyse von  
Dünnschnitten und Parametrisierung von Chlorophyll- und Salzgehaltsverteilungen“, von Hajo Eicken
  - Heft Nr. 83/1991** – „Das Fließen von Schelfeisen - numerische Simulationen  
mit der Methode der finiten Differenzen“, von Jürgen Determann
  - Heft Nr. 84/1991** – „Die Expedition ANTARKTIS-VIII/1-2, 1989 mit der Winter Weddell Gyre Study  
der Forschungsschiffe ‚Polarstern‘ und ‚Akademik Fedorov‘“, von Ernst Augstein,  
Nikolai Bagriantsev und Hans Werner Schenke
  - Heft Nr. 85/1991** – „Zur Entstehung von Unterwassereis und das Wachstum und die Energiebilanz  
des Meereises in der Atka Bucht, Antarktis“, von Josef Kipfstuhl
  - **Heft Nr. 86/1991** – „Die Expedition ANTARKTIS-VIII mit FS ‚Polarstern‘ 1989/90. Bericht vom  
Fahrtabschnitt ANT-VIII/5“, von Heinz Miller und Hans Oerter
  - Heft Nr. 87/1991** – „Scientific cruise reports of Arctic expeditions ARK VII/1-4 of RV ‚Polarstern‘  
in 1989“, edited by G. Krause, J. Meincke & H. J. Schwarz
  - Heft Nr. 88/1991** – „Zur Lebensgeschichte dominanter Copepodenarten (*Calanus finmarchicus*,  
*C. glacialis*, *C. hyperboreus*, *Metridia longa*) in der Framstraße“, von Sabine Diehl

- Heft Nr. 89/1991** – „Detaillierte seismische Untersuchungen am östlichen Kontinentalrand des Weddell-Meereres vor Kapp Norvegia, Antarktis“, von Norbert E. Kaul
- Heft Nr. 90/1991** – „Die Expedition ANTARKTIS-VIII mit FS ‚Polarstern‘ 1989/90. Bericht von den Fahrabschnitten ANT-VIII/6-7“, herausgegeben von Dieter Karl Fütterer und Otto Schrems
- Heft Nr. 91/1991** – „Blood physiology and ecological consequences in Weddell Sea fishes (Antarctica)“, by Andreas Kunzmann
- Heft Nr. 92/1991** – „Zur sommerlichen Verteilung des Mesozooplanktons im Nansen-Becken, Nordpolarmeer“, von Nicolai Mumm
- Heft Nr. 93/1991** – „Die Expedition ARKTIS VII mit FS ‚Polarstern‘, 1990. Bericht vom Fahrabschnitt ARK VII/2“, herausgegeben von Gunther Krause
- Heft Nr. 94/1991** – „Die Entwicklung des Phytoplanktons im östlichen Weddellmeer (Antarktis) beim Übergang vom Spätwinter zum Frühjahr“, von Renate Scharek
- Heft Nr. 95/1991** – „Radioisotopenstratigraphie, Sedimentologie und Geochemie jungquartärer Sedimente des östlichen Arktischen Ozeans“, von Horst Bohrmann
- Heft Nr. 96/1991** – „Holozäne Sedimentationsentwicklung im Scoresby Sund, Ost-Grönland“, von Peter Marienfeld
- Heft Nr. 97/1991** – „Strukturelle Entwicklung und Abkühlungsgeschichte von Heimefrontfjella (Westliches Dronning Maud Land/Antarktika)“, von Joachim Jacobs
- Heft Nr. 98/1991** – „Zur Besiedlungsgeschichte des antarktischen Schelfeis am Beispiel der Isopoda (Crustacea, Malacostraca)“, von Angelika Brandt
- **Heft Nr. 99/1992** – „The Antarctic ice sheet and environmental change: a three-dimensional modelling study“, by Philippe Huybrechts
  - **Heft Nr. 100/1992** – „Die Expeditionen ANTARKTIS IX/1-4 des Forschungsschiffes ‚Polarstern‘ 1990/91“ herausgegeben von Ulrich Bathmann, Meinhard Schulz-Baldes, Eberhard Fahrbach, Victor Smetacek und Hans-Wolfgang Hubberten
- Heft Nr. 101/1992** – „Wechselbeziehungen zwischen Schwermetallkonzentrationen (Cd, Cu, Pb, Zn) im Meerwasser und in Zooplanktonorganismen (Copepoda) der Arktis und des Atlantiks“, von Christa Pohl
- Heft Nr. 102/1992** – „Physiologie und Ultrastruktur der antarktischen Grünalge *Prasiola crista ssp. antarctica* unter osmotischem Stress und Austrocknung“, von Andreas Jacob
- **Heft Nr. 103/1992** – „Zur Ökologie der Fische im Weddellmeer“, von Gerd Hubold
- Heft Nr. 104/1992** – „Mehrkanaulige adaptive Filter für die Unterdrückung von multiplen Reflexionen in Verbindung mit der freien Oberfläche in marinen Seismogrammen“, von Andreas Rosenberger
- Heft Nr. 105/1992** – „Radiation and Eddy Flux Experiment 1991 (REFLEX I)“, von Jörg Hartmann, Christoph Kottmeier und Christian Wamser
- Heft Nr. 106/1992** – „Ostracoden im Epipelagial vor der Antarktischen Halbinsel - ein Beitrag zur Systematik sowie zur Verbreitung und Populationsstruktur unter Berücksichtigung der Saisonalität“, von Rüdiger Kock
- **Heft Nr. 107/1992** – „ARCTIC '91: Die Expedition ARK-VIII/3 mit FS ‚Polarstern‘ 1991“, von Dieter K. Fütterer
- Heft Nr. 108/1992** – „Dehnungsbeben an einer Störungszone im Ekström-Schelfeis nördlich der Georg-von-Neumayer-Station, Antarktis. – Eine Untersuchung mit seismologischen und geodätischen Methoden“, von Uwe Nixdorf.
- **Heft Nr. 109/1992** – „Spätquartäre Sedimentation am Kontinentalrand des südöstlichen Weddellmeeres, Antarktis“, von Michael Weber.
- **Heft Nr. 110/1992** – „Sedimentfazies und Bodenwasserstrom am Kontinentalhang des norwestlichen Weddellmeeres“, von Isa Brehme.
- Heft Nr. 111/1992** – „Die Lebensbedingungen in den Solekanälchen des antarktischen Meereises“, von Jürgen Weissenberger.
- Heft Nr. 112/1992** – „Zur Taxonomie von rezenten benthischen Foraminiferen aus dem Nansen Becken, Arktischer Ozean“, von Jutta Wollenburg.
- Heft Nr. 113/1992** – „Die Expedition ARKTIS VIII/1 mit FS ‚Polarstern‘ 1991“, herausgegeben von Gerhard Kattner.
- **Heft Nr. 114/1992** – „Die Gründungsphase deutscher Polarforschung, 1865 - 1875“, von Reinhard A. Krause.
- Heft Nr. 115/1992** – „Scientific Cruise Report of the 1991 Arctic Expedition ARK VIII/2 of RV ‚Polarstern‘ (EPOS II)“, by Eike Racher.
- Heft Nr. 116/1992** – „The Meteorological Data of the Georg-von-Neumayer-Station (Antarctica) for 1988, 1989, 1990 and 1991“, by Gert König-Langlo.
- Heft Nr. 117/1992** – „Petrogenese des metamorphen Grundgebirges der zentralen Heimefrontfjella (westliches Dronning Maud Land / Antarktis)“, von Peter Schulze.
- Heft Nr. 118/1993** – „Die mafischen Gänge der Shackleton Range / Antarktika: Petrographie, Geochemie, Isotopengeochemie und Paläomagnetik“, von Rüdiger Hotten.
- **Heft Nr. 119/1993** – „Gefrierschutz bei Fischen der Polarmee“, von Andreas P. A. Wöhrmann.
- **Heft Nr. 120/1993** – „East Siberian Arctic Region Expedition '92: The Laptev Sea - its Significance for Arctic Sea-Ice Formation and Transpolar Sediment Flux“, by D. Dethleff, D. Nürnberg, E. Reimnitz, M. Saarso and Y. P. Sacchenko. – „Expedition to Novaja Zemlja and Franz Josef Land with RV ‚Dainie Zelentsy‘“, by D. Nürnberg and E. Groth.

- **Heft Nr. 121/1993** – „Die Expedition ANTARKTIS X/3 mit FS ‚Polarstern‘ 1992“, herausgegeben von Michael Spindler, Gerhard Dieckmann und David Thomas
- Heft Nr. 122/1993** – „Die Beschreibung der Korngestalt mit Hilfe der Fourier-Analyse: Parametrisierung der morphologischen Eigenschaften von Sedimentpartikeln“, von Michael Diepenbroek.
- **Heft Nr. 123/1993** – „Zerstörungsfreie hochauflösende Dichteuntersuchungen mariner Sedimente“, von Sebastian Gerland.
- Heft Nr. 124/1993** – „Umsatz und Verteilung von Lipiden in arktischen marinen Organismen unter besonderer Berücksichtigung unterer trophischer Stufen“, von Martin Graeve.
- Heft Nr. 125/1993** – „Ökologie und Respiration ausgewählter arktischer Bodentischarten“, von Christian F. von Dorrien.
- Heft Nr. 126/1993** – „Quantitative Bestimmung von Paläoumweltparametern des Antarktischen Oberflächenwassers im Spätquartier anhand von Transferfunktionen mit Diatomeen“, von Ulrich Zielinski
- **Heft Nr. 127/1993** – „Sedimenttransport durch das arktische Meeres: Die rezente lithogene und biogene Materialfracht“, von Ingo Wollenburg.
- Heft Nr. 128/1993** – „Cruise ANTARKTIS X/3 of RV ‚Polarstern‘: CTD-Report“, von Marek Zwierz.
- Heft Nr. 129/1993** – „Reproduktion und Lebenszyklen dominanter Copepodenarten aus dem Weddellmeer, Antarktis“, von Frank Kurbjeweit
- Heft Nr. 130/1993** – „Untersuchungen zu Temperaturregime und Massenhaushalt des Filchner-Ronne-Schelfeises, Antarktis, unter besonderer Berücksichtigung von Anfrier- und Abschmelzprozessen“, von Klaus Grosfeld
- Heft Nr. 131/1993** – „Die Expedition ANTARKTIS X/5 mit FS ‚Polarstern‘ 1992“, herausgegeben von Rainer Gersonde
- Heft Nr. 132/1993** – „Bildung und Abgabe kurzketziger halogener Kohlenwasserstoffe durch Makroalgen der Polarregionen“, von Frank Laturnus
- Heft Nr. 133/1994** – „Radiation and Eddy Flux Experiment 1993 (REFLEX II)“, by Christoph Koltmeier, Jörg Hartmann, Christian Wamser, Axel Bochert, Christof Lüpkes, Dietmar Freese and Wolfgang Cohrs
- **Heft Nr. 134/1994** – „The Expedition ARKTIS-IX/1“, edited by Hajo Eicken and Jens Meincke
- Heft Nr. 135/1994** – „Die Expeditionen ANTARKTIS X/6-8“, herausgegeben von Ulrich Bathmann, Victor Smetacek, Hein de Baar, Eberhard Fahrbach und Gunter Krause
- Heft Nr. 136/1994** – „Untersuchungen zur Ernährungsökologie von Kaiserpinguinen (*Aptenodytes forsteri*) und Königspinguinen (*Aptenodytes patagonicus*)“, von Klemens Pütz
- **Heft Nr. 137/1994** – „Die kältezoische Vereisungsgeschichte der Antarktis“, von Werner U. Ehrmann
- Heft Nr. 138/1994** – „Untersuchungen stratosphärischer Aerosole vulkanischen Ursprungs und polarer stratosphärischer Wolken mit einem Mehrwellenlängen-Lidar auf Spitzbergen (79° N, 12° E)“, von Georg Beyerle
- Heft Nr. 139/1994** – „Charakterisierung der Isopodenfauna (Crustacea, Malacostraca) des Scotia-Bogens aus biogeographischer Sicht: Ein multivariater Ansatz“, von Holger Winkler.
- Heft Nr. 140/1994** – „Die Expedition ANTARKTIS X/4 mit FS ‚Polarstern‘ 1992“, herausgegeben von Peter Lemke
- Heft Nr. 141/1994** – „Satellitenaltimetrie über Eis – Anwendung des GEOSAT-Altimeters über dem Ekströmisien, Antarktis“, von Clemens Heidland
- Heft Nr. 142/1994** – „The 1993 Northeast Water Expedition. Scientific cruise report of RV ‚Polarstern‘ Arctic cruises ARK IX/2 and 3, USCG ‚Polar Bear‘ cruise NEWP and the NEWLAND expedition“, edited by Hans-Jürgen Hirche and Gerhard Kattner
- Heft Nr. 143/1994** – „Detaillierte refraktionsseismische Untersuchungen im inneren Scoresby Sund Ost-Grönland“, von Notker Fechner
- Heft Nr. 144/1994** – „Russian-German Cooperation in the Siberian Shelf Seas: Geo-System Laptev Sea“, edited by Heidemarie Kassens, Hans-Wolfgang Hubberten, Sergey M. Pryamikov and Rüdiger Stein
- **Heft Nr. 145/1994** – „The 1993 Northeast Water Expedition. Data Report of RV ‚Polarstern‘ Arctic Cruises IX/2 and 3“, edited by Gerhard Kattner and Hans-Jürgen Hirche.
- Heft Nr. 146/1994** – „Radiation Measurements at the German Antarctic Station Neumayer 1982 - 1992“, by Torsten Schmidt and Gerd König-Langlo.
- Heft Nr. 147/1994** – „Krustenstrukturen und Verlauf des Kontinentalrandes im Weddell-See / Antarktis“, von Christian Hübscher.
- **Heft Nr. 148/1994** – „The expeditions NORILSK/TAYMYR 1993 and BUNGER OASIS 1993/94 of the AWI Research Unit Potsdam“, edited by Martin Melles.
- \*\* **Heft Nr. 149/1994** – „Die Expedition ARCTIC '93. Der Fahrtabschnitt ARK-IX/4 mit FS ‚Polarstern‘ 1993“, herausgegeben von Dieter K. Fütterer.
- Heft Nr. 150/1994** – „Der Energiebedarf der Pygoscelis-Pinguine: eine Synopse“, von Boris M. Culik.
- Heft Nr. 151/1994** – „Russian-German Cooperation: The Transdrift I Expedition to the Laptev Sea“, edited by Heidemarie Kassens and Valeriy Y. Karpiy.
- Heft Nr. 152/1994** – „Die Expedition ANTARKTIS-X mit FS ‚Polarstern‘ 1992. Bericht von den Fahrtabschnitten / ANT-X / 1a und 2“, herausgegeben von Heinz Miller.
- Heft Nr. 153/1994** – „Aminosäuren und Huminstoffe im Stickstoffkreislauf polarer Meere“, von Ulrike Hubberten.
- Heft Nr. 154/1994** – „Regional and seasonal variability in the vertical distribution of mesozooplankton in the Greenland Sea“, by Claudio Richter.

- Heft Nr. 155/1995 – „Benthos in polaren Gewässern“, herausgegeben von Christian Wiencke und Wolf Arntz.
- Heft Nr. 156/1995 – „An adjoint model for the determination of the mean oceanic circulation, air-sea fluxes and mixing coefficients“, by Reiner Schlitzer.
- Heft Nr. 157/1995 – „Biochemische Untersuchungen zum Lipidstoffwechsel antarktischer Copepoden“, von Kirsten Fahl.
- \* Heft Nr. 158/1995 – „Die Deutsche Polarforschung seit der Jahrhundertwende und der Einfluß Erich von Drygalskis“, von Cornelia Lüdecke.
- \* Heft Nr. 159/1995 – „The distribution of  $\delta^{18}\text{O}$  in the Arctic Ocean: Implications for the freshwater balance of the halocline and the sources of deep and bottom waters“, by Dorothea Bauch.
- \* Heft Nr. 160/1995 – „Rekonstruktion der spätquartären Tiefenwasserzirkulation und Produktivität im östlichen Südatlantik anhand von benthischen Foraminiferenvergesellschaftungen“, von Gerhard Schmiedl.
- Heft Nr. 161/1995 – „Der Einfluß von Salinität und Lichtintensität auf die Osmolytkonzentrationen, die Zellvolumina und die Wachstumsraten der antarktischen Eisdiatomeen *Chaetoceros* sp. und *Navicula* sp. unter besonderer Berücksichtigung der Aminosäure Prolin“, von Jürgen Nothnagel.
- Heft Nr. 162/1995 – „Meerestransportiertes lithogenes Feinmaterial in spätquartären Tiefseesedimenten des zentralen östlichen Arktischen Ozeans und der Framstraße“, von Thomas Letzig.
- Heft Nr. 163/1995 – „Die Expedition ANTARKTIS-XI/2 mit FS „Polarstern“ 1993/94“, herausgegeben von Rainer Gersonde.
- Heft Nr. 164/1995 – „Regionale und altersabhängige Variation gesteinsmagnetischer Parameter in marinen Sedimenten der Arktis“, von Thomas Frederichs.
- Heft Nr. 165/1995 – „Vorkommen, Verteilung und Umsatz biogener organischer Spurenstoffe: Sterole in antarktischen Gewässern“, von Georg Hanke.
- Heft Nr. 166/1995 – „Vergleichende Untersuchungen eines optimierten dynamisch-thermodynamischen Meereismodells mit Beobachtungen im Weddellmeer“, von Holger Fischer.
- \* Heft Nr. 167/1995 – „Rekonstruktionen von Paläo-Umweltparametern anhand von stabilen Isotopen und Faunen-Vergesellschaftungen planktischer Foraminiferen im Südatlantik“, von Hans-Stefan Niebler
- Heft Nr. 168/1995 – „Die Expedition ANTARKTIS XII mit FS „Polarstern“ 1993/94. Bericht von den Fahrtabschnitten ANT XII/1 und 2“, herausgegeben von Gerhard Kattner und Dieter Karl Fütterer
- Heft Nr. 169/1995 – „Medizinische Untersuchung zur Circadianrhythmik und zum Verhalten bei Überwinterern auf einer antarktischen Forschungsstation“, von Hans Wortmann
- Heft-Nr. 170/1995 – DFG-Kolloquium: Terrestrische Geowissenschaften – Geologie und Geophysik der Antarktis.
- Heft Nr. 171/1995 – „Strukturentwicklung und Petrogenese des metamorphen Grundgebirges der nördlichen Heimfrontjella (westliches Dronning Maud Land/Antarktika)“, von Wilfried Bauer.
- Heft Nr. 172/1995 – „Die Struktur der Erdkruste im Bereich des Scoresby Sund, Ostgrönland: Ergebnisse refraktionseismischer und gravimetrischer Untersuchungen“, von Holger Mandler.
- Heft Nr. 173/1995 – „Paläozoische Akkretion am paläopazifischen Kontinentalrand der Antarktis in Nordvictorialand – P-T-D-Geschichte und Deformationsmechanismen im Bowers Terrane“, von Stefan Matzer.
- Heft Nr. 174/1995 – „The Expedition ARKTIS-X/2 of RV 'Polarstern' in 1994“, edited by Hans-W. Hubberten
- Heft Nr. 175/1995 – „Russian-German Cooperation: The Expedition TAYMYR 1994“, edited by Christine Siegart and Gmilyr Bolshiyarov.
- \* Heft Nr. 176/1995 – „Russian-German Cooperation: Laptev Sea System“, edited by Heidemarie Kassens, Dieter Piepenburg, Jörn Thiede, Leonid Timokhov, Hans-Wolfgang Hubberten and Sergey M. Priamikov.
- Heft Nr. 177/1995 – „Organischer Kohlenstoff in spätquartären Sedimenten des Arktischen Ozeans: Terrigener Eintrag und marine Produktivität“, von Carsten J. Schubert
- Heft Nr. 178/1995 – „Cruise ANTARKTIS XII/4 of RV 'Polarstern' in 1995: CTD-Report“, by Jüri Sildam.
- Heft Nr. 179/1995 – „Benthische Foraminiferenfaunen als Wassermassen-, Produktions- und Eisdriftanzeiger im Arktischen Ozean“, von Jutta Wollenburg.
- Heft Nr. 180/1995 – „Biogenopal und biogenes Barium als Indikatoren für spätquartäre Produktivitätsänderungen am antarktischen Kontinentalhang, atlantischer Sektor“, von Wolfgang J. Bonn.
- Heft Nr. 181/1995 – „Die Expedition ARKTIS X/1 des Forschungsschiffes „Polarstern“ 1994“, herausgegeben von Eberhard Fahrbach.
- Heft Nr. 182/1995 – „Laptev Sea System: Expeditions in 1994“, edited by Heidemarie Kassens.
- Heft Nr. 183/1995 – „Interpretation digitaler Parasound Echolotaufzeichnungen im östlichen Arktischen Ozean auf der Grundlage physikalischer Sedimenteigenschaften“, von Uwe Bergmann.
- Heft Nr. 184/1995 – „Distribution and dynamics of inorganic nitrogen compounds in the troposphere of continental, coastal, marine and Arctic areas“, by Maria Dolores Andrés Hernández.
- Heft Nr. 185/1995 – „Verbreitung und Lebensweise der Aphroditen und Polynoiden (Polychaeta) im östlichen Weddellmeer und im Lazarevmeer (Antarktis)“, von Michael Stiller.
- Heft Nr. 186/1995 – „Reconstruction of Late Quaternary environmental conditions applying the natural radionuclides  $^{230}\text{Th}$ ,  $^{10}\text{Be}$ ,  $^{234}\text{Pa}$  and  $^{238}\text{U}$ : A study of deep-sea sediments from the eastern sector of the Antarctic Circumpolar Current System“, by Martin Frank.
- Heft Nr. 187/1995 – „The Meteorological Data of the Neumayer Station (Antarctica) for 1992, 1993 and 1994“, by Gert König-Langlo and Andreas Herber.
- Heft Nr. 188/1995 – „Die Expedition ANTARKTIS-XI/3 mit FS „Polarstern“ 1994“, herausgegeben von Heinz Miller und Hannes Grobe.
- Heft Nr. 189/1995 – „Die Expedition ARKTIS-VII/3 mit FS „Polarstern“ 1990“, herausgegeben von Heinz Miller und Hannes Grobe

- Heft Nr. 190/1996** – "Cruise report of the Joint Chilean-German-Italian Magellan 'Victor Hensen' Campaign in 1994", edited by Wolf Arntz and Matthias Gorny.
- Heft Nr. 191/1996** – „Leitfähigkeits- und Dichtemessung an Eisbohrkernen“, von Frank Wilhelm.
- Heft Nr. 192/1996** – „Photosynthese-Charakteristika und Lebensstrategie antarktischer Makroalgen“, von Gabriele Weykam.
- Heft Nr. 193/1996** – „Heterogene Reaktionen von  $N_2O_5$  und Hbr und ihr Einfluss auf den Ozonabbau in der polaren Stratosphäre“, von Sabine Seisel.
- Heft Nr. 194/1996** – „Ökologie und Populationsdynamik antarktischer Ophiuroiden (Echinodermata)“, von Corinna Dahm.
- Heft Nr. 195/1996** – „Die planktische Foraminifere *Neogloboquadrina pachyderma* (Ehrenberg) im Weddellmeer, Antarktis“, von Doris Berberich.
- Heft Nr. 196/1996** – „Untersuchungen zum Beitrag chemischer und dynamischer Prozesse zur Variabilität des stratosphärischen Ozons über der Arktis“, von Birgit Heese.
- Heft Nr. 197/1996** – "The Expedition ARKTIS-XI/2 of 'Polarstern' in 1995", edited by Gunther Krause.
- Heft Nr. 198/1996** – „Geodynamik des Westantarktischen Riftsystems basierend auf Apatit-Spaltspuranalysen“, von Frank Lisker.
- Heft Nr. 199/1996** – "The 1993 Northeast Water Expedition. Data Report on CTD Measurements of RV 'Polarstern' Cruises ARKTIS IX/2 and 3", by Gerion Budéus and Wolfgang Schneider.
- Heft Nr. 200/1996** – "Stability of the Thermohaline Circulation in analytical and numerical models", by Gerrit Lohmann.
- Heft Nr. 201/1996** – „Trophische Beziehungen zwischen Makroalgen und Herbivoren in der Potter Cove (King George-Insel, Antarktis)“, von Katrin Iken.
- Heft Nr. 202/1996** – „Zur Verbreitung und Respiration ökologisch wichtiger Bodentiere in den Gewässern um Svalbard (Arktis)“, von Michael K. Schmid.
- Heft Nr. 203/1996** – „Dynamik, Rauigkeit und Alter des Meereises in der Arktis – Numerische Untersuchungen mit einem großskaligen Modell“, von Markus Harder.
- Heft Nr. 204/1996** – „Zur Parametrisierung der stabilen atmosphärischen Grenzschicht über einem antarktischen Schelfeis“, von Dörthe Handorf.
- Heft Nr. 205/1996** – "Textures and fabrics in the GRIP ice core, in relation to climate history and ice deformation", by Thorsteinn Thorsteinsson.
- Heft Nr. 206/1996** – „Der Ozean als Teil des gekoppelten Klimasystems: Versuch der Rekonstruktion der glazialen Zirkulation mit verschiedenen komplexen Atmosphärenkomponenten“, von Kerstin Fieg.
- Heft Nr. 207/1996** – „Lebensstrategien dominanter antarktischer Oithoridae (Cyclopoida, Copepoda) und Oncaeidae (Poecilostomatoida, Copepoda) im Bellingshausenmeer“, von Cornelia Metz.
- Heft Nr. 208/1996** – „Atmosphäreinfluss bei der Fernerkundung von Meereis mit passiven Mikrowellenradiometern“, von Christoph Oelke.
- Heft Nr. 209/1996** – „Klassifikation von Radarsatellitendaten zur Meereiserkennung mit Hilfe von Line-Scanner-Messungen“, von Axel Bochert.
- Heft Nr. 210/1996** – „Die mit ausgewählten Schwämmen (Hexactinellida und Demospongiae) aus dem Weddellmeer, Antarktis, vergesellschaftete Fauna“, von Kathrin Kunzmann.
- Heft Nr. 211/1996** – "Russian-German Cooperation: The Expedition TAYMYR 1995 and the Expedition KOLYMA 1995", by Dima Yu. Bolshiyarov and Hans-W. Hubberten.
- Heft Nr. 212/1996** – "Surface-sediment composition and sedimentary processes in the central Arctic Ocean and along the Eurasian Continental Margin", by Ruediger Stein, Gennadij I. Ivanov, Michael A. Levitan, and Kirsten Fahl.
- Heft Nr. 213/1996** – „Gonadenentwicklung und Eiproduktion dreier *Calanus*-Arten (Copepoda): Freilandbeobachtungen, Histologie und Experimente“, von Barbara Niehoff.
- Heft Nr. 214/1996** – „Numerische Modellierung der Übergangszone zwischen Eisschild und Eisschelf“, von Christoph Mayer.
- Heft Nr. 215/1996** – „Arbeiten der AWI-Forschungsstelle Potsdam in Antarktika, 1994/95“, herausgegeben von Ulrich Wand.
- Heft Nr. 216/1996** – „Rekonstruktion quartärer Klimaänderungen im atlantischen Sektor des Südpolarmeeres anhand von Radiolarien“, von Uta Brathauer.
- Heft Nr. 217/1996** – „Adaptive Semi-Lagrange-Finite-Elemente-Methode zur Lösung der Flachwassergleichungen: Implementierung und Parallelisierung“, von Jörn Behrens.
- Heft Nr. 218/1997** – "Radiation and Eddy Flux Experiment 1995 (REFLEX III)", by Jörg Hartmann, Axel Bochert, Dietmar Freese, Christoph Kottmeier, Dagmar Nagel and Andreas Reuter.
- Heft Nr. 219/1997** – „Die Expedition ANTARKTIS-XII mit FS 'Polarstern' 1995. Bericht vom Fahrabschnitt ANT-XII/3, herausgegeben von Wilfried Jokat und Hans Oerter.
- Heft Nr. 220/1997** – „Ein Beitrag zum Schwerfeld im Bereich des Weddellmeeres, Antarktis. Nutzung von Altimetermessungen des GEOSAT und ERS-1“, von Tilo Schöne.
- Heft Nr. 221/1997** – „Die Expeditionen ANTARKTIS-XIII/1-2 des Forschungsschiffes 'Polarstern' 1995/96“, herausgegeben von Ulrich Bathmann, Mike Lukas und Victor Smetacek.
- Heft Nr. 222/1997** – "Tectonic Structures and Glaciomarine Sedimentation in the South-Eastern Weddell Sea from Seismic Reflection Data", by László Oszkó.

**Heft Nr. 223/1997** – „Bestimmung der Meereisdicke mit seismischen und elektromagnetisch-induktiven Verfahren“, von Christian Haas.

**Heft Nr. 224/1997** – „Troposphärische Ozonvariationen in Polarregionen“, von Silke Wessel.

**Heft Nr. 225/1997** – „Biologische und ökologische Untersuchungen zur kryopelagischen Amphipodenfauna des arktischen Meeres“, von Michael Poltermann.

**Heft Nr. 226/1997** – „Scientific Cruise Report of the Arctic Expedition ARK-XI/1 of RV 'Polarstern' in 1995“, edited by Eike Rächor.

**Heft Nr. 227/1997** – „Der Einfluß kompatibler Substanzen und Kryoprotektoren auf die Enzyme Malatdehydrogenase (MDH) und Glucose-6-phosphat-Dehydrogenase (G6P-DH) aus *Acrosiphonia arctica* (Chlorophyta) der Arktis“, von Katharina Kück.

**Heft Nr. 228/1997** – „Die Verbreitung epibenthischer Mollusken im chilenischen Beagle-Kanal“, von Katrin Linse.

**Heft Nr. 229/1997** – „Das Mesozooplankton im Laptevmeer und östlichen Nansen-Becken - Verteilung und Gemeinschaftsstrukturen im Spätsommer“, von Hinrich Hanssen.

**Heft Nr. 230/1997** – „Modell eines adaptierbaren, rechnergestützten, wissenschaftlichen Arbeitsplatzes am Alfred-Wegener-Institut für Polar- und Meeresforschung“, von Lutz-Peter Kurdelski.

**Heft Nr. 231/1997** – „Zur Ökologie arktischer und antarktischer Fische: Aktivität, Sinnesleistungen und Verhalten“, von Christopher Zimmermann.

**Heft Nr. 232/1997** – „Persistente chlororganische Verbindungen in hochantarktischen Fischen“, von Stephan Zimmermann.

**Heft Nr. 233/1997** – „Zur Ökologie des Dimethylsulfoniumpropionat (DMSP)-Gehaltes temperierter und polarer Phytoplanktongemeinschaften im Vergleich mit Laborkulturen der Coccolithophoride *Emiliania huxleyi* und der antarktischen Diatomee *Nitzschia lecontei*“, von Doris Meyerdieter.

**Heft Nr. 234/1997** – „Die Expedition ARCTIC '96 des FS 'Polarstern' (ARK XIII) mit der Arctic Climate System Study (ACSYS)“, von Ernst Augstein und den Fahrteilnehmern.

**Heft Nr. 235/1997** – „Polonium-210 und Blei-210 im Südpolarmeer: Natürliche Tracer für biologische und hydrographische Prozesse im Oberflächenwasser des Antarktischen Zirkumpolarstroms und des Weddellmeeres“, von Jana Friedrich.

**Heft Nr. 236/1997** – „Determination of atmospheric trace gas amounts and corresponding natural isotopic ratios by means of ground-based FTIR spectroscopy in the high Arctic“, by Arndt Meier.

**Heft Nr. 237/1997** – „Russian-German Cooperation: The Expedition TAYMYR/SEVERNAYA ZEMLYA 1996“, edited by Martin Melles, Birgit Hagedorn and Dmitri Yu. Bolshiyarov.

**Heft Nr. 238/1997** – „Life strategy and ecophysiology of Antarctic macroalgae“, by Iván M. Gómez.

**Heft Nr. 239/1997** – „Die Expedition ANTARKTIS XIII/4-5 des Forschungsschiffes 'Polarstern' 1996“, herausgegeben von Eberhard Fahrbach und Dieter Gerdes.

**Heft Nr. 240/1997** – „Untersuchungen zur Chrom-Speziation in Meerwasser, Meereis und Schnee aus ausgewählten Gebieten der Arktis“, von Heide Giese.

**Heft Nr. 241/1997** – „Late Quaternary glacial history and paleoceanographic reconstructions along the East Greenland continental margin: Evidence from high-resolution records of stable isotopes and ice-rafted debris“, by Seung-II Nam.

**Heft Nr. 242/1997** – „Thermal, hydrological and geochemical dynamics of the active layer at a continuous permafrost site, Taymyr Peninsula, Siberia“, by Julia Boike.

**Heft Nr. 243/1997** – „Zur Paläoozeanographie hoher Breiten: Stellvertreterdaten aus Foraminiferen“, von Andreas Mackensen.

**Heft Nr. 244/1997** – „The Geophysical Observatory at Neumayer Station, Antarctica, Geomagnetic and seismological observations in 1995 and 1996“, by Alfons Eckstaller, Thomas Schmidt, Viola Graw, Christian Müller and Johannes Røgenhagen.

**Heft Nr. 245/1997** – „Temperaturbedarf und Biogeographie mariner Makroalgen - Anpassung mariner Makroalgen an tiefe Temperaturen“, von Bettina Bischoff-Bäsmann.

**Heft Nr. 246/1997** – „Ökologische Untersuchungen zur Fauna des arktischen Meeres“, von Christine Friedrich.

**Heft Nr. 247/1997** – „Entstehung und Modifizierung von marinen gelösten organischen Substanzen“, von Berit Kirchhoff.

**Heft Nr. 248/1997** – „Laptev Sea System: Expeditions in 1995“, edited by Heidemarie Kassens.

**Heft Nr. 249/1997** – „The Expedition ANTARKTIS XIII/3 (EASIZ I) of RV 'Polarstern' to the eastern Weddell Sea in 1996“, edited by Wolf Arntz and Julian Gutt.

**Heft Nr. 250/1997** – „Vergleichende Untersuchungen zur Ökologie und Biodiversität des Mega-Epibenthos der Arktis und Antarktis“, von Andreas Starmans.

**Heft Nr. 251/1997** – „Zeitliche und räumliche Verteilung von Mineralvergesellschaftungen in spätquartären Sedimenten des Arktischen Ozeans und ihre Nützlichkeit als Klimaindikatoren während der Glazial/Interglazial-Wechsel“, von Christoph Vogt.

**Heft Nr. 252/1997** – „Solitäre Ascidien in der Potter Cove (King George Island, Antarktis). Ihre ökologische Bedeutung und Populationsdynamik“, von Stephan Kühne.

**Heft Nr. 253/1997** – „Distribution and role of microprotozoa in the Southern Ocean“, by Christine Klaas.

**Heft Nr. 254/1997** – „Die spätquartäre Klima- und Umweltgeschichte der Bunge-Oase, Ostantarktis“, von Thomas Kulbe.

- Heft Nr. 255/1997** – "Scientific Cruise Report of the Arctic Expedition ARK-XIII/2 of RV 'Polarstern' in 1997", edited by Ruediger Stein and Kirsten Fahl.
- Heft Nr. 256/1998** – „Das Radionuklid Tritium im Ozean: Meßverfahren und Verteilung von Tritium im Südatlantik und im Weddellmeer“, von Jürgen Sültenfuß.
- Heft Nr. 257/1998** – „Untersuchungen der Saisonalität von atmosphärischem Dimethylsulfid in der Arktis und Antarktis“, von Christoph Kleefeld.
- Heft Nr. 258/1998** – „Bellingshausen- und Amundsenmeer: Entwicklung eines Sedimentationsmodells“, von Frank-Oliver Nitsche.
- Heft Nr. 259/1998** – "The Expedition ANTARKTIS-XIV/4 of RV 'Polarstern' in 1997", by Dieter K. Fütterer.
- Heft Nr. 260/1998** – „Die Diatomeen der Laptevsee (Arktischer Ozean): Taxonomie und biogeographische Verbreitung“, von Holger Cremer
- Heft Nr. 261/1998** – „Die Krustenstruktur und Sedimentdecke des Eurasischen Beckens, Arktischer Ozean: Resultate aus seismischen und gravimetrischen Untersuchungen“, von Estella Weigelt.
- Heft Nr. 262/1998** – "The Expedition ARKTIS-XIII/3 of RV 'Polarstern' in 1997", by Gunther Krause.
- Heft Nr. 263/1998** – „Thermo-tektonische Entwicklung von Oates Land und der Shackleton Range (Antarktis) basierend auf Spaltspuranalysen“, von Thorsten Schäfer.
- Heft Nr. 264/1998** – „Messungen der stratosphärischen Spurengase ClO, HCl, O<sub>3</sub>, N<sub>2</sub>O, H<sub>2</sub>O und OH mittels flugzeuggetragener Submillimeterwellen-Radiometrie“, von Joachim Urban.
- Heft Nr. 265/1998** – „Untersuchungen zu Massenhaushalt und Dynamik des Ronne Ice Shelves, Antarktis“, von Astrid Lambrecht.
- Heft Nr. 266/1998** – "Scientific Cruise Report of the Kara Sea Expedition of RV 'Akademic Boris Petrov' in 1997", edited by Jens Matthiessen and Oleg Stepanets.
- Heft Nr. 267/1998** – „Die Expedition ANTARKTIS-XIV mit FS ‚Polarstern‘ 1997. Bericht vom Fahrtabschnitt ANT-XIV/3“, herausgegeben von Wilfried Jokat und Hans Oerter.
- Heft Nr. 268/1998** – „Numerische Modellierung der Wechselwirkung zwischen Atmosphäre und Meereis in der arktischen Eisrandzone“, von Gerit Birnbaum.
- Heft Nr. 269/1998** – "Katabatic wind and Boundary Layer Front Experiment around Greenland (KABEG '97)", by Günther Heinemann.
- Heft Nr. 270/1998** – "Architecture and evolution of the continental crust of East Greenland from integrated geophysical studies", by Vera Schindwein.
- Heft Nr. 271/1998** – "Winter Expedition to the Southwestern Kara Sea - Investigations on Formation and Transport of Turbid Sea-Ice", by Dirk Dethleif, Per Loewe, Dominik Weiel, Hartmut Nies, Gesa Kuhmann, Christian Bahe and Gennady Tarasov.
- Heft Nr. 272/1998** – „FTIR-Emissionsspektroskopische Untersuchungen der arktischen Atmosphäre“, von Edo Becker.
- Heft Nr. 273/1998** – „Sedimentation und Tektonik im Gebiet des Agulhas Rückens und des Agulhas Plateaus („SETARAP“)", von Gabriele Uenzelmann-Neben.
- Heft Nr. 274/1998** – "The Expedition ANTARKTIS XIV/2", by Gerhard Kattner.
- Heft Nr. 275/1998** – „Die Auswirkung der 'NorthEastWater'-Polynya auf die Sedimentation von NO-Grönland und Untersuchungen zur Paläo-Ozeanographie seit dem Mittelweichsel“, von Hanne Notholt.
- Heft Nr. 276/1998** – „Interpretation und Analyse von Potentialfelddaten im Weddellmeer, Antarktis: der Zerfall des Superkontinents Gondwana“, von Michael Studinger.
- Heft Nr. 277/1998** – „Koordiniertes Programm Antarktisforschung“. Berichtskolloquium im Rahmen des Koordinierten Programms „Antarktisforschung mit vergleichenden Untersuchungen in arktischen Eisgebieten“, herausgegeben von Hubert Miller.
- Heft Nr. 278/1998** – „Messung stratosphärischer Spurengase über Ny-Ålesund, Spitzbergen, mit Hilfe eines bodengebundenen Mikrowellen-Radiometers“, von Uwe Raffalski.
- Heft Nr. 279/1998** – "Arctic Paleo-River Discharge (APARD). A New Research Programme of the Arctic Ocean Science Board (AOSB)", edited by Ruediger Stein.
- Heft Nr. 280/1998** – „Fernerkundungs- und GIS-Studien in Nordostgrönland“ von Friedrich Jung-Rothenhäusler.
- Heft Nr. 281/1998** – „Rekonstruktion der Oberflächenwassermassen der östlichen Laptevsee im Holozän anhand von aquatischen Palynomorphen“, von Martina Kunz-Pirrung.
- Heft Nr. 282/1998** – "Scavenging of <sup>231</sup>Pa and <sup>230</sup>Th in the South Atlantic: Implications for the use of the <sup>231</sup>Pa/<sup>230</sup>Th ratio as a paleoproductivity proxy", by Hans-Jürgen Walter.
- Heft Nr. 283/1998** – „Sedimente im arktischen Meereis - Eintrag, Charakterisierung und Quantifizierung“, von Frank Lindemann.
- Heft Nr. 284/1998** – „Langzeitanalyse der antarktischen Meereisbedeckung aus passiven Mikrowellendaten“, von Christian H. Thomas.
- Heft Nr. 285/1998** – „Mechanismen und Grenzen der Temperaturanpassung beim Pierwurm *Arenicola marina* (L.)“, von Angela Sommer.
- Heft Nr. 286/1998** – „Energieumsätze benthischer Filtrierer der Potter Cove (King George Island, Antarktis)“, von Jens Kowalke.
- Heft Nr. 287/1998** – "Scientific Cooperation in the Russian Arctic: Research from the Barents Sea up to the Laptev Sea", edited by Eike Rachor.

- Heft Nr. 288/1998** – „Alfred Wegener. Kommentiertes Verzeichnis der schriftlichen Dokumente seines Lebens und Wirkens“, von Ulrich Wutzke.
- Heft Nr. 289/1998** – “Retrieval of Atmospheric Water Vapor Content in Polar Regions Using Spaceborne Microwave Radiometry”, by Jungang Miao.
- Heft Nr. 290/1998** – „Strukturelle Entwicklung und Petrogenese des nördlichen Kristallingürtels der Shackleton Range, Antarktis: Proterozoische und Ross-orogene Krustendynamik am Rand des Ostantarktischen Kratons“, von Axel Brommer.
- Heft Nr. 291/1998** – „Dynamik des arktischen Meereises - Validierung verschiedener Rheologieansätze für die Anwendung in Klimamodellen“, von Martin Kreyscher.
- Heft Nr. 292/1998** – „Anthropogene organische Spurenstoffe im Arktischen Ozean, Untersuchungen chlorierter Biphenyle und Pestizide in der Laptevsee, technische und methodische Entwicklungen zur Probenahme in der Arktis und zur Spurenstoffanalyse“, von Sven Utschakovski.
- Heft Nr. 293/1998** – „Rekonstruktion der spätquartären Klima- und Umweltgeschichte der Schirmacher Oase und des Wohlthat Massivs (Ostantarktika)“, von Markus Julius Schwab.
- Heft Nr. 294/1998** – „Besiedlungsmuster der benthischen Makrofauna auf dem ostgrönländischen Kontinentalhang“, von Klaus Schnack.
- Heft Nr. 295/1998** – „Gehäuseuntersuchungen an planktischen Foraminiferen hoher Breiten: Hinweise auf Umweltveränderungen während der letzten 140.000 Jahre“, von Harald Hommers.
- Heft Nr. 296/1998** – “Scientific Cruise Report of the Arctic Expedition ARK-XIII/1 of RV ‘Polarstern’ in 1997”, edited by Michael Spindler, Wilhelm Hagen and Dorothea Stübing.
- Heft Nr. 297/1998** – „Radiometrische Messungen im arktischen Ozean - Vergleich von Theorie und Experiment“, von Klaus-Peter Johnsen.
- Heft Nr. 298/1998** – “Patterns and Controls of CO<sub>2</sub> Fluxes in Wet Tundra Types of the Taimyr Peninsula, Siberia - the Contribution of Soils and Mosses”, by Martin Sommerkorn.
- Heft Nr. 299/1998** – “The Potter Cove coastal ecosystem, Antarctica. Synopsis of research performed within the frame of the Argentinean-German Cooperation at the Dallmann Laboratory and Jubany Station (King George Island, Antarctica, 1991 - 1997)”, by Christian Wiencke, Gustavo Ferreyra, Wolf Arntz & Carlos Rinaldi.
- Heft Nr. 300/1999** – “The Kara Sea Expedition of RV ‘Akademik Boris Petrov’ 1997: First Results of a Joint Russian-German Pilot Study”, edited by Jens Matthiessen, Oleg V. Stepanets, Ruediger Stein, Dieter K. Fütterer, and Eric M. Galimov.
- Heft Nr. 301/1999** – “The Expedition ANTARKTIS XV/3 (EASIZ II)”, edited by Wolf E. Arntz and Julian Gutt.
- Heft Nr. 302/1999** – „Sterole im herbstlichen Weddellmeer (Antarktis): Großräumige Verteilung, Vorkommen und Umsatz“, von Anneke Mühlebach.
- Heft Nr. 303/1999** – „Polare stratosphärische Wolken: Lidar-Beobachtungen, Charakterisierung von Entstehung und Entwicklung“, von Jens Biele.
- Heft Nr. 304/1999** – „Spätquartäre Paläoumweltbedingungen am nördlichen Kontinentalrand der Barents- und Kara-See. Eine Multi-Parameter-Analyse“, von Jochen Knies.
- Heft Nr. 305/1999** – “Arctic Radiation and Turbulence Interaction Study (ARTIST)”, by Jörg Hartmann, Frank Albers, Stefania Argentini, Axel Bocher, Ubaldo Bonafé, Wolfgang Cohrs, Alessandro Conidi, Dietmar Freese, Teodoro Georgiadis, Alessandro Ippoliti, Lars Kaleschke, Christof Lüpkes, Uwe Maixner, Giangiuseppe Mastrantonio, Fabrizio Ravegnani, Andreas Reuter, Giuliano Trivellone and Angelo Viola.
- Heft Nr. 306/1999** – “German-Russian Cooperation: Biogeographic and biostratigraphic investigations on selected sediment cores from the Eurasian continental margin and marginal seas to analyze the Late Quaternary climatic variability”, edited by Robert R. Spielhagen, Max S. Barash, Gennady I. Ivanov, and Jörn Thiede.
- Heft Nr. 307/1999** – „Struktur und Kohlenstoffbedarf des Makrobenthos am Kontinentalhang Ostgrönlands“, von Dan Seiler.
- Heft Nr. 308/1999** – “ARCTIC '98: The Expedition ARK-XIV/1a of RV ‘Polarstern’ in 1998”, edited by Wilfried Jokat.
- Heft Nr. 309/1999** – „Variabilität der arktischen Ozonschicht: Analyse und Interpretation bodengebundener Millimeterwellenmessungen“, von Björn-Martin Sinnhuber.
- Heft Nr. 310/1999** – „Rekonstruktion von Meereisdrift und terrigenem Sedimenteintrag im Spätquartär: Schwermineralassoziationen in Sedimenten des Laptev-See-Kontinentalrandes und des zentralen Arktischen Ozeans“, von Marion Behrends.
- Heft Nr. 311/1999** – „Parameterisierung atmosphärischer Grenzschichtprozesse in einem regionalen Klimamodell der Arktis“, von Christoph Abegg.
- Heft Nr. 312/1999** – „Solare und terrestrische Strahlungswechselwirkung zwischen arktischen Eisflächen und Wolken“, von Dietmar Freese.
- Heft Nr. 313/1999** – “Snow accumulation on Ekströmsen, Antarctica”, by Elisabeth Schlosser, Hans Oerter and Wolfgang Graf.
- Heft Nr. 314/1999** – „Die Expedition ANTARKTIS XV/4 des Forschungsschiffes ‘Polarstern’ 1998“, herausgegeben von Eberhard Fahrbach.
- Heft Nr. 315/1999** – “Expeditions in Siberia in 1998”, edited by Volker Rachold.
- Heft Nr. 316/1999** – „Die postglaziale Sedimentationsgeschichte der Laptevsee: schwermineralogische und sedimentpetrographische Untersuchungen“, von Bernhard Peregovich.
- Heft-Nr. 317/1999** – „Adaption an niedrige Temperaturen: Lipide in Eisdiatomeen“, von Heidi Lehmal.
- Heft-Nr. 318/1999** – „Effiziente parallele Lösungsverfahren für elliptische partielle Differentialgleichungen in der numerischen Ozeanmodellierung“, von Natalja Rakowsky.

- Heft-Nr. 319/1999** – „The Ecology of Arctic Deep-Sea Copepods (Euchaetidae and Aetideidae). Aspects of their Distribution, Trophodynamics and Effect on the Carbon Flux“, by Holger Auel.
- Heft-Nr. 320/1999** – „Modellstudien zur arktischen stratosphärischen Chemie im Vergleich mit Meßdaten“, von Veronika Eyring.
- Heft-Nr. 321/1999** – „Analyse der optischen Eigenschaften des arktischen Aerosols“, von Dagmar Nagel.
- Heft-Nr. 322/1999** – „Messungen des arktischen stratosphärischen Ozons: Vergleich der Ozonmessungen in Ny-Ålesund, Spitzbergen, 1997 und 1998“, von Jens Langer
- Heft-Nr. 323/1999** – „Untersuchung struktureller Elemente des südöstlichen Weddellmeeres / Antarktis auf der Basis mariner Potentialfelddaten“, von Uwe F. Meyer.
- Heft-Nr. 324/1999** – „Geochemische Verwitterungstrends eines basaltischen Ausgangsgesteins nach dem spätpleistozänen Gletscherrückzug auf der Taimyrhalbinsel (Zentralsibirien) - Rekonstruktion an einer sedimentären Abfolge des Lama Sees“, von Stefanie K. Harwart.
- Heft-Nr. 325/1999** – „Untersuchungen zur Hydrologie des arktischen Meereises - Konsequenzen für den kleinskaligen Stofftransport“, von Johannes Freitag.
- Heft-Nr. 326/1999** – „Die Expedition ANTARKTIS XIV/2 des Forschungsschiffes 'Polarstern' 1998“, herausgegeben von Eberhard Fahrbach.
- Heft-Nr. 327/1999** – „Gemeinschaftsanalytische Untersuchungen der Harpacticoidenfauna der Magellanregion, sowie erste similaritätsanalytische Vergleiche mit Assoziationen aus der Antarktis“, von Kai Horst George.
- Heft-Nr. 328/1999** – „Rekonstruktion der Paläo-Umweltbedingungen am Laptev-See-Kontinentalrand während der beiden letzten Glazial/Interglazial-Zyklen anhand sedimentologischer und mineralogischer Untersuchungen“, von Claudia Müller.
- Heft-Nr. 329/1999** – „Räumliche und zeitliche Variationen atmosphärischer Spurengase aus bodengebundenen Messungen mit Hilfe eines Michelson Interferometers“, von Justus Notholt.
- Heft-Nr. 330/1999** – „The 1998 Danish-German Excursion to Disko Island, West Greenland“, edited by Angelika Brandt, Helge A. Thomsen, Henning Heide-Jørgensen, Reinhardt M. Kristensen and Hilke Ruhberg.
- Heft-Nr. 331/1999** – „Poseidon“ Cruise No. 243 (Reykjavik - Greenland - Reykjavik, 24 August - 11 September 1998): Climate change and the Viking-age fjord environment of the Eastern Settlement, sw Greenland“, by Gerd Hoffmann, Antoon Kuijpers, and Jörn Thiede.
- Heft-Nr. 332/1999** – „Modeling of marine biogeochemical cycles with an emphasis on vertical particle fluxes“, by Regina Usbeck.
- Heft-Nr. 333/1999** – „Die Tanaidaceenfauna des Beagle-Kanals und ihre Beziehungen zur Fauna des antarktischen Festlandssockels“, von Anja Schmidt.
- Heft-Nr. 334/1999** – „D-Aminosäuren als Tracer für biogeochemische Prozesse im Fluß-Schelf-Ozean-System der Arktis“, von Hans Peter Fitznar.
- Heft-Nr. 335/1999** – „Ökophysiologische Ursachen der limitierten Verbreitung reptanter decapoder Krebse in der Antarktis“, von Markus Frederich.
- Heft-Nr. 336/1999** – „Ergebnisse der Untersuchung des grönländischen Inlandeises mit dem elektromagnetischen Reflexionsverfahren in der Umgebung von NGRIP“, von Fidan Göktas.
- Heft-Nr. 337/1999** – „Paleozoic and mesozoic tectono-thermal history of central Dronning Maud Land, East Antarctica, – evidence from fission-track thermochronology“, by Stefanie Meier.
- Heft-Nr. 338/1999** – „Probleme hoher Stoffwechselraten bei Cephalopoden aus verschiedenen geographischen Breiten“, von Susanne Zielinski.
- Heft-Nr. 339/1999** – „The Expedition ARKTIS XV/1“, edited by Gunther Krause.
- Heft-Nr. 340/1999** – „Microbial Properties and Habitats of Permafrost Soils on Taimyr Peninsula, Central Siberia“, by Nicolé Schmidt.
- Heft-Nr. 341/1999** – „Photoacclimation of phytoplankton in different biogeochemical provinces of the Southern Ocean and its significance for estimating primary production“, by Astrid Bracher.
- Heft-Nr. 342/1999** – „Modern and Late Quaternary Depositional Environment of the St. Anna Trough Area, Northern Kara Sea“, edited by Ruediger Stein, Kirsten Fahl, Gennadij I. Ivanov, Michael A. Levitan, and Gennady Tarasov.
- Heft-Nr. 343/1999** – „ESF-IMPACT Workshop/Oceanic impacts: mechanisms and environmental perturbations, 15 - 17 April 1999 in Bremerhaven“, edited by Rainer Gersonde and Alexander Deutsch.

\* vergriffen/out of print.

\*\* nur noch beim Autor/only from the author.